This is to certify that the

dissertation entitled

Purification and Structural and Kinetic Characterizations of α-Galactosidases A and B from Human Liver

presented by

Francis E. Wilkinson

has been accepted towards fulfillment of the requirements for

Ph.D. degree in Biochemistry

Charles C. Sweeley
Major professor

Date October 11, 1985

PURIFICATION AND STRUCTURAL AND KINETIC CHARACTERIZATIONS OF α-GALACTOSIDASES A AND B FROM HUMAN LIVER

by

Francis Eugene Wilkinson

A DISSERTATION

Submitted to
Michigan State University
in partial fulfillment of the requirements
for the degree of

DOCTOR OF PHILOSOPHY

Department of Biochemistry

1985

ABSTRACT

Purification and Structural and Kinetic Characterization of α-Galactosidases A and B from Human Liver

Francis Eugene Wilkinson

α-Galactosidases A and B were purified to homogeneity in higher yields than has been reported for either enzyme from any other human tissue by a combination of a newly developed procedure to separate the α-galactosidases and previously published procedures. The α-galactosidase A preparation, but not B preparation, hydrolyzed a natural substrate, Gal α1-4Galß1-4Glcß1-1'-Ceramide, which indicates that the new method for separating the α-galactosidases is successful (Previous workers separated most of the α-galactosidase A from α-galactosidase B). The subunit molecular weights are 47,800 and 46,800 daltons for the A and B enzymes, respectively.

The amino acid compositions of both α-galactosidases were determined and were found to be fairly similar. Both α-galactosidases were carboxymethylated and then submitted for N-terminal sequencing. Each preparation yielded a unique N-terminal sequence, indicating that they are homodimers (the native molecular weights for both proteins had previously been shown to be about 100,000 daltons).

Nearly complete homology was found in the N-terminal region of these two proteins. These N-terminal sequences represent the first information obtained about the amino acid sequence of any human lysosomal glycosidase.

Tryptic peptides of both α-galactosidases were generated and separated by reversed-phase high performance liquid chromatography. Sufficient quantities of only α-galactosidase B peptides were obtained for N-terminal sequencing. Peptides accounting for twelve per cent of α-galactosidase B were sequenced. None of these α-galactosidase B peptides was found to have a sequence similar to the α-galactosidase A tryptic peptides determined by others, suggesting that the homology between α-galactosidases A and B is possibly restricted to the N-terminal region.

Some kinetic parameters of both enzymes were determined. The specific activities were determined to be 45.2 and 4.18 μmoles of 4-methylumbelliferyl-α-D-galactoside (4-MU-α-Gal) hydrolyzed per minute per mg of the A and B enzymes, respectively. α-Galactosidases A and B hydrolyzed the 4-MU-α-Gal with Km values of 1.83 and 13.1 mM, respectively. The Vmax were determined to be 52.9 and 13.9 μmol of 4-MU-α-Gal hydrolyzed per minute per mg of protein of the A and B enzymes, respectively. Both α-galactosidases A and B were competitively inhibited by D-galactose with respect to the hydrolysis of 4-MU-α-Gal; Ki values of 16.7 and 27.9 mM, respectively, were

observed. N-Acetyl-D-galactosamine was found to be a competitive inhibitor of α-galactosidase B with a Ki of 1.65 mM, but it did not inhibit α-galactosidase A.

Conduritol C epoxide, a structural analogue of α-D-galactose, inactivated α-galactosidase A, and very slowly B, in a time-dependent fashion. D-Galactose, a competitive inhibitor of α-galactosidase A, blocked the time-dependent inactivation of α-galactosidase A by conduritol C epoxide. These data strongly support the conclusion that conduritol C epoxide is a suicide inhibitor of α-galactosidase A. This is the first demonstration of a suicide inhibitor of any lysosomal glycosidase. Conduritol C epoxide appeared to be a competitive inhibitor of α-galactosidase A with a Ki of 330 mM.

This thesis is dedicated to my parents, Mr. and Mrs. Gilbert Wilkinson and to my brothers and sisters, whose love I cherish and whose finanacial support is very gratefully acknowledged.

I am also dedicating this work to those suffering from Fabry's disease and the other lysosomal storage diseases who have been praying for relief.

ACKNOWLEDGEMENTS

I would like to thank my major professor, Dr. Charles Sweeley, for his support and intellectual stimulation. I would also like to thank Dr's. Richard Anderson, William Deal, Walter Esselman, and William W. Wells for their input as committee members. A special thanks goes to Dr. James L. Fairley for his many suggestion during this project.

I would also like to thank the following post-docs, graduate students, and others who worked with me in Dr. Sweeley's lab over the past few years for their scientific insights and friendship: Matt Anderson, Diane Bloomer, John Burczak, Dorothy Byrne, Margaret Kabalin, Kimihiro Kanemitsu, Jos Kint, Norm LeDonne, Mike Lockney, Richard Lynch, Lyla Melkerson, Barb Myszkiewicz, Chris Marvel, Fumito Matsuura, Joe Moskal, Mitsuru Nakamura, Rob Soltysiak, Mike Thome, Mr. Wang, and Cliff Wong.

I would like to thank others in the department who were especially helpful: Doris Bauer, Betty Brazier, Steven Brookes, Lydia Coleman, David DeWitt, Theresa Fillwock, Susan Leavitt, Arlyne Garcia-Perez, and Dr. Clarence Suelter.

A special note of thanks goes to Dr. Shaun D. Black, formerly at the University of Michigan but now at Ohio State University, who gave me many helpful suggestions for the sequencing work.

I would also like to thank all my friends both back home and here in Michigan who have made these seven years just seem to fly by. And I should also thank all my ex-girlfriends who married the proverbial someone else so I could have enough time to do all this work.

TABLE OF CONTENTS

LIST OF TABLES

LIST OF FIGURES

Abbreviations

CBE	conduritol B epoxide
CCE	conduritol C epoxide
Con A	Concanavalin A-Sepharose
DMEM	Dulbelco's minimal essential medium
DE-52	DEAE-cellulose
DTT	dithiothreitol
FCS	fetal calf serum
α-Gal A	α-galactosidase A
α-Gal B	α-galactosidase B
GalNAc	N-acetyl-D-galactosamine
$GbOse_3$Ceramide	Galα1-4Galβ1-4Glcβ 1-1'-Ceramide
gc-ms	gas chromatography-mass spectroscopy
GlcNAc	N-acetyl-D-glucosamine
GM_2	The Tay-Sach's Ganglioside
HFBA	heptafluorobutyric acid
HPLC	high performance liquid chromatography
4-MU	4-Methylumbelliferyl
4-MU-α-Gal	4-Methylumbelliferyl-α-D-Galactoside
o-NP-α-GalNAc	o-Nitrophenyl-2-acetamido-2-deoxy-α-D-Galactoside
PEG	polyethyleneglycol
PMSF	phenylmethylsulfonylfluoride
p-NP	p-nitrophenol
p-NP-α-GalNAc	p-Nitrophenyl-2-acetamido-2-deoxy-α-D-galactoside
TFA	trifluoroacetic acid

LITERATURE REVIEW

The Physiological Importance of Lysosomal Enzymes The lysosome was recognized by deDuve as a distinct organelle in 1955 (1,2), and he postulated that its complement of hydrolytic enzymes can degrade any biomolecule (3). Several of these enzymes were studied by the use of synthetic substrates, while their in vivo functions were often discovered through correlations with disease states. An individual occasionally came to the attention of the medical profession because of life-threatening conditions which were due to a deficiency of one or more lysosomal enzymes. (Most of the deficient enzymes are glycosidases, but not all of them are even hydrolases: the terms lysosomal enzyme and hydrolase will be used interchangeably here). Such a deficiency commonly results in the accumulation in the lysosome of the natural substrate(s) of the enzyme. The accumulated material can disrupt normal cellular function, which is why these deficiencies are called lysosomal storage diseases. The lysosomes of some diseases have a characteristic appearance depending upon what material has accumulated. In several diseases, the chemical structure of the accumulated material has been determined and a correlation was made of an enzyme activity found in normal tissue capable of degrading the material with a deficiency of the enzyme in the tissues of the

afflicted individual (4). That a disease has not yet been associated with the deficiency of a lysosomal enzyme may reflect the severity of its absence so that the infant dies either *in utero* or shortly after birth. This is the case in caprine ß-mannosidosis (5,6).

The genetics of many of the lysosomal storage diseases have been determined, and all studied to date have proven to be recessive traits; two of these disorders, Fabry's and Hunter's diseases, are sex-linked (7). None of these diseases can be successfully managed. Studies are continuing on biochemical characterizations of the individual hydrolases as well as determinations of the biosynthesis and normal function of each in order to determine the molecular basis for the deficiency. The results of these studies may be useful in effecting a cure for these diseases.

A logical first step in the biochemical characterization of a lysosomal hydrolase is the purification of the enzyme so that a comparison can be made between the normal and mutant enzymes. The following lysosomal enzymes, among others, have been purified to apparent homogeneity from human tissues: N-acetylgalactosamine 6-sulfate sulfatase (8), α-N-acetylglucosaminidase (9), acid lipase (10), arylsulfatases A (11) and B (12), aspartylglucosaminidase (13), cathepsin D (14), α-L-fucosidase (15), α-galactosidases A (16) and B (17), galactocerebrosidase

(18), ß-galactosidase A_2 (19), glucosylceramidase (20), ß-glucuronidase (21), α-glucosidase (22), β-hexosaminidase (23), and sphingomyelinase (24). Several of these enzymes have been partially chemically characterized. Some of these characterizations have included amino acid composition (11-15, 19, 21, and 24), partial amino acid or cDNA sequence (25-27), carbohydrate composition (28,29), or a general structure of the carbohydrate moieties attached to the enzyme (30-33).

In general, these hydrolases degrade biomolecules that are delivered to the lysosome by receptor-mediated endocytosis (34) or by other mechanisms. The digestion products are amino acids, simple sugars, lipids, and nucleotides and are thought to be removed from the cell by a process similar to a reversal of receptor-mediated endocytosis.

These hydrolases generally have an acidic pH optimum, and <u>in vivo</u> measurements have shown that lysosomes have an internal pH of 4.7 to 4.8 (35). Some of the hydrolases that degrade neutral glycosphingolipids and gangliosides utilize a specific activator protein that appears to be involved in both solubilizing the lipid and stabilizing the glycosidase (36). The AB variant of GM_2 gangliosidosis (37) and a variant of metachromatic leukodystrophy (38,39) are due to deficiencies of the respective activator proteins.

The kinetic parameters and substrate specificities of

many lysosomal hydrolases have been determined (4). The determination of the mechanism of catalysis is especially important since the inability of these enzymes to perform properly has such drastic consequences. One of the methods of determining the mechanism of catalysis has involved suicide inhibitors. These have been used to isolate the active site peptide of a few non-lysosomal glycosidases (40-44): the results of these (Table 1) and other studies on the mechanism of glycosidases have been reviewed (45). Among the lysosomal glycosidases, van Diggelen *et al.* (46) have reported an *in vivo* inactivation of lysosomal ß-galactosidase by ß-galactosyl p-nitrophenol triazene which had previously been shown to be a suicide inhibitor of *E. coli* ß-galactosidase (44). They (46) also showed inhibition of the lysosomal ß-glucosidase with the ß-glucosyl derivative. It has been suggested that conduritol B epoxide is a suicide inhibitor of the lysosomal enzyme β-glucocerebrosidase because injection of conduritol B epoxide into mice significantly reduces the levels of this enzyme in the brain, liver, and spleen (47) and because it is a suicide inhibitor of two non-lysosomal glycosidases (40,42). Conduritol B epoxide has been shown to be a competitive inhibitor of calf brain ß-glucosidase (48). But to date no compound has been shown to be a suicide inhibitor of any lysosomal glycosidase, nor has the amino acid sequence around the active site of any lysosomal glycosidase been determined.

Table 1. Active site sequences of non-lysosomal hydrolases.

1. Val-Met-Ser-<u>Asp</u>-Trp-Ala-Ala-His-His-Ala-Gly-Val-Ser-

2. Ile-Thr-Glx-Glx-Gly-Val-Phe-Gly-<u>Asp</u>-Ser-Glx-

3. Ile-<u>Asp</u>-Met-Asn-Gln-Pro-Asn-Ser-Ser

4. Gln-Ala-Thr-Asn-Arg-Asn-Thr-Asp-Gly-Ser-Thr-<u>Asp</u>-Tyr

5. Thr-Thr-Ala-Thr-Asp-Ile-Ile-Cys-Pro-<u>Met</u>-Tyr-Ala-Arg

1. ß-Glucosidase A_3 from <u>Aspergillus wentii</u> (40). The active site label was conduritol B epoxide.

2. ß-Glucosidase A from bitter almonds (41). The active site label was 6-bromo-3,4,5-trihydroxy cyclonex-1-ene oxide.

3. Rabbit intestinal sucrase·isomaltase complex (42). The active site label was condurtiol B epoxide.

4. Hen egg lysosyme (43). The active site label was 2',3'-epoxypropyl-O-ß-N-acetyl-<u>D</u>-glucosaminyl-ß-(1-4)-N-acetyl-<u>D</u>-glucosaminide.

5. <u>E. coli</u> ß-galactosidase (44). The active site label was ß-<u>D</u>-galactopyranosylmethyl p-nitrophenyl triazene.

The underlined amino acid was derivatized by the respective active site label.

Biosynthesis of Lysosomal Enzymes. The biosynthesis of the lysosomal hydrolases is a complicated process that involves at least two peptide cleavages, the action of glycosyltransferases and glycosidases, and includes the proper sorting of the enzymes within the endomembrane system to either the lysosome or to secretory vesicles (Table 2 lists the main steps of lysosomal enzyme biosynthesis). Understanding the biosynthesis of these enzymes is epecially important since a few of the lysosomal storage disorders, I-cell disease and pseudo-Hurler dystrophy (49,50) and a variant of GM_2 gangliosidosis (51-53), are due to an improper biosynthesis of the respective lysosomal hydrolase. The early stage of the biosynthesis of lysosomal enzymes is exactly the same as that of secreted mammalian proteins, and is similar to the synthesis of some secreted bacterial proteins (54). The mRNA's coding for the pre-pro form of the lysosomal hydrolases are translated on cytoplasmic ribosomes until a leader sequence of about twenty, mostly hydrophobic amino acids comprises the nascent chain (55). At this point a complex of six proteins known as the signal recognition particle, SRP, binds the leader sequence with high affinity and interacts with the ribosome, thereby stopping further translation (56). The complex then binds with a docking protein (57) on the rough endoplasmic reticulum, the SRP is released, the nascent peptide goes through a pore in the membrane to the lumen of the endoplasmic reticulum, and

Table 2. Biosynthesis of Lysosomal Enzymes.

1) Transcription of the gene coding for the lysosomal enzyme and processing of the hnRNA to mRNA. These events occur in the nucleus.

2) Translation begins on a cytoplasmic ribosome, and as soon as the leader sequence has been translated, the Signal Recognition Particle, SRP, binds the ribosome, and translation ceases. The SRP-ribosome-mRNA-nascent protein binds with a docking protein on the endoplasmic reticulum, and translation resumes with the nascent protein being in the lumen of the endoplasmic reticulum.

3) The leader sequence is proteolytically removed,and the protein is glycosylated during translation. Both of these events occur in the endoplasmic reticulum.

4) Carbohydrate processing events converting the $Glc_3Man_9GlcNAc_2$ oligosaccharide to the high mannose, complex, or hybrid chains occur next. The enzymes responsible for the initial reactions such as α-glucosidases I and II are in the endoplasmic reticulum, while those responsible for the last events such as the glycosyltransferases involved in the formation of complex chains are in the Golgi apparatus.

5) If the enzyme has subunits, the subunits presumably associate in the Golgi apparatus before transport to lysosome.

6) The lysosomal enzyme is then transported to the lysosome where a C- or N-terminal peptide is removed from the enzyme, and this cleavage is sometimes necessary for the enzyme to be functional.

translation continues. An as yet unidentified protease cleaves the leader sequence of hydrophobic amino acids from the N-terminus shortly after translation resumes, yielding the pro-form of the enzyme (55). The balance of the nascent protein is then translated directly into the lumen of the endoplasmic reticulum. Cell-free translation of mRNA of secreted proteins in the absence of microsomes results in the translation of the pre-pro form of the lysosomal enzyme that cannot be further processed (55), the implications of which will be discussed later.

Studying the carbohydrates and processing events of the carbohydrate moieties on the lysosomal enzymes is of special importance because 1) two lysosomal storage diseases are due to a deficiency of a processing enzyme, 2) the carbohydrates are involved in directing the lysosomal enzymes to their proper cellular location, and 3) the carbohydrates are involved in maintaining the lysosomal enzymes in circulation. During translation the protein is N-glycosylated on certain asparagine residues. Lennarz and coworkers (58) found that a sequence of -Asn-X-Ser(Thr)- (X probably cannot be Asp) is required for glycosylation although not all such sequences are glycosylated. Assessments of the three-dimensional structures of the proteins around possible glycosylation sites showed that those sites in ß-turns or loops tend to be glycosylated, while those in α-helices are not (59). Other factors may be involved because bovine pancreatic ribonucleases A and B

translation continues. An as yet unidentified protease cleaves the leader sequence of hydrophobic amino acids from the N-terminus shortly after translation resumes, yielding the pro-form of the enzyme (55). The balance of the nascent protein is then translated directly into the lumen of the endoplasmic reticulum. Cell-free translation of mRNA of secreted proteins in the absence of microsomes results in the translation of the pre-pro form of the lysosomal enzyme that cannot be further processed (55), the implications of which will be discussed later.

Studying the carbohydrates and processing events of the carbohydrate moieties on the lysosomal enzymes is of special importance because 1) two lysosomal storage diseases are due to a deficiency of a processing enzyme, 2) the carbohydrates are involved in directing the lysosomal enzymes to their proper cellular location, and 3) the carbohydrates are involved in maintaining the lysosomal enzymes in circulation. During translation the protein is N-glycosylated on certain asparagine residues. Lennarz and coworkers (58) found that a sequence of -Asn-X-Ser(Thr)- (X probably cannot be Asp) is required for glycosylation although not all such sequences are glycosylated. Assessments of the three-dimensional structures of the proteins around possible glycosylation sites showed that those sites in ß-turns or loops tend to be glycosylated, while those in α-helices are not (59). Other factors may be involved because bovine pancreatic ribonucleases A and B

have the same amino acid sequence, but only the B form is glycosylated.

An oligosaccharide is transferred en bloc from a dolicholpyrophosphate lipid intermediate to the asparagine by a membrane-bound enzyme. The transferred oligosaccharide contains three glucosyl, nine mannosyl, and two N-acetylglucosaminyl residues (60,61) (Figure 1 Structure A). Subsequent glycoprotein processing, which includes the removal and/or addition of sugars on the core oligosaccharide, commences shortly after N-glycosylation. The oligosaccharide processing generally results in various kinds of high mannose chains, complex chains which usually indicate the presence of sialic acid, or hybrid chains which are a combination of high mannose and complex (Figure 2 shows representative examples of all three types of chains). All three types of oligosaccharides have been found on lysosomal hydrolases. The control mechanisms for determining which types of oligosaccharides will be formed have not yet been determined, but data support two possible models. The first is that the control is inherent in the conformation of the protein (62) such that some high mannose chains become inaccessible to the processing enzymes because of the folding of the nascent protein (63). The second is that the complement of processing enzymes in the respective cell type (64) varies among the cell types so that the enzymes themselves regulate the extent of processing. The main processing events and their

Figure 1. The Carbohydrate Processing Events.

Structure A is transferred from a dolichol pyrophosphate lipid intermediate to the amide of specific asparaginyl residues of some proteins as described in the text. The three α-glucosyl residues of Structure A are removed by the successive action of α-glucosidases I and II to yield Structure B. The starred mannoses on Structure B can be phosphorylated at carbon six on lysosomal enzymes by the successive action of a GlcNAc phosphotransferase and an α-N-acetylglucosamine-1-phosphodiesterase. α-Mannosidase I can remove the four α1-2 linked mannoses from Structure B to yield Structure C, which is an intermediate in the biosynthesis of both complex and hybrid type oligosaccharides. α-Mannosidase I digestion is not always complete so that one or more of the α1-2 linked mannoses remain on the oligosaccharide; such molecules are of the high mannose type.

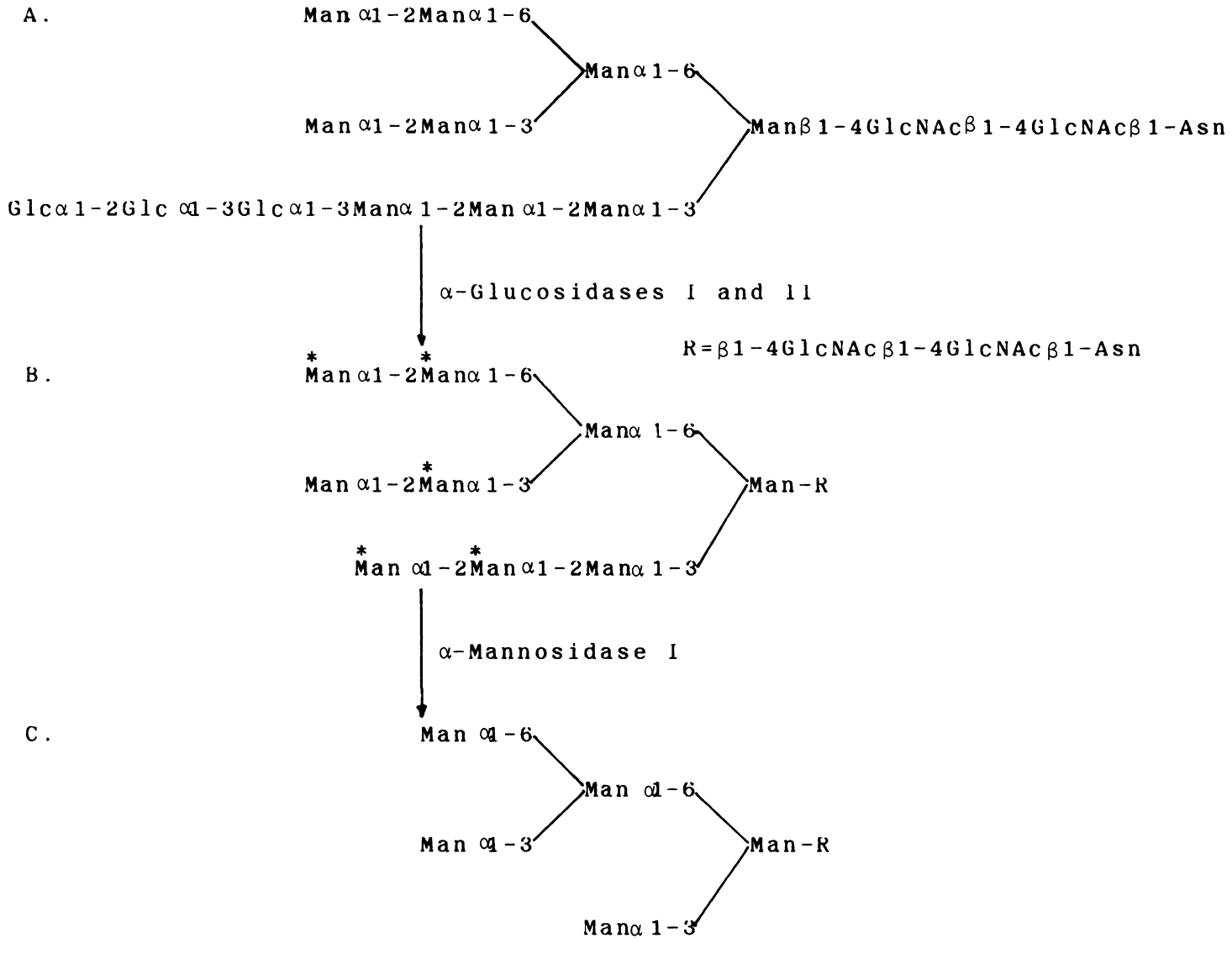
A.
Manα1-2Manα1-6
Manα1-6
Manα1-2Manα1-3
Manβ1-4GlcNAcβ1-4GlcNAcβ1-Asn
Glcα1-2Glcα1-3Glcα1-3Manα1-2Manα1-2Manα1-3
α-Glucosidases I and II
R=β1-4GlcNAcβ1-4GlcNAcβ1-Asn
B.
Manα1-2Manα1-6
Manα1-6
Manα1-2Manα1-3
Man-R
Manα1-2Manα1-2Manα1-3
α-Mannosidase I
C.
Manα1-6
Manα1-6
Manα1-3
Man-R
Manα1-3

Figure 1. Continued

Structure C is the substrate for GlcNAc transferase I which yields Structure D. Structure D can be converted to Structure E by the action of α-mannosidase II. Structure E can be the substrate for the successive action of GlcNAc, galactosyl, sialyl, and fucosyltransferases to yield bi-, tri-, or tetraantennary complex chains. Structure D can also be the substrate of GlcNAc transferase III resulting in Structure F, which can be the the substrate for GlcNAc and galactosyl transferases resulting in bisected structures.

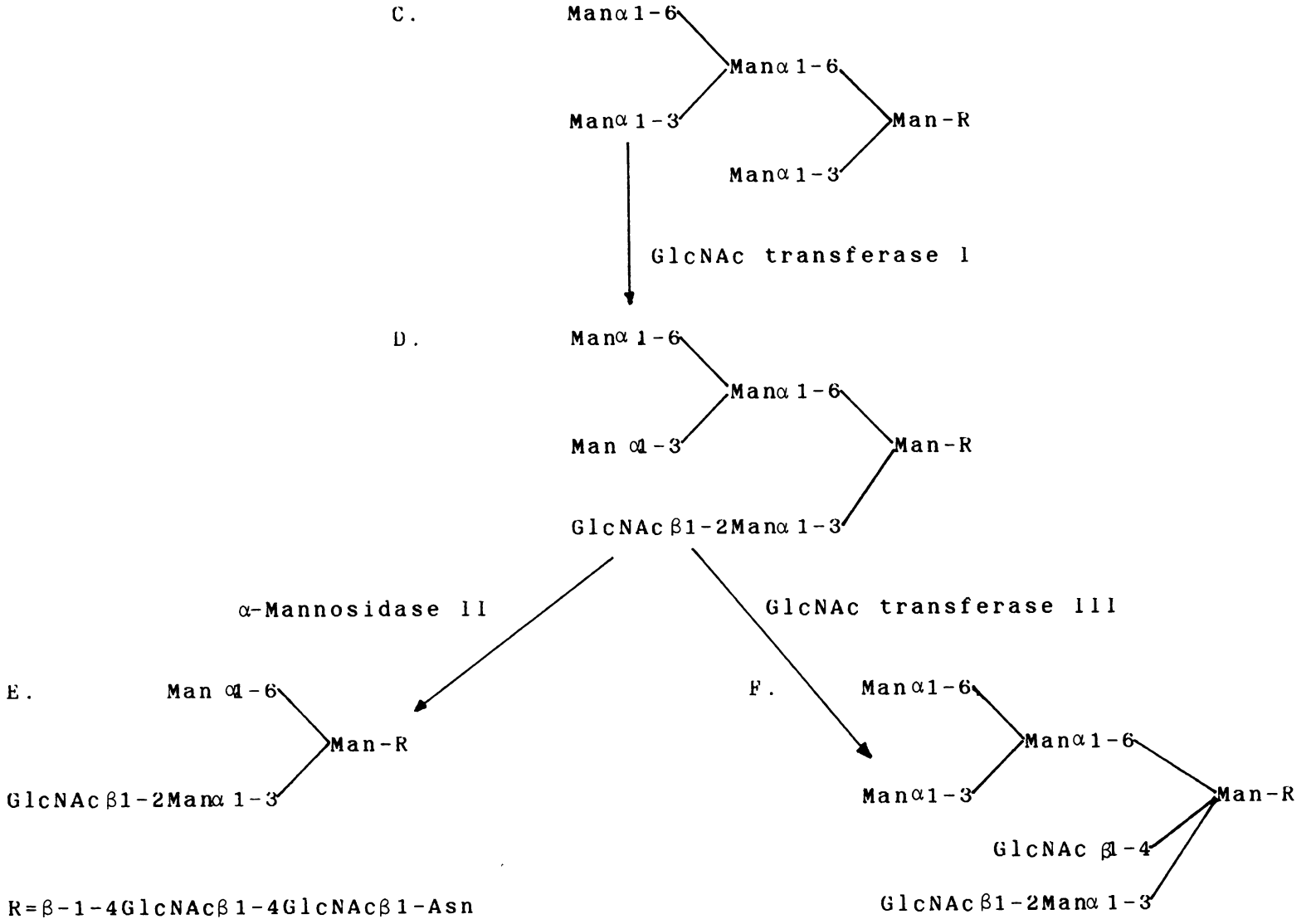
C.
Manα1-6
Manα1-6
Manα1-3
Man-R
Manα1-3
GlcNAc transferase I
D.
Manα1-6
Manα1-6
Man α1-3
Man-R
GlcNAcβ1-2Manα1-3
α-Mannosidase II
GlcNAc transferase III
E.
Man α1-6
Man-R
GlcNAcβ1-2Manα1-3
F.
Manα1-6
Manα1-6
Manα1-3
Man-R
GlcNAc β1-4
GlcNAcβ1-2Manα1-3
R=β-1-4GlcNAcβ1-4GlcNAcβ1-Asn

Figure 2. The major types of N-linked oligosaccharides.

A. High mannose type found on porcine cathepsin D (32)

B. Hybrid type found on ovalbumin (81)

C. Complex type found on human placental glucocerebrosidase (33)

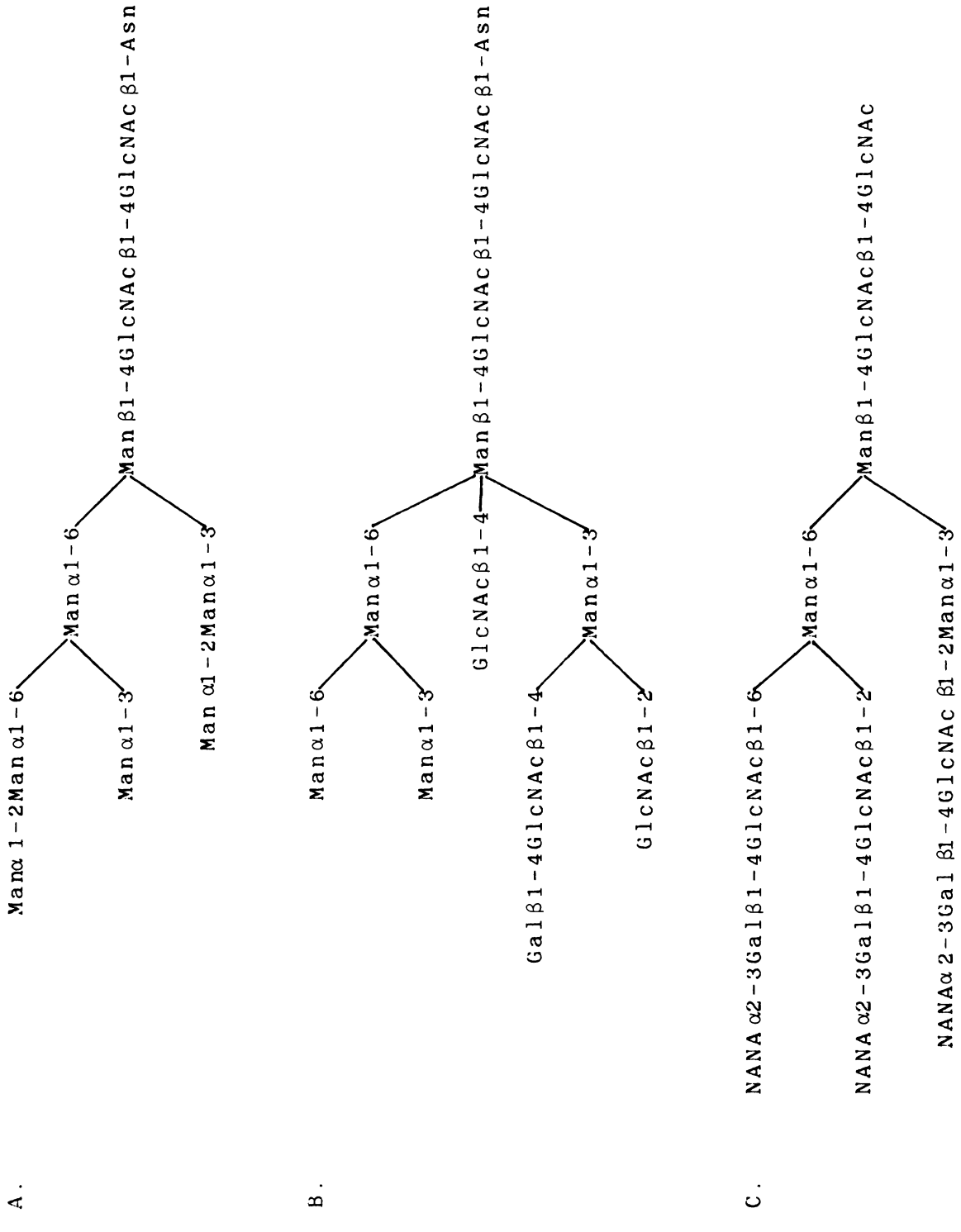
A.
Manα 1-2Man α1-6
Man α1-6
Man α1-3
Man β1-4GlcNAc β1-4GlcNAc β1-Asn
Man α1-2Man α1-3
B.
Man α1-6
Man α1-6
Man α1-3
Man β1-4GlcNAc β1-4GlcNAc β1-Asn
GlcNAc β1-4
Gal β1-4GlcNAc β1-4
Man α1-3
GlcNAc β1-2
C.
NANA α2-3Gal β1-4GlcNAc β1-6
Man α1-6
NANA α2-3Gal β1-4GlcNAc β1-2
Man β1-4GlcNAc β1-4GlcNAc
NANA α2-3Gal β1-4GlcNAc β1-2Man α1-3

regulation are presented briefly below.

The first step in the processing of N-linked carbohydrates is the removal of the three glucosyl units from the tetradecasaccharide by two unique enzymes, α-glucosidases I and II. α-Glucosidase I removes the terminal glucosyl residue and α-glucosidase II removes the two remaining α-glucosyl residues (Figure 1 Structure A to B) (61,65). Both of these α-glucosidases have been partially characterized and are localized in the rough endoplasmic reticulum. Most N-linked oligosaccharides studied to date are normally processed in this fashion, but an exception is the human myeloma IgD:WAH in which there is incomplete removal of the internal glucosyl residue (66).

High mannose chains result from the removal of few, if any, α-mannosyl residues from the oligosaccharide by α-mannosidase I (Figure 1 Structure B to C) (67).

The mannose-6-phosphate recognition system has been of intense research interest for several years and has recently been elucidated. In brief, primarily in fibroblasts and a few other tissues, a GlcNAc-phosphotransferase in the Golgi apparatus (68) transfers GlcNAc-phosphate from UDP-GlcNAc to carbon six of one or two of any of five mannosyl residues on the high mannose chains (69) (Figure 1 Structure B the starred positions) after the three glucosyl residues have been removed. This GlcNAc-phosphotransferase is highly specific. Non-lysosomal proteins having a high mannose chain as well

as heat-denatured lysosomal enzymes are poor substrates for the enzyme. It has been postulated that a structural determinant in the protein portion of lysosomal hydrolases is required for recognition by the GlcNAc-phosphotransferase (70). This GlcNAc-phosphotransferase is deficient in I-cell disease (49) and very low in pseudo-Hurler dystrophy (50), two lysosomal storage diseases in which functional lysosomal enzymes including ß-hexosaminidase and arylsulfatase A are secreted by fibroblasts but are not retained by the cells (71). The GlcNAc is removed by a Golgi apparatus-associated α-N-acetyglucosaminylphosphodiesterase (68). The mannose-6-phosphate then binds to a receptor protein of M_r=215,000 (72,73) that directs the hydrolase to the lysosome where it is thought that acid phosphatase removes the phosphate from the mannose-6-phosphate (74). This mannose-6-phosphate receptor also exists on the cell surface and functions in directing extracellular mannose-6-phosphate-containing lysosomal hydrolases to the lysosomes via receptor-mediated endocytosis. It is important to remember that this mannose-6-phosphate recognition system functions mainly in fibroblasts because I-cell patients have normal levels of lysosomal hydrolases in other cell types (75,76). An additional mechanism of transporting these enzymes to lysosomes must operate in tissues other than fibroblasts. In this connection, a second mannose-6-phosphate receptor of M_r=46,000 has

recently been reported (77).

The complex chains are formed by a series of several reactions. The first is the removal of the four α 1-2 linked mannosyl residues by α-mannosidase I (Figure 1 Structure B to C) (67), which is a membrane-bound enzyme localized in the Golgi apparatus. The next step is the addition of a GlcNAc residue by GlcNAc transferase I (Figure 1 C to D), which is a necessary step for the formation of both complex and hybrid carbohydrates (78). Structure D shown in Figure 1 is necessary for the action of α-mannosidase II, which removes two of the remaining α-mannosyl residues (79) so that Structure D can be a substrate for successive GlcNAc, galactosyl, sialyl, and fucosyl transferases resulting in complex chains (80) (Figure 2 Structure C). Structure D in Figure 1 can also be the substrate for GlcNAc transferase III with Structure F being the product of the reaction; this last structure can be the substrate of the glycosyltransferases listed above which results in a hybrid carbohydrate (Figure 2B).

Once processing of the carbohydrate moieties, whether high mannose or complex, has been completed, a high molecular weight form of the enzyme can be secreted by the cell, and a lower molecular weight protein is directed to the lysosome. One or more peptides are generally removed from the lysosomal hydrolase before its delivery to the lysosome, and two lysosomal enzymes have been shown to be formed by the removal of a C-terminal peptide (82).

Many of the lysosomal enzymes are comprised of two or more subunits, and the assembly of these subunits into active enzymes is only now being addressed. Subunit association in the one case studied to date occurs only among the precursor subunits after most or all of the carbohydrate processing reactions, but before the final proteolytic cleavages and shipment of the enzyme to the lysosome have occurred (51). It has recently been shown (52,53) that a variant of Tay-Sach's disease is due to an improper association of the α and ß chains of ß-hexosaminidase A so that the large molecular weight precursor of the α chain is not converted to the mature form. The precursor of the mutant α chain appears to have the same molecular weight and carbohydrate as the normal, but the reason for the faulty assembly has not yet been determined.

Therapeutic Approaches

Organ Transplantation. There is currently no effective treatment for any of the lysosomal storage diseases in contrast to the treatment of juvenile (Type I) diabetes with insulin.. One of the current strategies is to reduce the incidence of the respective diseases by performing enzyme assays on amniotic cells derived from at-risk patients and then performing a therapeutic abortion if the patient lacks the respective lysosomal hydrolase. Research

is continuing for a more viable alternative.

Progress is especially being made in the area of organ transplantation. A kidney transplanted into a Fabry's patient (83) appears to metabolize the lipid that would otherwise accumulate there and cause kidney failure, which is a major cause of death of Fabry's patients. However, the transplanted kidney may not secrete enough of the deficient enzyme, α-galactosidase A, to metabolize the lipid accumulating in endothelial cells, the other major site of accumulation, causing heart disease and death in some Fabry's patients. Therefore the ideal organ for transplantation therapy would be one that could be transplanted with low risk to the patient and that is either the only organ involved in the disease or one that is able to secrete enzyme that can be endocytosed by the organs where the substrate has accumulated.

Recently (84), an eight-month-old infant suffering from Hurler's syndrome received a bone marrow transplant in the hope that the bone marrow-derived leukocytes would produce enough of the deficient enzyme, α-L-iduronidase, to halt both the progression of the disease and reverse the clinical symptoms that had already occurred. The non-neural tissues appeared normal up to eleven months after the bone marrow transplant, but the mental development of the child was low perhaps due to his having been kept in isolation for five months or to the inability of the enzyme to cross the blood-brain barrier. A less

detailed report has appeared (85) about a bone marrow transplant in an infant with metachromatic leukodystrophy. This patient was progressing well up to ten months after the bone marrow transplant. In addition, an adult cat having arylsulfatase B deficiency received a bone marrow transplant (86). The cat's physical and biochemical symptoms were all markedly improved, including its skeletal abnormalities. Collectively, these experiments indicate that the plasma forms of these lysosomal hydrolases are synthesized and secreted by bone marrow-derived cells and that the plasma forms of these enzymes degrade the material that would otherwise accumulate in the lysosome, possibly by being endocytosed by the somatic cells where the respective substrate would accumulate.

Enzyme Replacement Therapy. There are currently two variations of enzyme replacement therapy. The first involves the purification, or nearly total purification, of the respective enzyme from human sources and injecting the enzyme into the bloodstream. This procedure has both positive and negative features. The positive side is that since the enzyme is of human origin, it will not elicit an antibody response, and the respective enzyme should function *in vivo* (87). The drawbacks to this procedure include 1) the tissue source is frequently autopsy specimens which are difficult to obtain, 2) there is only a small quantity of these enzymes in human tissue, 3) the purification procedures generally give low yields, 4) the

infused enzyme may not reach the organ(s) where the substrate has accumulated, 5) the infused enzymes can be quickly removed from circulation by the Ashwell receptor (88), and 6) the enzyme may not be able to cross the blood-brain barrier. The second general strategy is the infusion of genetically engineered enzyme. This would require the isolation of the entire gene coding for the lysosomal enzyme, which would have to be cloned into a mammalian cell in order for the requisite carbohydrate processing (55) necessary for uptake by the respective cells and possibly for avoiding an immune response. Another drawback is that neither the amino acid nor cDNA sequence of any human lysosomal enzyme has yet been completely determined, but 80% of the sequence of α-L-fucosidase (25) and lesser amounts of three other human lysosomal glycosidases have been determined (26-27).

α-Galactosidases A and B: Association with Disease States, Function, Biosynthesis, and Structures.

Fabry's Disease and its Association with α-Galactosidase A Deficiency. Fabry's disease is a fatal, sex-linked recessive error of glycosphingolipid metabolism. There is a deficiency of an α-galactosidase so that lipids accumulate in the tissues of Fabry's patients. This lipid accumulation is responsible for a variety of ailments including skin lesions, renal impairments, cardiovascular

disease, ocular opacities, cataracts, retinal edema, and dysfunction of the central nervous system and gastrointestinal tract. The patient usually dies of kidney failure in his fourth or fifth decade. Heterozygous females are affected to a much smaller extent (89). The accumulated lipid was identified by Sweeley and Klionsky (90) as ceramide trihexoside, $GbOse_3Ceramide$, with digalactosylceramide as a minor component. Wherrett and Hakomori (95) found blood group B glycosphingolipids accumulating in Fabry's patients whose blood type was B (See Figure 3 for the structures of these and other glycoconjugates likely to be metabolized by this enzyme).

Later Brady et al. (98) correlated the deficiency of an enzyme, which they called ceramide trihexosidase, with Fabry's disease. It was initially thought that this ceramide trihexosidase was a ß-galactosidase, since the non-reducing terminus of ceramide trihexoside is galactose. However, Kint (99) clearly demonstrated by the use of a synthetic substrate that the deficient enzyme in Fabry's disease is an α-galactosidase. Beutler and Kuhl (100) and Kint et al. (101) found that there are two different α-galactosidases, which they called the A and B forms. It was reported that the A form is absent while the B form persists or even increases in Fabry's disease.

An activator protein, shown to be necessary for the in vivo hydrolysis of ceramide trihexoside, has been partially purified from human liver (36). No case of Fabry's disease

Figure 3. Glycoconjugates catabolized by α-galactosidase A.

(I) Digalactosyl Ceramide (90)

(II) Ceramide Trihexoside (90)

(III) Cytolipin R (91)

(IV) P_1 Antigen (92)

(V) Rabbit erythrocyte pentaglycosylceramide (93)

(VI) Glycolipid X of rat granuloma and macrophage (94)

(VII) Glycolipids from the pancreas of a Fabry's patient whose blood type was B (95)

(VIII) Blood Group B II glycolipid (96)

(IX) Blood Group I active ganglioside from bovine RBC's (97)

(I) Galα1-4Galβ1-1'-Ceramide

(II) Galα1-4Galβ1-4Glcβ1-1'-Ceramide

(III) GalNAcβ1-3Galα1-3Galβ1-4Glcβ1-1'-Ceramide

(IV) Galα1-4Galβ1-4GlcNAcβ1-3Galβ1-4Glcβ1-1'-Ceramide

(V) Galα1-3Galβ1-3GlcNAcβ1-3Galβ1-4Glcβ1-1'-Ceramide

(VI) Galα1-3Galβ1-3GalNAcβ1-3Galβ1-4Glcβ1-1'-Ceramide
|
Fucα1-2

(VII) Galα1-3Galβ1-3/4GlcNacβ1-3Galβ1-4Glcβ1-1'-Ceramide
|
Fucα1-2

(VIII) Galα1-3Galβ1-4GlcNAcβ1-3Galβ1-4GlcNAcβ1-3Galβ1-4Glcβ1-1'-Ceramide
|
Fucα1-2

(IX) Galα1-3Galβ1-4GlcNAcβ1-6Galβ1-4GlcNAcβ1-3Galβ1-4Glcβ1-1'-Ceramide
NANAα2-3Galβ1-4GlcNAcβ1-3

having a deficient activator protein has yet been reported.

Purification of the α-Galactosidases. Several attempts were made to purify the two α-galactosidases to determine if they have a precursor-product relationship, as had been postulated (101), or are interconvertible (102), and to determine the lesion responsible for Fabry's disease. Major contributions towards the purification of these enzymes were made by Beutler and Kuhl (103), who separated the two α-galactosidases by DEAE-cellulose chromatography, which is still used by some of the major investigators in the field (16,104-106). Mayes and Beutler (107) purportedly purified from placenta the A enzyme which has a subunit of M_r=67,500, and a contaminant of M_r=47,000 that appeared as a diffuse band on an SDS-polyacrylamide gel; this contaminant was probably α-galactosidase A. The first successful purification of either α-galactosidase was by Kusiak et al. (17), who obtained the B form from human placenta. This protein had a subunit M_r=47,700 and was reported to be a homodimer. Their preparation of the A form contained many contaminants as revealed by SDS-gel electrophoresis and had a subunit M_r=57,700 which is significantly higher than the M_r=49,800 that has since been determined (16). Dean and Sweeley purified the B form (104) and almost completely purified the A form (105) from human liver. They also compared the kinetic parameters and substrate specificities for both enzymes (108). The first successful purification of α-galactosidase A was by Bishop

and Desnick (16). Their purification scheme was a tremendous improvement over others in terms of yield, purity and the number of steps required; their success was primarily due to the use of an affinity ligand developed by Harpaz and Flowers (109) for the purification of coffee bean α-galactosidase.

Oligosaccharides on the α-Galactosidases. Digestions of the α-galactosidases with neuraminidase showed that the A form has sialic acid while the B form does not (110,111). It was inferred that the B form is a glycoprotein by its binding to concanavalin A-Sepharose during purification (17). The biological importance of the carbohydrate moieties on α-galactosidase A was demonstrated by *in vivo* experiments by Desnick *et al.* (87). They infused partially purified human splenic and plasma α-galactosidase A into two brothers with Fabry's disease to determine: (1) what effect these enzymes would have on the plasma level of ceramide trihexoside, (2) if these enzymes would remain in the plasma, and (3) if the gross symptoms would improve in either patient. They found that, although the splenic form has a higher specific activity than the plasma form, the plasma form persisted much longer in circulation and cleared much more of the circulating $GbOse_3Cer$ than did the splenic enzyme. It is thought that the *in vivo* efficacy of the plasma form relative to the splenic form was due to the higher degree of sialylation of the plasma form. The rapid clearance of the splenic enzyme is

consistent with the clearance of desialylated glycoproteins from serum by the Ashwell receptor (88). These experiments also demonstrated the potential use of the plasma form of α-galactosidase A for enzyme replacement therapy in Fabry's patients.

Biosynthesis of α-Galactosidases A and B. Due to the biological importance of the carbohydrate moieties of α-galactosidase A and to determine the biosynthetic processing events of lysosomal hydrolases, others in this laboratory studied the carbohydrate processing events of these two lysosomal glycosidases (30,31). The largest glycosylated precursor of α-galactosidase A is M_r=58,000; that of α-galactosidase B is M_r=65,000, while the molecular weights of the fully processed enzymes are 49,000 and 48,000, respectively, which indicates that one or more peptides are removed from the precursors of both enzymes. Half of the carbohydrate chains of α-galactosidase A are processed to the complex type having a tri- or tetraantennay structure, while the other half are high mannose chains with eight or nine mannoses. On the other hand α-galactosidase B has only high mannose chains containing 7 to 9 mannoses. A phosphorylated biosynthetic intermediate of α-galactosidase B was found (30) in fibroblasts but, not surprisingly, such an intermediate was not found for α-galactosidase A from Chang liver cells (31). However, 50% of the α-galactosidase A purified from human placenta (106) has one or more phosphorylated

carbohydrate chains.

Biological Significance of α-Galactosidase B.

α-Galactosidase B has been studied primarily as an adjunct to the studies of α-galactosidase A, and in a sense has been seen as a contaminant that is difficult to separate from α-galactosidase A. Until recently the principal biological importance of α-galactosidase B has been its demonstration as an α-N-acetylgalactosaminidase (17,112,113). The porcine (114) and human (105) liver enzymes have been shown to cleave the terminal α-N-acetygalactosaminyl residue from the Forssman glycolipid (See Figure 4 for the degradation of the principal neutral glycosphinglipids by the lysosomal glcosidases) and is presumably also involved in the catabolism of blood group A antigens and α-N-acetylgalatosamine in O-linked glycoproteins (See Figure 5 for the structures of these and other glycoconjugates likely to be catabolized by α-galactosidase B). Julia Frei of this laboratory (119) showed that the hepatic level of α-galactosidase B in a patient who died of malignant histiocytosis was either 2 or 30% of normal, depending upon which artificial substrate was used. The correlation between α-galactosidase B deficiency and malignant histiocytosis has not been firmly determined. Glucosylceramide is the only glycoconjugate found thus far in higher concentration in malignant histiocytosis relative to a normal control, but the patient

did not have any of the recognized forms of Gaucher's disease.

Figure 4. Degradation of Neutral Glycosphingolipids

The glycosphingolipids of the globo series, the major group of neutral glycosphingolipids of human erythrocytes, are degraded by five lysosomal hydrolases to ceramide and neutral sugars as shown.

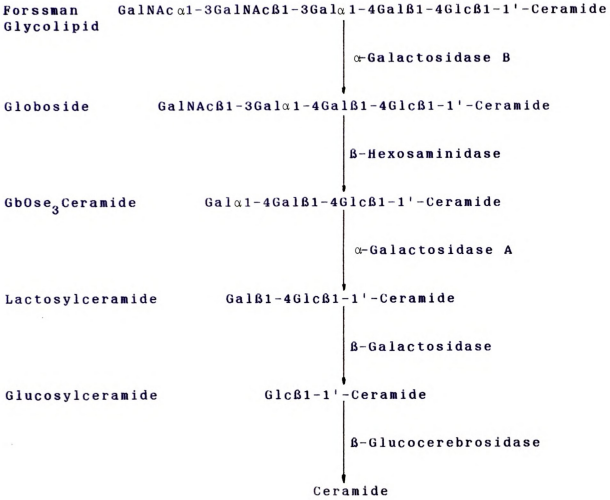
Forssman Glycolipid
GalNAcα1-3GalNAcß1-3Galα1-4Galß1-4Glcß1-1'-Ceramide
α-Galactosidase B
Globoside
GalNAcß1-3Galα1-4Galß1-4Glcß1-1'-Ceramide
ß-Hexosaminidase
GbOse3Ceramide
Galα1-4Galß1-4Glcß1-1'-Ceramide
α-Galactosidase A
Lactosylceramide
Galß1-4Glcß1-1'-Ceramide
ß-Galactosidase
Glucosylceramide
Glcß1-1'-Ceramide
ß-Glucocerebrosidase
Ceramide

Figure 5. Glycoconjugates Catabolized by α-Galactosidase B.

(I) The major carbohydrate found on glycophorin (115).

(II) Forssman tetraglycosyl ceramide of hamster fibroblasts (116).

(III) Forssman glycolipid (117).

(IV) Glycolipid A^a of human RBC's (118).

(V) Glycolipid A^c of human RBC's (118).

(I) NANA-α2-Galβ1-3GalNAcα1-3-Ser(Thr)
|
NANAα2-

(II) GalNAcα1-3GalNAcβ1-3Galβ1-4Glcβ1-1'-Ceramide

(III) GalNAcα1-3GalNAcβ1-3Galα1-4Galβ1-4Glcβ1-1'-Ceramide

(IV) GalNAcα1-3Galβ1-4GlcNAcβ1-3Galβ1-4Glcβ1-1'-Ceramide
|
Fucα1-2

(V) GalNAcα1-3Galβ1-4GlcNAcβ1-6
|
Fucα1-2
\
Galβ1-4GlcNAcβ1-3Galβ1-4Glcβ1-1-Ceramide
/
GalNAcα1-3Galβ1-4GlcNAcβ1-3
|
Fucα1-2

STATEMENT OF THE PROBLEM

Most of the lysosomal storage diseases have been associated with a deficiency of one or another specific lysosomal hydrolase. For most of these enzymes little is known about the primary sequence, the lesion responsible for the lysosomal storage disease or the molecular mechanism of catalysis. Furthermore, our understanding of the biosynthesis of these enzymes is incomplete. This project was undertaken to characterize chemically the human α-galactosidases and to determine their kinetic properties. The specific goals of this project were as follows:

a) To purify α-galactosidases A and B from human liver and to determine enough of the primary sequence of each enzyme so that cDNA probes based upon the amino acid sequences could be synthesized and used by others to isolate and sequence the genes of both α-galactosidases.

b) To induce monospecific antibodies to -galactosidase A so that others could study the biosynthesis of α-galactosidase A.

c) To determine the kinetic parameters of both α-galactosidases and to synthesize a suicide inhibitor of one or both enzymes so that information pertinent to the mechanism of catalysis could be obtained.

These studies should lead to a better understanding of the structures and mechanisms of catalysis of both α-galactosidases, and provide a basis for future investigators to determine the entire structures of both enzymes. Conceivably this could lead to an effective treatment of Fabry's disease.

MATERIALS

Enzyme Assays

ethylenediamine	Eastman Kodak, Co. Rochester, NY
N-acetyl-D-galactosamine	Sigma Chemical Co. St. Louis, MO
4-MU-α-D-Galactoside	Sigma Chemical Co. St. Louis, MO
p-NP-α-GalNAc	Sigma Chemical Co. St. Louis, MO
Lactosylceramide $GbOse_3Cer$	Purified by John Burczak of this laboratory from bovine liver
Sodium taurocholate	Calbiochem San Diego, CA

Preparation of the Affinity Resin

6-aminohexanoic acid	Sigma Chemical Co. St. Louis, MO
ammonia, anhydrous	Matheson East Rutherford, NJ
benzylchloroformate	Aldrich Chemical Co., Inc. Milwaukee, WI
CNBr	Sigma Chemical Co. St. Louis, MO
D-galactose	Sigma Chemical Co. St. Louis, MO
hydrogen gas	Airco, Inc. Montvale, NJ
isobutyl chloroformate	Eastman Kodak, Co. Rochester, NY
Iatrobeads	Iatron Laboratories, Inc. Tokyo, Japan
methanol, anhydrous	reagent grade methanol refluxed over magnesium turnings and iodine then redistilled

Pd on activated charcoal	Aldrich Chemical, Co., Inc. Milwaukee, WI
Sepharose 4-B	Sigma Chemical Co. St. Louis, MO

Enzyme Purification

Ampholytes (pH 3 to 5)	Bio-Rad Laboratories Richmond, CA
concanavalin A-Sepharose	Sigma Chemical Co. St. Louis, MO
DE-52 (DEAE cellulose)	Whatman, Laboratory Products Inc. Clifton, NJ
human liver	autopsy specimens obtained through the courtesy of Dr. Kevin Cavanaugh at Ingham County Hospital and Dr. Harold Bowman at St. Lawrence Hospital
Hypatite C (Hydroxylapatite)	Clarkson Chemical Co., Inc. Williamsport, PA
α-methylmannoside	Sigma Chemical Co. St. Louis, MO
PMSF	Sigma Chemical Co. St. Louis, MO
Sephadex G-150	Pharmacia Fine Chemicals, Inc. Piscataway, NJ

Protein Derivitization and Peptide Generation andSeparation

μBondapak Phenyl column	Waters Associates Milford, MA
dithiothreitol	Boehringer Mannheim Biochemicals Indianapolis, IN
heptafluorobutyric acid	Aldrich Chemical Company, Inc. Milwaukee, WI
HPLC solvent filters, FHUP 04700 for organics, and HATF 04700 for water	Millipore Corp. Bedford, MA

HPLC solvents, water, acetonitrile, and isopropanol	Burdick and Jackson Laboratories, Inc. Muskegon, MI
iodoacetic acid	Sigma Chemical Co. St. Louis, MO
Sephadex G-50	Pharmacia Fine Chemicals, Inc. Piscataway, NJ
Synchropak RP-8 column 250 X 4.1 mm	SynChrom,Inc. Linden, IN
TPCK-trypsin	A generous gift from Dr. John Wilson of this department
4-vinyl pyridine	Aldrich Chemical Co., Inc. Milwaukee, WI

Antibody Induction-Polyclonal and Monoclonal

albino Swiss mice, females	Spartan Animal Services Michigan State University
aminopterin	Sigma Chemical Co. St. Louis, MO
DMEM	KC Biological, Inc. Lenexa, KS
Fetal Calf Serum	KC Biological, Inc. Lenexa, KS
Freund's Complete Adjuvant	Gibco Laboratories Grand Island, NY
Freund's Incomplete Adjuvant	Gibco Laboratories Grand, Island, NY
glutamine	KC Biological, Inc. Lenexa, KS
horse serum	Flow Laboratories, Inc. McClean, VA
hypoxanthine	Sigma Chemical Co. St. Louis, MO
NCTC 109	MA Bioproducts Bethesda, MD
Polyethylene Glycol 1000	Baker Chemical Co. Phillipsburg, NJ

penicillin	KC Biological, Inc. Lenexa, KS
Rabbit anti-mouse IgG	Miles Laboratories Elkhart, IN
SP2/0-Ag14 mouse myeloma cells	Cell Distribution Center of the Salk Institute LaJolla, CA
Staphylococcus aureus cells, heat killed	Kindly provided by Dr. William Smith of this department
thymidine	Signa Chemical Co. St. Louis, MO

Synthesis of Conduritol C Epoxide

conduritol B and conduritol B epoxide	Dr. Norman Radin Department of Biochemistry University of Michican
methyl red hydrochloride	J. T. Baker Chemical Co. Phillipsburg, NJ
m-chloroperoxybezoic acid	Aldrich Chemical Co., Inc. Milwaukee, WI

METHODS

Synthesis of the Affinity Ligand N-6-Aminohexanoyl-α-D-Galactopyranosylamine

The affinity ligand was synthesized according to the method of Harpaz and Flowers (109), who combined several well-known organic reactions to prepare an affinity ligand for the successful purification of coffee bean α-galactosidase. The synthesis is shown in Figure 6, which should be helpful in following the steps of the synthesis.

Synthesis of N-Benzyloxycarbonyl-6-Aminohexanoic Acid. The synthesis is that of Schwyzer et al. (120). The reaction mixture contained 0.02 moles of 6-aminohexanoic acid in 250 ml of 1.0 N NaOH, 0.25 moles of benzyloxycarbonyl chloride (Figure 6, Compound II) dissolved in 250 ml of diethyl ether, and 250 ml of 4 N NaOH. The solutions of aminohexanoic acid and 4 N NaOH were pre-cooled to 4^{o}, and the three solutions were combined with vigorous stirring over 15 minutes. The reaction mixture was stirred for an addtional hour at room temperature. The organic and aqueous phases separated, and the organic phase was removed. The aqueous phase was re-extracted three times with 250 ml of diethyl ether. The aqueous phase was acidified with 6 N HCl to pH 2.0 and kept overnight at

Figure 6. Synthesis of the Affinity Ligand.

The affinity ligand, N-6-Aminohexanoyl-α-D-galactopyranosylamine, was synthesized as described in the Methods section. The principal reactants and products are as follows:

I	6-Aminohexanoic acid
II	Benzylchloroformate
III	N-Benzyloxycarbonyl-6-aminohexanoic acid
IV	D-galactose
V	α-D-galactopyranosylamine ammonia complex
VI	Isobutyl chloroformate
VII	Mixed anhydride of III and VI
VIII	N-(N-Benzyloxycarbonyl-6-aminohexyl)-α-D-galactopyranosylamine
IX	N-6-Aminohexanoyl-α-D-galactopyranosylamine

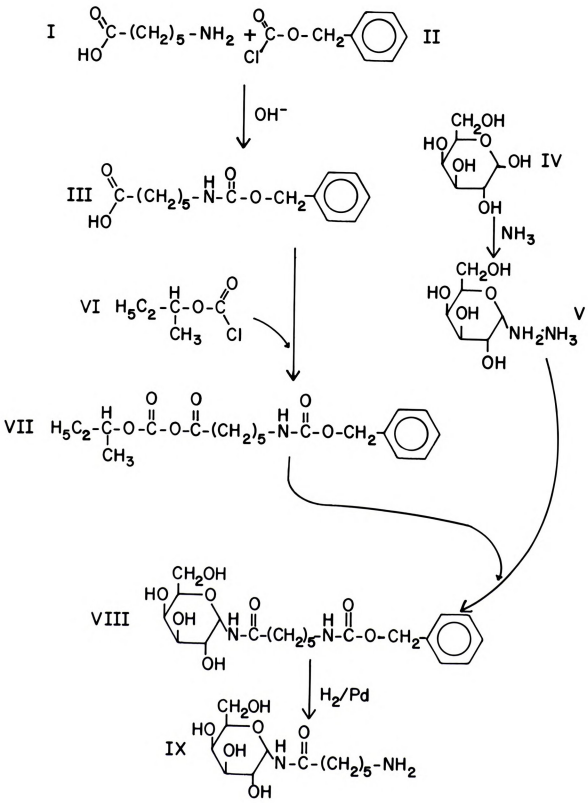
I
II
OH⁻
III
IV
NH₃
V
VI
VII
VIII
H₂/Pd
IX

4°. The white product was recrystallized twice from 25 ml of CCl_4, and its melting point was compared to the reported value of 54-55° (120).

Synthesis of α-Galactosylamine Ammonia Complex. The synthesis of Compound V (Figure 6) is that of Frusch and Isbell (121). The reaction conditions were anhydrous because α-galactosylamine, the principal reaction product, undergoes inversion of configuration to the ß-form in water. The reaction mixture contained 1.0 g of dessicated NH_4Cl and 39.6 g of dessicated D-galactose mixed with 200 ml of anhydrous methanol; this was not a solution as galactose is sparingly soluble in methanol. Anhydrous ammonia was bubbled into the reaction mixture, which was gently stirred for eight hours at room temperature. The product crystallized for four days at 4°. Approximately 10 g of product, one fourth of the reaction mixture, was filtered and recrystallized from 50 ml of 3% NH_4OH to which was added 200 ml of dry methanol saturated with ammonia. The product was recrystallized at 4° overnight. The product was reported to have a melting point of 95-96° (16), that of ß-galactosylamine is 136-137° (122). The identity of the product being α- rather than ß- was confirmed by ^{13}C-NMR spectroscopy. A ^{13}C-NMR spectrum of the product was recorded on a Bruker WP-60 Spectrometer by Dr. Hernan Nunez (as are all other ^{13}C-NMR spectra). The spectrum of ß-galactosylamine was obtained after the product had been dissolved in water for

thirty-four hours.

Synthesis of N-(N-Benzyloxycarbonyl-6-aminohexyl)-α-D-galactopyranosylamine. The reaction mixture contained 1.50 ml of isobutylchloroformate (Figure 6, Compound VI), 1.58 ml of triethylamine, and 3.06 g of N-benzyloxycarbonyl-6-aminohexanoic acid (Figure 6, Compound III) dissolved in 19 ml of dry DMF. The reaction mixture was stirred for 25 minutes at -5^{o}. The mixture was filtered, and to the filtrate (Figure 6, Compound VII) was added 942 mg of α-galactosylamine (Figure 6, Compound V) and an additional 19 ml of dry DMF. This latter mixture was stirred in a stoppered vessel overnight at 4^{o}. The solvents were then removed by rotary evaporation using a water bath heated to 60^{o}. The product (Figure 6, Compound VIII) was purified on a column of Iatrobeads (2.5 X 45 cm) eluted with chloroform-methanol-water (30:10:1, v/v/v), solvent A. Fractions were collected, and aliquots were spotted on silica gel G plates which were developed in solvent A and sprayed with orcinol reagent to detect the carbohydrate-containing material. The main product proved to be Compound VIII (Figure 6), and those fractions having the pure product were pooled and the solvents removed by rotary evaporation.

Synthesis of N-6-Aminohexanoyl-α-D-galactopyranosylamine. A vacuum flask containing 2.0 g of Compound VIII (Figure 6), 100 mg of Pd on charcoal, and 100 ml of 80% methanol was attached to both a water aspirator and a cylinder of

thirty-four hours.

Synthesis of N-(N-Benzyloxycarbonyl-6-aminohexyl)-α-D-galactopyranosylamine. The reaction mixture contained 1.50 ml of isobutylchloroformate (Figure 6, Compound VI), 1.58 ml of triethylamine, and 3.06 g of N-benzyloxycarbonyl-6-aminohexanoic acid (Figure 6, Compound III) dissolved in 19 ml of dry DMF. The reaction mixture was stirred for 25 minutes at -5°. The mixture was filtered, and to the filtrate (Figure 6, Compound VII) was added 942 mg of α-galactosylamine (Figure 6, Compound V) and an additional 19 ml of dry DMF. This latter mixture was stirred in a stoppered vessel overnight at 4°. The solvents were then removed by rotary evaporation using a water bath heated to 60°. The product (Figure 6, Compound VIII) was purified on a column of Iatrobeads (2.5 X 45 cm) eluted with chloroform-methanol-water (30:10:1, v/v/v), solvent A. Fractions were collected, and aliquots were spotted on silica gel G plates which were developed in solvent A and sprayed with orcinol reagent to detect the carbohydrate-containing material. The main product proved to be Compound VIII (Figure 6), and those fractions having the pure product were pooled and the solvents removed by rotary evaporation.

Synthesis of N-6-Aminohexanoyl-α-D-galactopyranosylamine. A vacuum flask containing 2.0 g of Compound VIII (Figure 6), 100 mg of Pd on charcoal, and 100 ml of 80% methanol was attached to both a water aspirator and a cylinder of

was dissolved in pure water and a catalyst of
87. 100 mg of Pd on C (5%, 11 500 DLC 1 of EtOH, methanol
A vacuum flask equipped with a
flapper of a Schlenk adapter. The
compound:

bule to avoid mass boiling and decomposition of the
Compound with IR:
ent. The mixture was
shaking with occasional
silica gel 0 petroleum ether/ether 9
five times more cautiously. Finally
chloride to
on a column of
oc. The product (1.1 g, 2
removed by drying
stopper, cooled
19 ml of dry DMF.
Hydrolysis: Weigh
filtrate (pink
mmoles at -5°. The mixture was
19 ml of dry DMF. The mixture
8-aminoquinoline
ml of triethylamine
ml of isobutylchloroformate
Sajtherapie

hydrogen gas. The vacuum flask was alternately evacuated and flushed with hydrogen gas at least twice to remove all the air from the flask. The hydrogen gas was let into the flask, and hydrogenolysis (123) proceeded for four and a half hours at room temperature and atmospheric pressure with stirring. The reaction mixture was filtered to remove the charcoal, and the methanol was removed by rotary evaporation. A ^{13}C-NMR spectrum indicated that the product (Figure 6, Compound IX) was pure. Coupled spectra (^{1}H-^{13}C) were made of α-galactosylamine, ß-galactosylamine, and the product to determine the coupling constant between the anomeric carbon and its proton which would indicate the anomerity of the product.

Coupling of the Affinity Ligand N-6-Aminohexanoyl-α-D-galactosylpyranosylamine to Sepharose 4B. The affinity ligand (Figure 6, Compound IX) was attached to Sepharose 4B by the method of March et al. (124). Approximately 50 ml of packed beads were washed with 500 ml of water and then activated by the addition of 7 g of CNBr dissolved in 5 ml of acetonitrile. The suspension of beads was stirred gently, kept between pH 11 and 12 by the addition of 5 N NaOH as needed, and the temperature was maintained at 20° by the addition of ice. The beads were then quickly vacuum filtered, washed with 300 ml of 0.2 M sodium phosphate, pH 9.5, and mixed with 100 ml of 0.2 M sodium phosphate, pH 9.5, containing 200 mg of the affinity ligand (Figure 6, Compound IX). This last reaction was kept at 23° for

about 5 minutes and then chilled to 4° by the addition of ice. Coupling of the ligand to the beads continued for two days at 4°. The affinity ligand attached to Sepharose 4B will be called the affinity resin.

Enzyme Assays

Enzyme Activity. One unit of enzyme is the amount of enzyme that hydrolyzes one μmol of substrate in one minute.

Assays Using Artificial Substrates

α-Galactosidase A plus B Activity. This is a modification of the procedure of Desnick et al. (125) that measures both enzymes, but it cannot be used to distinguish them. Up to 25 μl of enzyme was put into a 10 X 75 mm test tube and 150 μ l of 5.0 mM 4-MU-α-D-galactoside in Gomori Citrate-Phosphate pH 4.6 (126) was added to the enzyme. The enzyme and substrate were incubated at 37° for a minute or longer as they were previously at 4°, and the assay was begun by the addition of substrate. The reaction was carried out at 37° and was terminated by the addition of 2.35 ml of 0.1 M ethylenediamine. The fluorescence of the liberated 4-MU was determined in an Aminco J4-7439 which was calibrated with standard 4-MU.

α-Galactosidase A. This assay is based upon the fact that

α-galactosidase B is an α-N-acetylgalactosaminidase and is competitively inhibited by N-acetyl-D-galactosamine. The assay was performed exactly as the α-Gal A plus B assay except that the substrate also contained 58.3 mM N-acetyl-D-galactosamine in addition to the 4-MU-α-Gal. α-Galactosidase A was inhibited by less than five per cent under these conditions while α-galactosidase B was inhibited by over ninety-five per cent.

α-Galactosidase B. α-Galactosidase B was assayed by the method of Sung and Sweeley (127). Up to 50 µl of enzyme was mixed with 50 µl of 10 mM p-NP-α-GalNAc in 0.1 M Na Citrate pH 4.3. The enzyme and substrate were incubated at 37° for at least one minute as they were previously at 4°, and the reaction was begun by the addition of substrate to the enzyme. The reaction was carried out at 37° and terminated by the addition of 3.0 ml of saturated sodium tetraborate. The absorbance of the liberated p-nitrophenol was measured in a Gilford 2400 Spectrophotometer at 410 nm using p-nitrophenol as the standard.

Non-Quantitative Assay Using a Natural Substrate

To demonstrate that α-galactosidase A, but not α-galactosidase B, could hydrolyze $GbOse_3Cer$, both highly purified enzymes were reacted with bovine $GbOse_3Cer$

according to the method of Dean (128). Ten milliunits of each enzyme was added to 100 nmol of bovine $GbOse_3Cer$, 50 µg of sodium taurocholate, and 50 µl of Gomori Citrate-Phosphate pH 4.2. The reaction mixtures were incubated at 37^{o} for one hour when an additional 10 milliunits of the respective enzyme was added to each. The reactions proceeded for an additional hour and were terminated by boiling for one minute. The reaction mixtures were lyophilized, dissolved in chloroform-methanol 2:1, and an aliquot was spotted on a silica gel G plate. The TLC plate was developed in chloroform-methanol-water (65:25:4, v/v/v), sprayed with 0.5% orcinol in 4 N H_2SO_4, and heated to 100^{o} to visualize the carbohydrates. Standard sodium taurocholate, $GbOse_3Cer$, LacCer, the expected hydrolysis product, and a blank reaction mixture were also run on the TLC plate.

Purification of α-Galactosidases A and B from Human Liver

General Methods. α-Galactosidases A and B were purified from human liver by a combination of the procedures of Dean and Sweeley (104,105) and Bishop and Desnick (16). Approximately one kg of frozen human liver was thawed overnight in two volumes (w,v) of cold 1 mM PMSF. The liver was homogenized four times for 30 seconds at top speed in a Waring Commercial Blendor. The homogenate was filtered through cheesecloth to remove connective tissue

and then centrifuged at 16,000 X g in a Sorvall RC2-B for 30 minutes at 4^{o} (as are all steps in the enzyme purification unless otherwise noted). The pellets were re-extracted with two volumes of water, recentrifuged, and the supernatants assayed with 4-MU-α-Gal until 90% of the activity was solubilized. The supernatants were pooled, brought to 60% saturation with solid ammonium sulfate, and centrifuged at 16,000 X g for 30 minutes. The supernatants were discarded, and the precipitates were resuspended in 500 ml of distilled water. This solution was dialyzed versus ten liters of 10 mM sodium phosphate pH 6.5 (buffer A) with two changes of buffer. The dialysate was centrifuged at 16,000 X g for 30 minutes to remove protein that precipitated during dialysis, and the pellets were discarded.

The α-galactosidases were extracted from the supernatant by stirring with 100 ml of Concanavalin A-Sepharose for one hour at room temperature. The solution was re-extracted until greater then 90% of the -galactosidases had been removed. The beads were removed from this solution by filtration using a Buchner funnel with a nylon mesh filter. The filtered beads were washed with about 50 ml of buffer A, packed in a column (2 X 20 cm), and eluted with 0.1 M α-methylmannoside in buffer A until all the enzyme, which was yellow, had been eluted.

The Concanavalin A extract was then applied to a DE-52 column (4.2 X 11 cm) that had been pre-equilibrated with

buffer A. The column was washed with 200 ml of buffer A to remove nonbinding proteins. The α-galactosidases were eluted with a linear NaCl gradient (4 liters total, 0 to 300 mM) in buffer A. Fractions were collected and assayed with both 4-MU-α-Gal, 4-MU-α-Gal with GalNAc, and p-NP-α-GalNAc. Fractions containing only α-galactosidase A were pooled, and those containing both A and B were pooled. The two fractions were separately concentrated in an Amicon Model 52 using a PM 10 membrane to about 20 ml. The enzymes were then applied to a Sephadex G-150 column (3.5 X 110 cm) and eluted with buffer A at a flow rate of approximately 20 ml/hour to maximize protein separation. Fractions were collected, assayed with 4-MU-α-Gal, and the A_{280} determined. Fractions having more than 100 milliunits/ml were pooled and concentrated to about 1.0 units/ml of α-Gal A and 5.0 units/ml of α-Gal B.

Affinity Chromatography of α-Galactosidase A. The α-galactosidase A from the G-150 step was diluted with one-half its volume with 0.15 M NaCl in Gomori Citrate-Phosphate pH 4.6 (buffer B) and acidified with dilute HCl to pH 5.0. The enzyme mixture was centrifuged for 1 minute at 12,000 X g in a Brinkman Eppendorf Centrifuge Model 5412, and the supernatant fraction was applied to a column of N-6-Aminohexanoyl-α-galactopyranosylamine-Sepharose (0.75 X 10 cm). Fractions of 2 ml were collected. The non-binding proteins

were eluted with buffer C (buffer B adjusted to pH 5.0) until the A_{280} was zero, after which a linear pH and salt gradient was begun from buffer C to 0.5 M NaCl in Gomori Citrate-Phosphate pH 6.0 (buffer D, 20 ml of each). The gradient was stopped at pH 5.6, and the α-galactosidase A was eluted with 0.4 M galactose in buffer D. The fractions were assayed with 4-MU-α-Gal. The most active fractions were pooled and dialyzed versus either buffer A or Gomori Citrate-Phosphate pH 6.0. The purity of the enzyme was determined by SDS polyacrylamide gel electrophoresis. Impurities were removed by either gel filtration on the 3.5 X 110 cm Sephadex G-150 column or rechromatographing on the affinity resin.

Dual Affinity Chromatography of α-Galactosidase B. The pooled enzyme from the G-150 step containing both α-galactosidase A and B was diluted with half its volume of buffer B and adjusted to pH 4.7 with dilute HCl. Solid GalNAc was added to the enzyme to make the solution 50 mM in GalNAc. The enzyme mixture was then applied to the affinity column (0.75 X 10 cm) that had been pre-equilibrated with 50 mM GalNAc in buffer B. Fractions of 2 ml were collected. The non-binding proteins were eluted with buffer B until the A_{280} was zero. The pH-salt gradient as for the α-galactosidase A was begun, and the α-galactosidase A was eluted with 0.4 M galactose in buffer C. The GalNAc eluted fractions were assayed with

4-MU-α-Gal. The active fractions were pooled, concentrated to less than 10 ml, and dialyzed versus buffer A to remove the GalNAc. The enzyme was acidified to pH 4.7 with dilute HCl, centrifuged to remove precipitated proteins, and reapplied to the affinity column that had been pre-equilibrated with buffer B. The column was eluted with buffer B, and fractions of 2 ml were collected. The A_{280} and the α-galactosidase activity of the fractions were closely monitored. Since α-galactosidase B does not tightly bind to this affinity ligand, not all of the contaminating proteins can be washed from the column before the enzyme is eluted. One must exercise judgment when deciding to elute the α-galactosidase B. The enzyme should be eluted after the bulk of non-absorbing proteins have passed through the column and while the amount of α-galactosidase B that has non-specifically eluted is small. The α-galactosidase B was eluted with 0.4 M galactose in buffer B. The fractions were assayed with 4-MU-α-Gal. The most active fractions were pooled and dialyzed versus either buffer A or Gomori Citrate-Phosphate, pH 6.0. The purity of the enzyme was determined by SDS gel electrophoresis.

Gel Electrophoresis. Denaturing polyacrylamide gel electrophoresis was performed according to the method of Laemmli (129). Protein bands were generally visualized by staining with Coomassie Brilliant Blue R, but were stained

with alkaline silver reagent (130) when the amount of protein was small as in assessing the purity of individual fractions eluted from the affinity resin.

Protein Determination. Protein concentration was determined in a number of ways: The Lowry method (131) with BSA as a standard, a modified Lowry (132) using BSA as a standard, with fluorescamine (133), and determining the A_{280} in a Gilford 2400 Spectrophotometer. The last three methods were used when either the protein concentration or sample size was low.

Carboxymethylation. The α-galactosidases were carboxymethylated by the method of Gracy (134). The lyophilized proteins were dissolved at a concentration of 0.5 mg/ml in a solution containing 0.5 M Tris hydrochloride, 25 mM EDTA, 6 M guanidine hydrochloride, and 8 mM 2-mercaptoethanol adjusted to pH 8.5. The mixture was flushed with N_2 to remove oxygen and stirred for one hour at room temperature. Ten microliters of iodoacetic acid (10 mg/ml) were added per 100 µg of protein being carboxymethylated. The mixture was flushed with N_2, and the carboxymethylation continued for twenty minutes in the dark. The carboxymethylation was terminated by the addition of 10 µl of 2-mercaptoethanol per 100 µg of protein. The protein solution was desalted by dialysis in the dark or by gel filtration on Sephadex G-50.

Pyridethylation. The α-galactosidases were pyridethylated by the method of Hermodson et al. (135). The proteins were

dissolved at up to 30 mg/ml in a solution containing 6.0 M guanidine hydrochloride, 0.13 M Tris, and 0.10 mg/ml EDTA adjusted to pH 7.5. A twenty-fold molar excess of DTT relative to protein sulfhydryl content, which was assumed to be five per cent of the residues of the proteins, was added and the mixture was stirred for three hours at room temperature. A three-fold molar excess of 4-vinylpyridine relative to DTT was then added and the solution was stirred for an additional ninety minutes. Alkylation was terminated by acidification of the protein solution to pH 2.0 with 88% formic acid. The protein solutions were desalted by either dialysis or gel filtration on Sephadex G-50.

Trypsin Digestion. The alkylated α-galactosidases were suspended in either 1% NH_4OH or 10 mM sodium phosphate, pH 7.0, at a concentration of 2 to 5 mg/ml, and TPCK-trypsin was added at a ratio of 50:1 (w,w of protein, trypsin). The α-galactosidases were digested at room temperature for 10 hours. The digestion was terminated either by freezing or lyophilization.

Separation of Peptides by HPLC. All peptide separations were performed using a Beckman 112 Solvent Delivery System connected to an Altex 210 Sample Injecter and a Beckman 160 Absorbance Detector which was connected to an Isco-strip chart recorder. The detector was set at 229 nm by using a Beckman 229 filter and a Cadmium lamp. The flow rate for all separations was 1.0 ml/minute. HPLC grade solvents

were used, and the solvents were vacuum-filtered to remove any particles and to de-gas the solvents. The aqueous solvents were filtered with an HATF 04700 filter, and the organic solvents were filtered with an FHUP 04700 filter.

TFA was added to the tryptic digest to give a 1% solution which was injected onto the RP-8 column. The primary separation utilized a solvent system of H_2O to CH_3CN/2-propanol (3:1, v/v) with 0.1% TFA throughout (136). The tryptic peptides were separated by starting with water and having a linear gradient of the organic phase which increased at one per cent per minute. The eluate corresponding to peaks on the chromatogram were collected, and the solvents were removed under a water aspirator vacuum, but not lyophilized. The peptides were generally rechromatographed prior to N-terminal sequencing. The peptides were initially redissolved in 0.1% TFA in either water or the organic phase used in the primary separation, but neither of these solvents were very effective. The best system was to dissolve the peptide in a small volume of 6 M guanidine HCl which was diluted to less than 0.5 M guanidine with 0.1% TFA in water prior to injection. Two systems were used for rechromatographing the peptides: The first was exactly like the primary separation except that 0.1% HFBA replaced TFA and there was an increase of the organic phase of 2% per minute. The other system was also like the primary separation except that a μBondapak Phenyl column was used and there was an

increase of the organic phase of 2% per minute.

Antibody Production

Polyclonal. Purified human liver α-galactosidase A was injected at several sites on the back of each of two rabbits. The first injection contained 20 μg of enzyme in an emulsion of Freund's Complete Adjuvant. The booster injections on days 14 and 28 contained 10 μg of enzyme in Freund's Incomplete Adjuvant. The rabbits were bled on day 42. The specificity of the antibodies was determined by Dr. Norman C. LeDonne Jr. of this laboratory by immunoprecipitating [2-^{3}H]-Mannose labelled α-galactosidase A from Chang liver cells (31).

Monoclonal. Monoclonal antibodies to human liver α-galactosidase A were induced in mice by a variation of the method of Galfre et al. (137). Female Swiss white mice were injected i.p. with 10 μg of partially purified α-galactosidase A (approximately 450 munits) emulsified with Freund's Complete Adjuvant. The first booster injection was two weeks later with 10 μg of enzyme in Freund's Incomplete Adjuvant. The second booster was like the first booster and followed it by at least two weeks. Three days after the second booster injection the mouse was sacrificed by cervical dislocation. Blood from a heart puncture was saved for determination of anti-α-

galactosidase A antibodies. The spleen was aseptically removed, washed with DMEM containing 20 mM HEPES, then cut, and teased into a single cell suspension. The cells were centrifuged at 1000 X g for 10 minutes at room temperature (all subsequent steps are at room temperature unless otherwise noted). The RBC's were lysed by gently resuspending the cell pellet in 5 ml of 0.2% NaCl for 30 seconds, then mixed with 5 ml of 1.6% NaCl and then with 10 ml of DMEM with HEPES. The cells were recentrifuged for 10 minutes at 1000 X g, resuspended in DMEM with HEPES, and an aliquot was counted in a hemocytometer to determine cell number.

Approximately 1-5 X 10^7 mouse spleen cells were mixed with 1-5 X 10^6 (a 10:1 mixture) hypoxanthine guanine phosphoribosyl transferase-negative SP2/0-Ag14 mouse myeloma cells. The SP-2 cells had been grown in 10% FCS in DMEM containing 100 µ g/ml of both penicillin and streptomycin at 37^o in a 7% CO_2-water saturated atmosphere. The mixture of cells was centrifuged at 1000 X g for 10 minutes, the supernatant removed, and 1.0 ml of fusion medium, PEG, DMSO, DMEM, (7:1:12, w/v/v), was added at 37^o. The cell pellet was gently disrupted and mixed with the tube in the palm of the hand to keep the fusion warm for one minute. One ml of DMEM with HEPES was added and mixed gently for one minute, after which 2 ml of DMEM with HEPES were added and mixed for one minute. Four ml of HT medium [DMEM containing 10% (v,v) FCS, 10% (v,v) horse

serum, 10% (v,v) NCTC 109 media, 2 mM glutamine, 100 μM hypoxanthine, 16 μM thymidine, 3 μM glycine, 100 mg/l penicillin, and 100 mg/l streptomycin] were added and mixed for 3 minutes, then 8 ml of HT media were added and mixed for an additional 3 minutes. The fusion mixture was centrifuged at 500 X g for 10 minutes. The cell pellet was resuspended in 50 ml of HT media, and 0.1 ml were added to the wells of five 96-well Costar plates.

The plates were incubated at 37° in a 7% CO_2-water saturated atmosphere. After two days 0.1 ml of HAT media (HT media containing 1.0 μM aminopterin) was added to each well. This media was removed two days later when an additional 0.1 ml of HAT media was added. The hybridoma cells were grown until the media became acidic (yellow), and an aliquot was pipetted into a 10 X 75 mm dispo tube to test for anti α-Gal A antibodies.

Heat-killed Staphylococcus aureus cells were washed 3 times with one volume of 0.1 M sodium phosphate, pH 8.0 (buffer E), containing 0.5% Triton X-100 and 10 mg/ml BSA. The S. aureus was resuspended in one volume of buffer E. Rabbit anti-mouse IgG (Miles) was added to the washed S. aureus (1:20, v/v), and it was bound by incubating at 37° for 5 minutes. The mixture was centrifuged and resuspended in one volume of buffer E. 100 μl of the S. aureus rabbit anti-mouse IgG complex was added to the media from each of the clones and incubated for 5 minutes at 37°. The tubes were centrifuged, and the supernatants were removed.

Approximately 1 milliunit of partially purified α-galactosidase A in Gomori Citrate-Phosphate pH 6.0 was added to the pellet which was vortexed, incubated at 37° for 10 minutes, centrifuged, and the supernatant removed. The pellet containing the S. aureus-rabbit anti-mouse mouse anti-human liver α-Gal A antibody was resuspended in 25 µl of Gomori Citrate-Phospate pH 4.6 and assayed with 4-MU-α-Gal. Pre-immune and immune mouse sera were used for negative and positive controls, respectively.

Synthesis of Conduritol C Epoxide

Conduritol C tetraacetate was synthesized by the procedure of Stegelmeier (138) and converted to conduritol C epoxide by the method of Radin and Vunnam (139). Mr. James Grove and Dr. Fumito Matsuura of this laboratory performed the first four steps of the synthesis; I performed the last three steps. Refer to Figure 7 for details of the synthesis.

Synthesis of 5,6-dibromo-2-cyclohexene-1,4-dione. The reaction mixture contained 43.2 g of benzoquinone dissolved in 600 ml of ice cold CCl_4 to which was added over a period of 30 minutes 20 ml of Br_2 in 600 ml of CCl_4 with stirring. The reaction continued for 30 minutes at 4° when 100 g of sodium sulfate was added with stirring. The reaction mixture was filtered, and warmed to room

Procedure

Add 1.0 mL of 0.1 M $AgNO_3$ to 50 mL of 0.1 M KBr in a 125 mL Erlenmeyer flask. Add 1 mL of 6 M HNO_3 and 2 mL of saturated $Fe(NO_3)_3$ indicator. Titrate with 0.1 M KSCN to the first permanent reddish-brown color. Record the volume of KSCN used. Repeat with a second 50 mL portion of KBr solution.

Calculations

Moles of $AgNO_3$ added = $0.1000 \times 0.0100 = 1.00 \times 10^{-3}$ mol

Moles of KSCN used = $0.1000 \times 0.0042 = 4.2 \times 10^{-4}$ mol

Moles of KBr = $1.00 \times 10^{-3} - 4.2 \times 10^{-4} = 5.8 \times 10^{-4}$ mol

Mass of KBr = $5.8 \times 10^{-4} \times 119.00 = 0.069$ g

Percent KBr = $\frac{0.069}{0.1000} \times 100 = 69\%$

Discussion

The Volhard method is specific for bromide and iodide because $AgBr$ and AgI are less soluble than $AgSCN$. Chloride must be removed or the titration will overestimate the halide content. Nitrobenzene is sometimes added to coat the $AgCl$ precipitate and prevent it from reacting with thiocyanate.

Figure 7. Synthesis of Conduritol C Epoxide.

Conduritol C Epoxide was synthesized as described in the Methods section, and the reactions of the synthesis are illustrated here. The principal reactants and products are as follows:

I	Benzoquinone
II	5,6-dibromo-2-cyclohexene-1,4-dione
III	5c,6t-dibromo-2-cyclohexene-1r,4t-diol
IV	1r,4t-diacetoxy-2t,3c-dibromo-5-cyclohexene
V	1r,2c,3c,4t-tetraacetoxy-5c,6t-dibromo-cyclohexane
VI	Conduritol C Tetraacetate
VII	Conduritol C
VIII	Conduritol C Epoxide

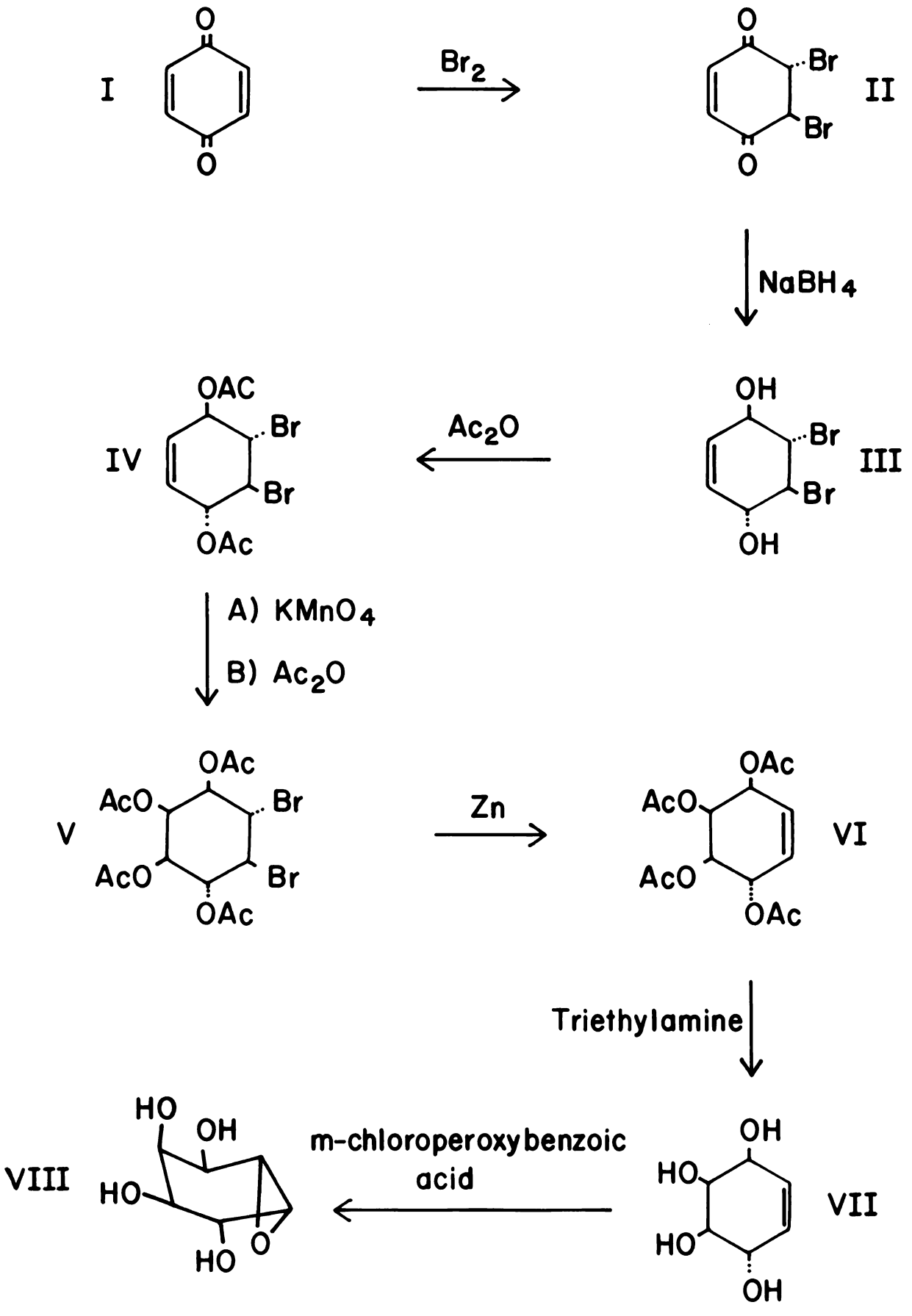
I
Br_2
II
$NaBH_4$
III
Ac_2O
IV
A) $KMnO_4$
B) Ac_2O
V
Zn
VI
Triethylamine
VII
m-chloroperoxybenzoic acid
VIII

temperature. The crystals were dissolved by the addition of 500 ml of CCl_4, and the excess Br_2 was extracted with 1.5 l of water. The solvents were removed by rotary evaporation, and the product (Figure 7, Compound II) was recrystallized four times from CCl_4. The product was analyzed by infrared and mass spectrometry.

Synthesis of 5c,6t-dibromo-2-cyclohexene-1r,4t-diol. The reaction mixture contained 26.8 g of Compound II (Figure 7) dissolved in 600 ml of diethyl ether to which was slowly added 9.5 g of sodium borohydride dissolved in 150 ml of water. The reaction proceeded for 140 minutes until the solution became almost colorless. The reaction mixture was transferred to a separatory funnel, and the ether phase was removed. The aqueous phase was extracted three times with 100 ml of diethyl ether. Solid sodium sulfate was added to the combined ether phases, which were then filtered, and the filtrate was evaporated by rotary evaporation. The product was recrystallized from acetone-pentane (2:1, v/v) and analyzed by infrared and mass spectrometry.

Synthesis of 1r,4t-diacetoxy-2t,3c-dibromo-5-cyclohexene. The reaction mixture contained 15.4 g of Compound III (Figure 7) dissolved in 150 ml of pyridine to which was added 150 ml of acetic anhydride with stirring on an ice bath. The reaction was stirred overnight at room temperature, and 300 ml of ice water was then added with stirring. The mixture was transferred to a separatory funnel and extracted three times with 200 ml of $CHCl_3$.

The $CHCl_3$ extracts were pooled and washed three times with 100 ml of each of the following in order: 6 N HCl, saturated sodium bicarbonate, and water. Solid anhydrous sodium sulfate was added to the $CHCl_3$ layer, which was then filtered and the solvents removed by rotary evaporation. The oily product was dissolved in 150 ml of ethanol which was allowed to stand for three days at room temperature. Crystals developed which were collected by filtering. The filtrate was concentrated to 50 ml by rotary evaporation and allowed to stand at room temperature for additional crystallization. The crystals were washed with cold ethanol. This entire procedure was repeated with 14.6 g of Compound III (Figure 7). The product was analyzed by infrared and mass spectrometry.

Synthesis of 1r,2c,3c,4t-tetraacetoxy-5c,6t-dibromo cyclohexane. The reaction mixture contained 3.65 g of Compound IV (Figure 7) dissolved in 125 ml of absolute ethanol to which was added 3 g of $MgSO_4$ in 20 ml of water. This solution was cooled on an ice bath, and 3.2 g of $KMnO_4$ in 200 ml of water was added dropwise over a period of three hours with stirring at 4^o. After 90 minutes an additional 3 g of $MgSO_4$ in 20 ml of water and 125 ml of absolute ethanol, both of which were pre-cooled, were added to the reaction mixture. The reaction continued an additional 3 hours when 100 g of activated charcoal were added, and the reaction continued overnight at 4^o. The mixture was then filtered and the activated charcoal was

The procedure was repeated with a fresh portion of the same sample, this time using 0.0200 M $KMnO_4$ in 2.0 M H_2SO_4 as the titrant. The initial volume of the sample was 50.00 mL, and the titration was carried out at room temperature (approximately 25 °C). The first endpoint was observed after the addition of 18.45 mL of titrant, and the second endpoint after a total of 36.90 mL. The difference between the two endpoints, 18.45 mL, corresponds to the oxalate content. Because the stoichiometry of the reaction between permanganate and oxalate is 2:5, the amount of oxalate is calculated from the permanganate volume using the factor 5/2. The mean of the two determinations was used in all subsequent calculations.

Blank titrations were also performed to correct for the small amount of reductant present in the reagents and water. Three blanks were run, each containing 50.00 mL of deionized water and 5 mL of 2.0 M H_2SO_4, titrated to the same endpoint color. The mean blank volume was 0.12 mL, with a standard deviation of 0.03 mL. This blank was subtracted from every sample titration before any further calculation was carried out.

Replicate analyses were carried out on three separate aliquots of the same stock solution, each aliquot being 50.00 mL measured with a volumetric pipette. The relative standard deviation of the corrected titrant volumes was 0.8%, which is consistent with the precision expected for a manual endpoint detection by visual color change. No outliers were rejected by the Q-test at the 95% confidence level.

Spike recovery experiments were carried out by adding a known mass of sodium oxalate to a second aliquot of the sample before titration. The spike was prepared by dissolving 0.1000 g of primary standard $Na_2C_2O_4$ in 100.0 mL of deionized water, and 5.00 mL of this solution was added to 50.00 mL of the sample. The recovered oxalate corresponded to 99.4% of the added amount, indicating that no significant loss or interference occurs under the conditions used.

The ionic strength of the titration medium was estimated to be approximately 0.5 M, dominated by the sulfuric acid and the sodium and potassium ions introduced with the sample. Activity coefficients were not applied, since the concentrations of the analyte and titrant are low relative to the ionic strength and the correction would be smaller than the precision of the method.

Temperature was recorded at the start and end of each titration. The solution warmed by about 2 °C during the titration because of the heat of reaction, and the titrant was standardized at the mean temperature. Titrations carried out at 20 °C and at 30 °C showed that the endpoint volume changes by less than 0.1% over this range, so temperature control is not critical for routine work.

For additional characterization, the sample was also examined by infrared spectroscopy. A small portion was dried at 110 °C for 2 h and mixed with potassium bromide. The spectrum was recorded from 4000 to 400 cm^{-1}. The carboxylate bands appear at 1615 and 1315 cm^{-1}, and the absence of a broad band above 3200 cm^{-1} indicates that the material is anhydrous. This spectrum is used as a reference for identity checks on subsequent batches.

washed three times with 20 ml of ethanol. The ethanol washings and the filtrate were combined, and the solvents were removed by rotary evaporation. The intermediate product was dried overnight over P_2O_5. Acetylation of this intermediate was performed as in the conversion of Compound III to IV in Figure 7 with crystallization of the product performed at 4°. The product was analyzed by an infrared spectrum, mass spectrometry, and by comparing its melting point to the literature value of 144° (138).

Synthesis of Conduritol C Tetraacetate. The reaction mixture contained 1.5 g of Compound V (Figure 7) dissolved in 70 ml of diethyl ether, 3.0 g of powdered zinc, and 3.0 ml of glacial acetic acid. The reaction mixture was stirred for four hours at room temperature. The mixture was filtered, the zinc was washed with 40 ml of diethyl ether, and the ether washings were pooled. The ether fraction was washed once with 50 ml of saturated sodium bicarbonate, dried over sodium sulfate in a vacuum dessicator, and the ether removed by rotary evaporation. The product was identified by obtaining an infrared spectrum, a mass spectrum, and a melting point which was compared to the reported value of $91-92^{\circ}$ (143).

Synthesis of Conduritol C . The reaction mixture contained 600 mg of Compound VI (Figure 7) dissolved in 30 ml of methanol-water (7:3, v/v) and 2.12 ml of triethylamine. The reaction was stirred overnight at room temperature, and the solvents were then removed by rotary evaporation. The

reaction was repeated until the melting point of the product was the same as the literature value of 148-151° (140). The removal of acetyl groups was also monitored by low resolution ^{1}H-NMR spectra which were made by Mr. Royal Truman of the MSU Department of Chemistry on a Varian T-60 NMR Spectrometer. The identity of the product was also confirmed by a mass spectrum of the TMS derivative and an infrared spectrum, which were compared to the respective spectra of conduritol B. The purity of the product was determined by gas chromatography of the TMS derivative (144). The GC was a Hewlett-Packard 5840 A Gas Chromatograph with a six foot long 3% SE-30 column. The GC was programmed for a linear increase in temperature of 2° per minute starting at 140°. In order to determine the stereochemistry of the product, high resolution coupled and decoupled ^{1}H-NMR spectra of the product were made by Dr. Klaas Hallenga and associates of the M.S.U. Department of Chemistry on a Bruker WM-250 Spectrometer.

Synthesis of Conduritol C Epoxide. The reaction mixture contained 121 mg of Compound VII (Figure 7) and 221 mg of m-chloroperoxybenzoic acid suspended in 15 ml of methanol. The suspension was stirred for five days at room temperature. The solvents were removed by rotary evaporation, and the chloro-compounds were extracted from the flask with 10 ml of diethyl ether. The product was applied to an Iatrobeads column (2 X 23 cm) and eluted with ethanol-ethyl acetate-water (2:8:1, v/v/v), solvent B.

Fractions containing the epoxide were identified by spotting an aliquot on a Fisher Redi-Plate, developing the plate in solvent B, and spraying the plate with methyl red reagent (141). Those fractions having only the principal product were pooled and the solvents removed. The conduritol C epoxide was recrystallized from 1 ml of methanol with 5 ml of absolute ethanol at -80^{o}. The purity of the product was determined by gas chromatography of the TMS derivative as described above for conduritol C. The identity of the product was established by comparing its melting point to the literature values of $135-137^{o}$ (140) and 145^{o} (142), a mass spectrum of the TMS derivative which was compared with the TMS derivative of conduritol B epoxide, and by inhibition of pure human liver α-galactosidase A. The stereochemistry of the product was determined by high resolution ^{1}H-NMR as described above for conduritol C.

Purification of Commercially Tritiated Conduritol C Epoxide. A sample of 112 mg of conduritol C epoxide was labelled by the Wilzbach method with tritium gas by the Amersham Corp. The solvents were removed under a stream of nitrogen. The product was suspended in solvent B and applied to a column of Iatrobeads (2 X 20 cm) and eluted with solvent B. Aliquots of the fractions were counted for radioactivity as well as checked for epoxide as described above. The radioactive fractions that also contained the

Fractions containing the epoxide were identified by spotting an aliquot on a Fisher Redi-Plate, developing the plate in solvent B, and spraying the plate with methyl red reagent (141). Those fractions having only the principal product were pooled and the solvents removed. The conduritol C epoxide was recrystallized from 1 ml of methanol with 5 ml of absolute ethanol at -80^{o}. The purity of the product was determined by gas chromatography of the TMS derivative as described above for conduritol C. The identity of the product was established by comparing its melting point to the literature values of $135-137^{o}$ (140) and 145^{o} (142), a mass spectrum of the TMS derivative which was compared with the TMS derivative of conduritol B epoxide, and by inhibition of pure human liver α-galactosidase A. The stereochemistry of the product was determined by high resolution ^{1}H-NMR as described above for conduritol C.

Purification of Commercially Tritiated Conduritol C Epoxide. A sample of 112 mg of conduritol C epoxide was labelled by the Wilzbach method with tritium gas by the Amersham Corp. The solvents were removed under a stream of nitrogen. The product was suspended in solvent B and applied to a column of Iatrobeads (2 X 20 cm) and eluted with solvent B. Aliquots of the fractions were counted for radioactivity as well as checked for epoxide as described above. The radioactive fractions that also contained the

epoxide were pooled, and the solvents were removed under a stream of nitrogen. The material was then dissolved in water, applied to a G-25 column (1 X 115 cm), and eluted with water. Fractions were collected and assessed for both radioactivity and epoxide. The radio-chemical purity of the material was assessed by TLC using unlabelled CCE as a standard and scanning the TLC plate with a Berthold LB 2760 TLC Scanner. The approximate concentration of the ^{3}H-CCE was determined by chromatographing an aliquot of the material along with known amounts of unlabelled CCE on TLC and spraying with methyl red reagent. The specific radioactivity was determined by counting an aliquot of the material by scintillatiion counting.

Weekend of site installation troubles

Labor day fix deployment broke staging. The on-call engineer had to roll back the entire release at midnight. Customer reported that the dashboard showed stale data for hours. Root cause: a missing migration in the deploy script. Lesson learned: always run migrations before restarting the app server.

Slept on the floor of the server room. Power outage during the storm. Generator kicked in after twelve minutes. Lost two hard drives in the array. Rebuild took the rest of the night. Coffee was the only thing keeping anyone upright.

Fire drill. The whole team evacuated the building. Alarm went off at 2:47 PM. Nobody knew if it was real or a test. Turned out to be a burnt toaster in the breakroom. Cost us an hour of productivity.

Migration failed halfway through. Rollback script also failed. Had to restore from backup. Lost about 30 minutes of transactions. Customers were not happy. Apologized and issued credits.

RESULTS

Synthesis of the Affinity Ligand. The synthesis of the affinity ligand (Figure 6, Compound IX) was straight-forward as all the reactions were facile. The melting point of synthetic N-benzyloxycarbonyl-6-amino hexanoic acid (Figure 6, Compound III) was 53.5-54.5^{o} compared to the literature value of 54-55^{o} (119). The melting point of the α-galactosylamine-ammonia complex (Figure 6, Compound V) was 94-98^{o} compared to the literature value of 95-96^{o} (16); the reported melting point of ß-galactosylamine is 136-137^{o} (122). Neither the melting points nor spectra of the other intermediates in the synthesis of the affinity ligand were available to verify the identity of the respective compounds. However, the N-(N-benzyloxycarbonyl-6-aminohexyl)-α-D -galactopyranosylamine Compound VIII (Figure 6) had a migration on thin-layer chromatography, relative to the minor products, that was similar to that found by Bishop and Desnick (16). The purity of the affinity ligand Compound IX (Figure 6), was determined by ^{13}C-NMR spectroscopy (Figure 8). There were twelve peaks, as expected in the spectrum; peaks 2 through 7 were from the sugar, the others were from the spacer arm derived from 6-aminohexanoic acid. The ^{13}C-NMR spectra of α- and ß-galactosylamine were also obtained (Figure 9) and

Figure 8. ^{13}C-NMR spectrum of the affinity ligand

The affinity ligand was dissolved at a concentration of 200 mg in 3 ml of water, and a ^{13}C-NMR spectrum of the sample was made in a Bruker WP-60 Spectrometer by Dr. Hernan Nunez as are all other ^{13}C-NMR spectra. The spectrum is a compilation of 54,955 scans. The chemical shifts in ppm of the principal peaks are:

1	180.39
2	78.34
3	73.53
4	71.00
5	70.51
6	67.89
7	62.78
8	41.44
9	36.87
10	30.11
11	26.71
12	26.27

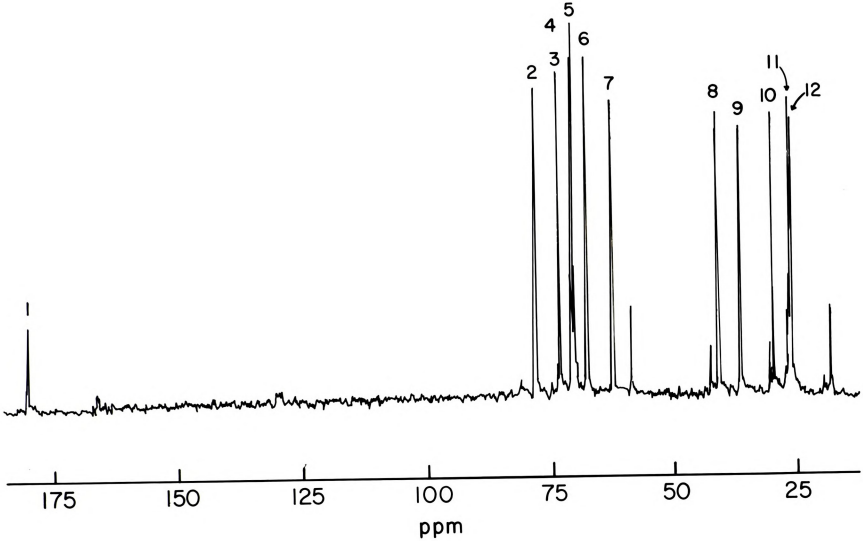
1
2
3
4
5
6
7
8
9
10
11
12
175
150
125
100
75
50
25
ppm

Figure 9. ^{13}C-NMR spectra of α- and β-Galactosylamine.

Panel A. α-Galactosylamine, synthesized as described in the Methods section, was dissolved at 100 mg/ml in water, and the spectrum was made. This spectrum was a compilation of 257 scans. The chemical shifts in ppm of the major peaks are:

1 82.96
2 71.44
3 70.80
4 70.66
5 69.54
6 62.73

Panel B. The above sample of α-galactosylamine was scanned for 34 hours starting two hours after the sample was dissolved in water. α-Galactactosylamine has been reported to undergo inversion of configuration to the β-form shortly after dissolving in water (121). Peaks X and Y have the same chemical shifts as listed above for peaks 1 and 5 of α-galactosylamine. The spectrum was a compilation of 86,315 scans. The chemical shifts in ppm of the major peaks are:

1 87.24
2 77.61
3 75.18
4 73.82
5 70.66
6 62.83

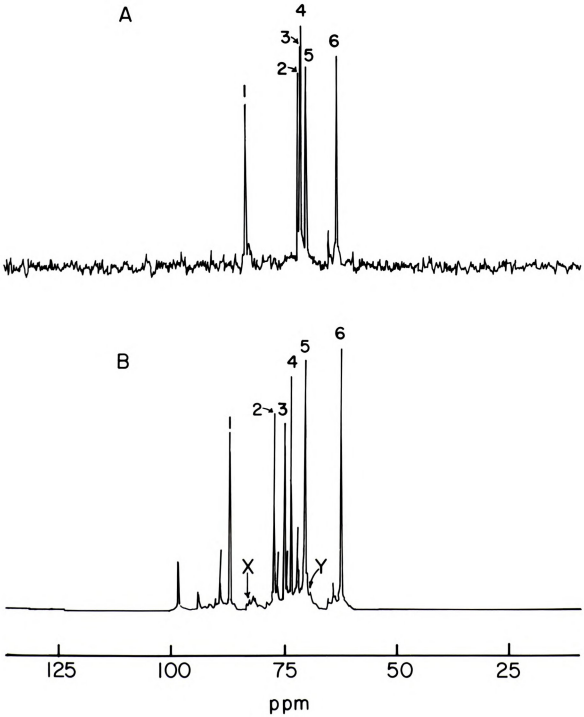
A
4
3
5
6
2
1
B
6
5
4
2
3
1
X
Y
125
100
75
50
25
ppm

Figure 10. Coupled spectra (^{1}H-^{13}C) of the affinity ligand and the galactosylamines

Panel A. 200 mg of the affinity ligand were dissolved in 3 ml of water. The spectrum is a compilation of 18,541 scans. The coupling constant of the anomeric carbon and its hydrogen was found to be 164.2 Hz, and the chemical shift of the anomeric carbon was 78.24 ppm. The chemical shifts in ppm of some of the principal peaks are:

1 83.7
2 75.5
3 72.8
4 68.6
5 65.6
6 62.8
7 26.4

Panel B. Synthetic α-galactosylamine was dissolved in water. The spectrum is a compilation of 16,755 scans and lasted seven hours so that most of the α-galactosylamine had undergone inversion of configuration to the β-form. The coupling constants of the anomeric carbon and its hydrogen of the α- and β-galactosylamine are 162.8 and 150.3 Hz, respectively. The chemical shifts, as determined from these data of the anomeric carbon of the α- and β-galactosylamine, are 87.17 and 82.95 ppm, respectively. The chemical shifts in ppm of some of the principal peaks are:

1 92.2
2 82.2
3 75.4
4 65.7
5 62.8
6 53.2

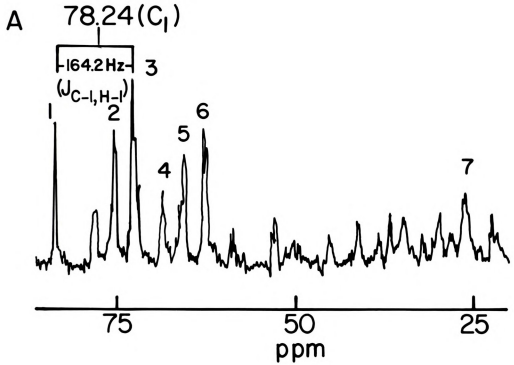
A
78.24(C1)
164.2 Hz
(JC-1,H-1)
1
2
3
4
5
6
7
75
50
25
ppm

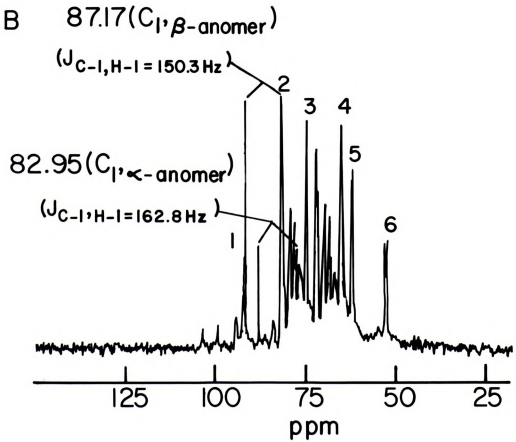
B
87.17(C1, β-anomer)
(JC-1,H-1 = 150.3 Hz)
82.95(C1, α-anomer)
(JC-1,H-1 = 162.8 Hz)
1
2
3
4
5
6
125
100
75
50
25
ppm

compared to the spectrum of the affinity ligand with the hope that the peaks from the sugar of the affinity ligand would match those of either galactosylamine; they did not. For example, the chemical shifts of the anomeric carbon, which is one of the most distinctive for a sugar, were 78.34, 82.96, and 87.24 ppm for the affinity ligand, α-galactosylamine, and ß-galactosylamine, respectively. Upon consulting with Dr. Hernan Nunez, it was decided that the chemical shift information was insufficient to determine the anomeric configuration of the purported affinity ligand. Coupled spectra (^{1}H-^{13}C) were made of the affinity ligand and of both galactosylamines in order to determine the coupling constant of the anomeric carbon and its hydrogen. The size of this coupling constant in sugars is characteristic of the anomerity of the sugar. The coupling of the hydrogens of the carbons splits the individual peaks previously due to each carbon, and the midpoint of the two new peaks should be extremely close to the chemical shift of the original peak. The distance in Hz between the two new peaks represents the coupling constant. The coupling constants of the anomeric carbon and its hydrogen for the affinity ligand, α-galactosylamine, and ß-galactosylamine were 164.2, 162.8, and 150.3 Hz respectively (Figure 10). These data show that the anomeric configuration of the affinity ligand is α. That the affinity ligand was successfully used in purifying two α-galactosidases is post facto evidence that

the anomeric configuration of the affinity ligand is α.

Purification of α-Galactosidases A and B from Human Liver

This purification scheme was devised in order to maximize the yield of pure α-galactosidase A rather than the B enzyme because the A enzyme, but not B, has been associated with a lysosomal storage disease and is found in much lower concentration than the B enzyme. Since the A enzyme is of such low abundance in the liver, which has one of the higher concentrations of the enzyme of any major organ, and because human livers are so difficult to obtain, extra procedures were taken in order to maximize the yield of the A form even though the additional contaminants would have to be removed at subsequent steps.

The data from three purifications of human liver α-galactosidases are summarized in Table 3. It is not apparent from the table, but the pellets from the initial 16,000 X g centrifugation had to be re-extracted with water at least twice in order to obtain greater than 90% yield at the first step. Previously (104,105) a 30-60% $(NH_4)_2SO_4$ cut was made of the first supernatant; here it was found that the same specific activity of the α-galactosidases was found in the 0-30% as in the 30-60% $(NH_4)_2SO_4$ cut so that only a 0-60% $(NH_4)_2SO_4$ cut was subsequently made.

The introduction of concanavalin A-Sepharose into the

The distribution of [illegible] in the [illegible] was [illegible] $[M^{+}]^{2}$ [illegible] so that only a one-one $[M^{+}]^{2}$ [illegible] was [illegible] the [illegible] [illegible] $[M^{+}]^{2}$ [illegible] [illegible] [illegible]

Table 3. The purification of human liver α-galactosidases.

These data represent the yields and specific acitivities of the human liver α-galactosidases at each step of the purification scheme and are the average of three purifications of the enzymes. The yield at the affinity chromatography step represents only the most recent data as the optimal conditions for affinity chromatography were only recently determined.

Step	Yield	Sp. Act.	Fold	% α-Gal A
Total Homogenate	100*	0.00101*	1.0*	58
16,000 X g supernatant	95*	0.00166*	1.66*	ND
0-60% $(NH_4)_2SO_4$	88*	0.00228*	2.26*	ND
Con A Extract	87*	0.0509*	50.4*	ND
DEAE	70*			74
A only	90**	0.140*	139*	
B+A		0.0956*	95*	
G-150	66*			72
A only	82**	0.495*	490*	
B+A		0.370*	370*	
Affinity Chromatography				
A only	58**	45.2	77,200**	
B only	37**	4.18	9,850**	

*Data based upon the yield of both α-galactosidases.

**Data based upon the fact that the initial mixture of α-galactosidases is 58% A.

Figure 11. Column chromatography of α-galactosidases A and B on DE-52.

The concanavalin A-Sepharose extract was applied to a column of DE-52 (4.05 X 24 cm) pre-equilibrated in buffer A. The column was washed with 200 ml of buffer A to removed non-binding proteins. The α-galactosidases were eluted with a linear NaCl gradient (4 liters total, 0 to 300 mM) in buffer A. Fractions of 15.5 ml were collected and assayed for α-gal A (closed circles), α-gal B (open circles), and α-gal A+B (open squares) activities. Protein ws monitored by A_{280} (closed squares). Fractions containing only α-galactosidase A and those containing A and B were pooled separately, as indicated, and concentrated to 25 ml in an Amicon Model 52 for gel filtration on Sephadex G-150.

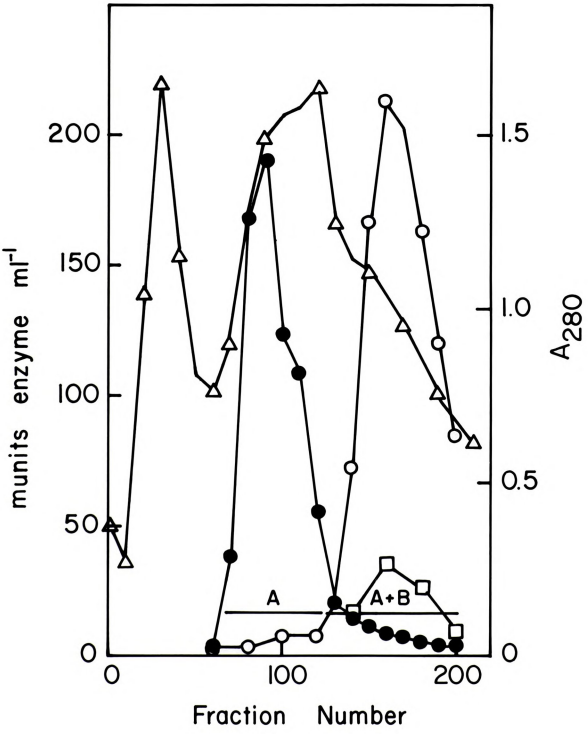
munits enzyme ml⁻¹
200
150
100
50
0
1.5
1.0
0.5
0
A280
A
A+B
0
100
200
Fraction Number

purification scheme, as was previously done for the splenic and placental enzymes (16,17), greatly facilitated the purification of both enzymes. There was a nearly quantitative yield of the enzymes and a purification of twenty-fold at the Con-A step, which also meant that the enzyme could be more easily managed.

The DE-52 afforded only a two- to three-fold increase in specific activity of the α-galactosidases, but there was an apparent separation of the A from the B enzyme. As can be seen in Figure 11, the first peak of α-galactosidase to elute from the DEAE contains only α-galactosidase A (Fractions 67-124). The second peak of enzyme eluting from the column hydrolyzes p-NP- -GalNAc and is apparently α-galactosidase B. However, a significant amount of the second peak of α-galactosidase hydrolyzes 4-MU-α-Gal in the presence of 50 mM GalNAc which indicates that half of this second peak is α-galactosidase A. The presence of so much α-galactosidase A in a preparation of α-galactosidase B would surely invalidate any kinetic or substrate specificity studies.

The two pools of α-galactosidase from the DE-52 were separately concentrated and applied to a large G-150 column. The sample size was generally about 2% of the column volume, and the flow rate was 2 ml/hour/cm^2 of the cross sectional area of the column as was suggested in the Pharmacia manual for optimizing protein separations. As can be seen from the data in Table 3, there is about a

three-fold increase in specific activity of the enzymes and about a ninety per cent yield at this step. This increase in specific activity is primarily due to the removal of high molecular weight proteins (Figure 12). The enzyme preparation was reddish brown up to this point, and the fractions from the G-150 column having the α-galactosidases were light yellow; those with the unwanted proteins were brown or red.

Affinity Chromatography of α-Galactosidase A. The yield of pure α-galactosidase A from the affinity chromatography step was initially around 25%, but occasionally as high as 50%. The enzyme must be acidified prior to affinity chromatography in order for the enzyme to bind to the affinity resin because the enzyme elutes from the resin at pH 5.5 or above. Initially the enzyme was acidified to pH 4.7 as Bishop and Desnick (16) used for the splenic enzyme, but the pI of the human liver enzyme is 4.6 (105). In the last enzyme purification, the enzyme was acidified to pH 5.0, and the yield at the affinity chromatography step in both a trial run and a large preparation was 70%.

Affinity Chromatography of α-Galactosidase B. As can be seen in Figure 13, the 50 mM GalNAc prevented the α-galactosidase B from binding to the affinity resin so that the enzyme passed through the column with the unwanted proteins (Fractions 2-12), while the α-galactosidase A was retained. The α-galactosidase A was eluted with galactose at pH 6.0 (Fractions 32-40). After the GalNAc was

The Chromatography Laboratory

Dr. Elena Vasquez had been working in the chromatography lab at Meridian Institute of Technology for seven years when she first noticed the anomaly. It was a Tuesday afternoon in late October, and she was preparing samples for a routine analysis of plant pigments. The lab was quiet, lit only by the fluorescent panels overhead and the soft glow of her monitor. She had run the same protocol hundreds of times before, and she knew exactly what to expect.

The sample was a chloroform extract of spinach leaves, a standard test material used to calibrate the column's separation efficiency. Vasquez injected the solution into the gas chromatograph and watched the detector trace appear on the screen. The first peak arrived at 4.2 minutes, as it always did. The second peak arrived at 6.8 minutes, also as it always did. But then a third peak appeared at 9.1 minutes, and Vasquez frowned. She had never seen a third peak in this analysis.

She checked the baseline, the flow rate, the temperature of the column oven. Everything was within specification. She ran the sample again. The third peak appeared in exactly the same position, with exactly the same height. She ran a blank solvent sample. The third peak did not appear. She ran a standard mixture of the three known pigments. The third peak appeared in the standard, at the same retention time as in the spinach extract.

Vasquez sat back in her chair and looked at the ceiling. She had been working with chromatography long enough to know that a reproducible peak was not an artifact. It was a real compound, present in the sample, and it had been there all along. The question was what it was.

She began by calculating the retention index of the unknown peak relative to the n-alkane standards. The value was 1,347. She consulted her reference tables and found no match. The closest known compound was limonene, with a retention index of 1,029, and the next was beta-carotene, at 1,520. Neither was close enough to account for the observed value. She checked the literature for essential oils, for terpenes, for anything that might elute in that range. Nothing matched.

Over the next three days, Vasquez repeated the analysis under different conditions. She changed the column temperature ramp, the carrier gas flow rate, the injection volume. She prepared fresh extracts from new leaves, from different plants, from a commercial supplier. The peak appeared every time, in every sample, at every temperature. It was not a contaminant. It was not a degradation product. It was something that belonged in the sample, something that had been overlooked by every analyst who had ever run a spinach standard.

Figure 12. Column chromatography of α-galactosidase A on Sephadex G-150.

Those fractions from the DE-52 step containing only α-galactosidase A were pooled and concentrated to 25 ml. The enzyme was appled to a Sephadex G-150 column (3.5 X 110 cm) pre-equilibrated in buffer A. The enzyme was eluted with buffer A at a flow rate of approximately 20 ml per hour, and fractions of 5.4 ml were collected. Enzyme activity was determined with 4-MU-α-Gal (closed circles), and protein was monitored by determining A_{280} (open circles). Fractions containing greater than 100 munits per ml were pooled and concentrated in the Amicon Model 52 to approximately 1.0 unit per ml for purification by affinity chromatography.

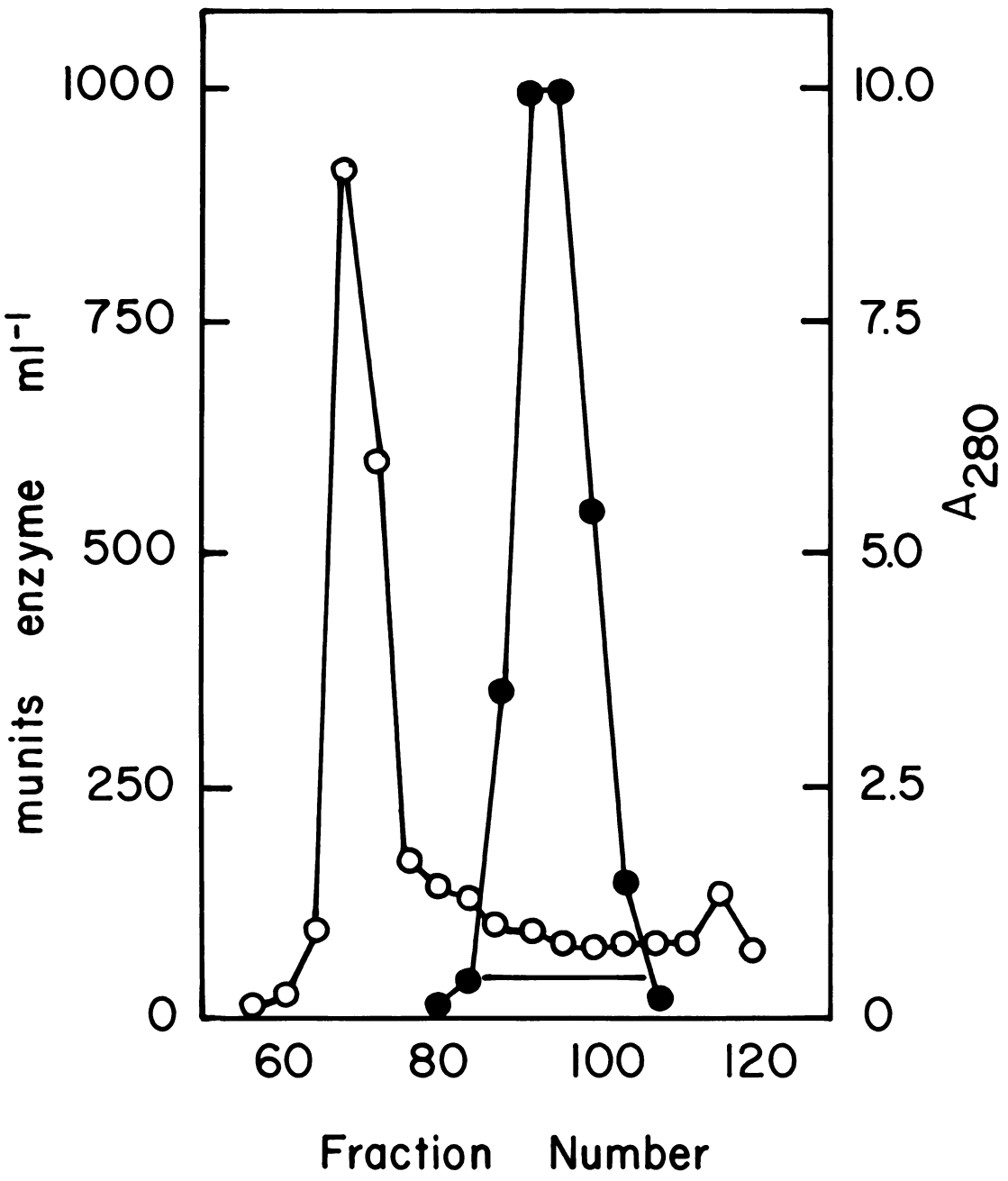
1000
750
500
250
0
munits enzyme ml-1
10.0
7.5
5.0
2.5
0
A280
60
80
100
120
Fraction Number

Figure 13. Dual affinity chromatographic separation of α-galactosidases A and B.

The mixture of partially purified α-galactosidases A and B from the G-150 step was acidified with HCl to pH 4.7, and solid GalNAc was added so that the concentration of GalNAc was 50 mM. The enzyme was then applied at 4° to a 0.75 X 10 cm affinity column at that had been pre-equilibrated with Gomori Citrate-Phosphate pH 4.6, containing 0.15 M NaCl and 50 mM GalNAc. Fractions of 2 ml were collected. The balance of the α-galactosidase B was eluted with 15 ml of the GalNAc buffer. α-Galactosidase activity was measured with 4-MU-α-Gal (solid line), and the A_{280} (dashed line) of the fractions was determined. The unbound proteins were eluted with Gomori Citrate-Phosphate pH 4.6 containing 0.15 M NaCl until the A_{280} of the effluent was zero. The α-galactosidase A was eluted with Gomori Citrate-Phosphate pH 6.0 containing 0.4 M galactose and 0.5 M NaCl, fractions 31-40. The fractions containing α-galactosidase B, 2-14, were pooled, concentrated to less than 10 ml, and were dialyzed versus 10 mM sodium phosphate pH 6.5 to remove the GalNAc. The α-galactosidase B was then purified by affinity chromatography as described in the Methods section.

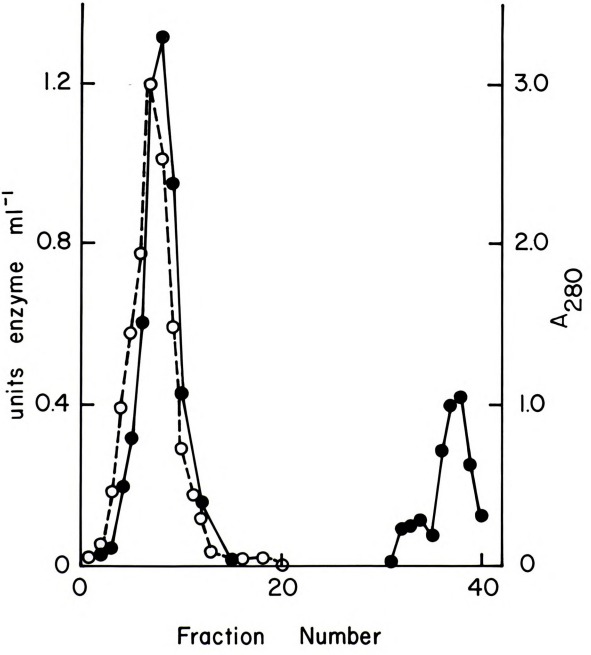
1.2
0.8
0.4
0
units enzyme ml⁻¹
3.0
2.0
1.0
0
A280
0
20
40
Fraction Number

dialyzed from the α-galactosidase B, the enzyme was re-applied to the affinity resin at pH 4.7. The yield of α-galactosidase B at the affinity chromatography step was around 80% even though the pI of the enzyme is 4.5 (104).

Chemical Characterizations of the Purified α-Galactosidases A and B. Human liver α-galactosidases A and B had previously been shown to have native molecular weights of 104,000 and 90,000 (105) respectively. I have found that the subunit molecular weights of A and B are 47,800 and 46,800 daltons, respectively, as determined by SDS-gel electrophoresis (Figure 14). Both α-galactosidases appear as very diffuse bands in the gel, which is characteristic of glycoproteins.

Approximately 100 μg of each enzyme was dialyzed versus water and submitted to Doris Bauer of this department for amino acid analysis. An additional 10 μg of α-galactosidase A was submitted to Dr. Al Smith of the Department of Biochemistry of the University of California at Davis for another analysis of amino acid composition. Both analyses of α-galactosidase A gave similar results. The composition of α-galactosidase A, as determined by Dr. Smith, and the composition of α-galactosidase B are given in Table 4 which also has the composition of several other human lysosomal enzymes.

Eight nmol of carboxymethylated α-galactosidase A and approximately 36 nmol of carboxymethylated α-galactosidase

Figure 14. Molecular weight determination and assessment of purity of human liver α-galactosidases A and B.

Five μg of each protein was applied to the respective well, electrophoresis was performed according to the method of Laemmli (129), and the gel was stained with Coomassie Brilliant Blue R. Lane 1 contained the following standard proteins whose subunit molecular weights X 10^{-3} are listed in the figure in decreasing order: phosphorylase a, bovine serum albumin, ovalbumin, aldolase, and α-chymotrypsinogen A. Lanes 2 and 3 contained α-galactosidase A and B, respectively. The subunit molecular weights of the α-galactosidases were determined from a plot of R_f versus log MW of the standards and are 47,800 and 46,800 for α-galactosidase A and B, respectively.

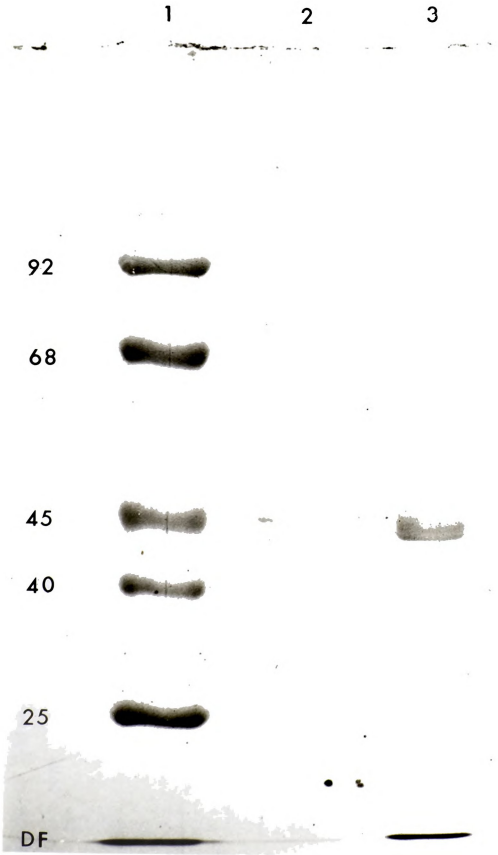
1
2
3
92
68
45
40
25
DF

Table 4. Amino Acid Composition of Human Lysosomal Enzymes

Amino Acid	(I)	(II)	(III)	(IV)	(V)	(VI)	(VII)
Asx	10.7	12.4	13.1	10.7	9.3	11.7	10.9
Thr	4.2	4.4	4.0	5.9	6.6	5.7	6.3
Ser	10.2	9.2	6.6	6.6	8.5	7.7	9.3
Glx	12.6	12.2	10.4	9.6	8.3	9.9	11.5
Pro	4.8	5.2	6.6	7.2	7.3	9.6	5.5
Gly	12.3	11.6	9.0	9.6	7.7	8.3	6.9
Ala	9.0	8.2	6.6	6.4	8.1	5.2	8.4
Val	5.5	5.4	3.9	5.0	5.8	4.7	6.6
Met	2.0	2.7	4.5	1.1	1.4	1.2	0.4
Ile	4.2	4.5	5.9	4.0	3.3	3.0	3.9
Leu	8.2	7.4	11.5	11.0	10.8	9.3	8.8
Tyr	3.0	3.0	3.8	5.9	3.5	4.2	2.5
Phe	3.1	4.2	3.0	5.8	5.0	6.7	4.2
His	2.4	2.7	1.9	2.0	3.3	3.1	2.0
Lys	3.7	3.7	3.9	5.0	4.4	6.3	4.4
Arg	4.0	2.5	5.2	3.6	4.2	3.1	4.1
Cys	ND	0.5	ND	1.0	1.2	0.4	2.0
Trp	ND	ND	ND	ND	1.4	ND	2.3

(I) α-Galactosidase A from liver (Present work).

(II) α-Galactosidase A from placenta (26).

(III) α-Galactosidase B from liver (Present work).

(IV) β-Galactosidase A_2 from liver (19).

(V) β-Glucocerebrosidase from placenta (26).

(VI) α-L-Fucosidase from liver (15).

(VII) Aspartylglucosaminidase from liver (13).

Table 4. continued.

Amino Acid	(VIII)	(IX)	(X)	(XI)	(XII)	(XIII)	(XIV)
Asx	10.5	11.4	9.7	7.4	8.5	10.3	9.5
Thr	5.1	4.9	6.0	5.2	8.8	4.4	6.0
Ser	8.1	8.5	6.0	5.9	9.4	7.1	8.6
Glx	9.4	11.5	11.1	7.8	5.9	12.2	9.1
Pro	6.7	5.5	6.5	10.4	5.2	7.5	6.1
Gly	11.0	9.4	7.2	10.2	8.2	9.3	6.5
Ala	5.6	7.7	6.1	9.2	5.5	6.1	5.5
Val	7.3	6.0	6.7	5.2	5.8	7.2	5.0
Met	1.6	1.7	1.4	1.8	1.1	ND	2.1
Ile	4.8	4.0	3.6	1.8	3.5	4.3	4.1
Leu	9.1	9.1	10.0	12.0	7.3	11.7	9.2
Tyr	4.6	1.9	5.5	3.1	4.2	3.7	5.0
Phe	3.5	4.0	4.4	4.5	3.6	5.4	5.5
His	1.3	2.6	3.4	3.1	3.8	2.0	3.3
Lys	6.7	5.8	5.5	2.4	5.1	4.7	5.6
Arg	2.7	3.4	7.1	4.5	3.5	4.2	4.6
Cys	---	2.7	0.0	3.2	1.3	ND	2.5
Trp	Tr	ND	---	2.3	9.4	ND	1.7

(VIII) Cathepsin D from placenta (14)

(IX) Sphingomyelinase from placenta (24)

(X) β-Glucuronidase from placenta (21)

(XI) Arylsulfatase A from liver (11)

(XII) Arylsulfatase B from liver (12)

(XIII) β-Hexosaminidase from placenta, α-chain (23)

(XIV) β-Hexosaminidase from placenta, β-chain (23)

B were submitted for N-terminal sequencing to Dr. Al Smith of the University of California at Davis Department of Biochemistry. The results are given in Table 5, which also includes the N-terminal sequences of other human lysosomal glycosidases.

Since the N-terminal sequences of both α-galactosidases are so similar, it was decided to compare more of the sequence of the two enzymes by sequencing internal peptides derived from both enzymes. Each enzyme was carboxymethylated and digested with trypsin, and the tryptic peptides were separated by reversed-phase HPLC as shown in Figures 15 and 16. Several peptides of α-galactosidase B (Figure 16), but few of α-galactosidase A (Figure 15) were separated by HPLC.

One peptide of α-galactosidase A was been purified (Figure 17), but there was not enough material for N-terminal sequencing. Several peptides of α-galactosidase B from the chromatogram shown in Figure 16 were repurified using the HFBA system as described in the Methods section. These peptides as well as several peaks from Figure 16 that seemed likely to have a single peptide were submitted to the Protein Sequencing Facility of the University of Michigan for N-terminal sequencing. Unfortunately, there was not enough of any of these peptides for sequencing (50 or more pmol is a reasonable amount). There was enough α-galactosidase B for two additional primary separations of tryptic peptides, one of which is shown in Figure 18.

Table 5. N-Terminal Sequences of Human Lysosomal Hydrolases

1	Leu-Asp-Asn-Gly-Leu-Ala-Arg-X^a-Pro-Tyr/Thr-Met-Gly-X^a-X^a-Leu-
2	Leu-Asp-Asn-Gly-Leu-Ala-Arg-Thr-Pro-Thr-Met-Gly-Trp-Leu-X^a-Trp-Glu-Arg-Phe-X^a-Gly-Asn-
3	Leu-Asp-Asn-Gly-Leu-Ala-Arg-Thr-Pro-Thr-Met-Gly-Trp-Leu-Leu-Trp-Glu-Arg-Phe-X^a-Gly-Asn
4	Leu-Asp-Asn-Gly-Leu-Leu-Gln-Thr-Pro-Pro-Met-Gly-Trp-Leu-Ala-Trp-Glu-Arg-Phe-
5	Ala-Arg-Pro-Cys-Ile-Pro-Lys-Ser-Phe-Gly-Tyr-Ser-Ser-Val-Val-Cys-Val-Cys-X^a-Ala-Thr-
6	Leu-Trp-Trp-His-Trp-Gln-Gly-Glu-Gly-Arg-Pro-Gln-Tyr-Gln-Arg-Phe-Met-Arg-Asp-Asn-Tyr-

1	Liver α-galactosidase A (Present work)
2	Placental α-galactosidase A (26)
3	A composite of the liver and placental forms of α-galactosidase A
4	Liver α-galactosidase B (Present work)
5	Placental β-glucocerebrosidase (26)
6	Liver α-L-fucosidase (25)

Figure 15. Primary separation of tryptic peptides of human liver α-galactosidase A.

Approximately 250 μg of carboxymethylated α-galactosidase A were digested with 5 μg of TPCK-trypsin for ten hours at room temperature in one per cent NH_4HCO_3. The digest was lyophilized, resuspended in 0.1% TFA, and applied to a Synchrom RP-8 HPLC column. The solvent system was H_2O-CH_3CN/2-propanol (3:1, v/v) with 0.1% TFA throughout. The flow rate was 1.0 ml per minute, and the absorbance detector was set at 229 nm. The effluent corresponding to the peak on the chromatogram as shown by the bar was collected; this peak was further purified as shown in Figure 17.

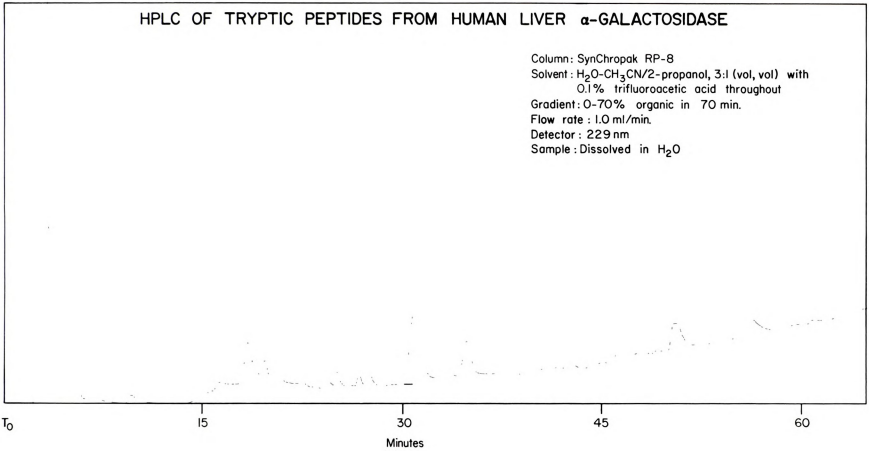
HPLC OF TRYPTIC PEPTIDES FROM HUMAN LIVER α-GALACTOSIDASE
Column: SynChropak RP-8
Solvent: H_2O-CH_3CN/2-propanol, 3:1 (vol, vol) with 0.1% trifluoroacetic acid throughout
Gradient: 0-70% organic in 70 min.
Flow rate: 1.0 ml/min.
Detector: 229 nm
Sample: Dissolved in H_2O
T_0
15
30
45
60
Minutes

Figure 16. Primary separation of tryptic peptides of human liver α-galactosidase B.

Approximately 250 μg of carboxymethylated α-galactosidase B were digested with 10 μg of TPCK-trypsin for ten hours at room temperature in one per cent NH_4HCO_3. The digest was lyophilized, resuspended in 0.1% TFA, and applied to a Synchrom RP-8 HPLC column. The solvent system was H_2O-CH_3CN/2-propanol (3:1, v/v) with 0.1% TFA throughout. The flow rate was 1.0 ml per minute, and the absorbance detector was set at 229 nm. Peptides from other primary separations of α-galactosidase B, but corresponding to the numbered peaks in this separation, gave the following amino acid sequences:

1. Met-Ala-Gln-Asp-Gly-X^a-Arg and Thr-Asp-Met-Pro-Tyr-Arg

2. Leu-Asp-Asp

3. Leu-Leu-Ile-X^a-(Val)-, Ser-Ala-Asp-(Gln)-(Val)-, and

   Val-Val-Gln-Asp-Ala-(Glu)-Thr-Phe-Ala-(Glu)-X^a-(Lys)

4. Asp-Met-Gly-Tyr-Thr-Tyr-(Leu)-(Gly/Asn)-

5. Leu-Asp-Asp-Gly-

7. Val-Glu-Tyr-

8. Ala-Gln-Met-Ala-

X^a-The identity of the amino acid was not determined.

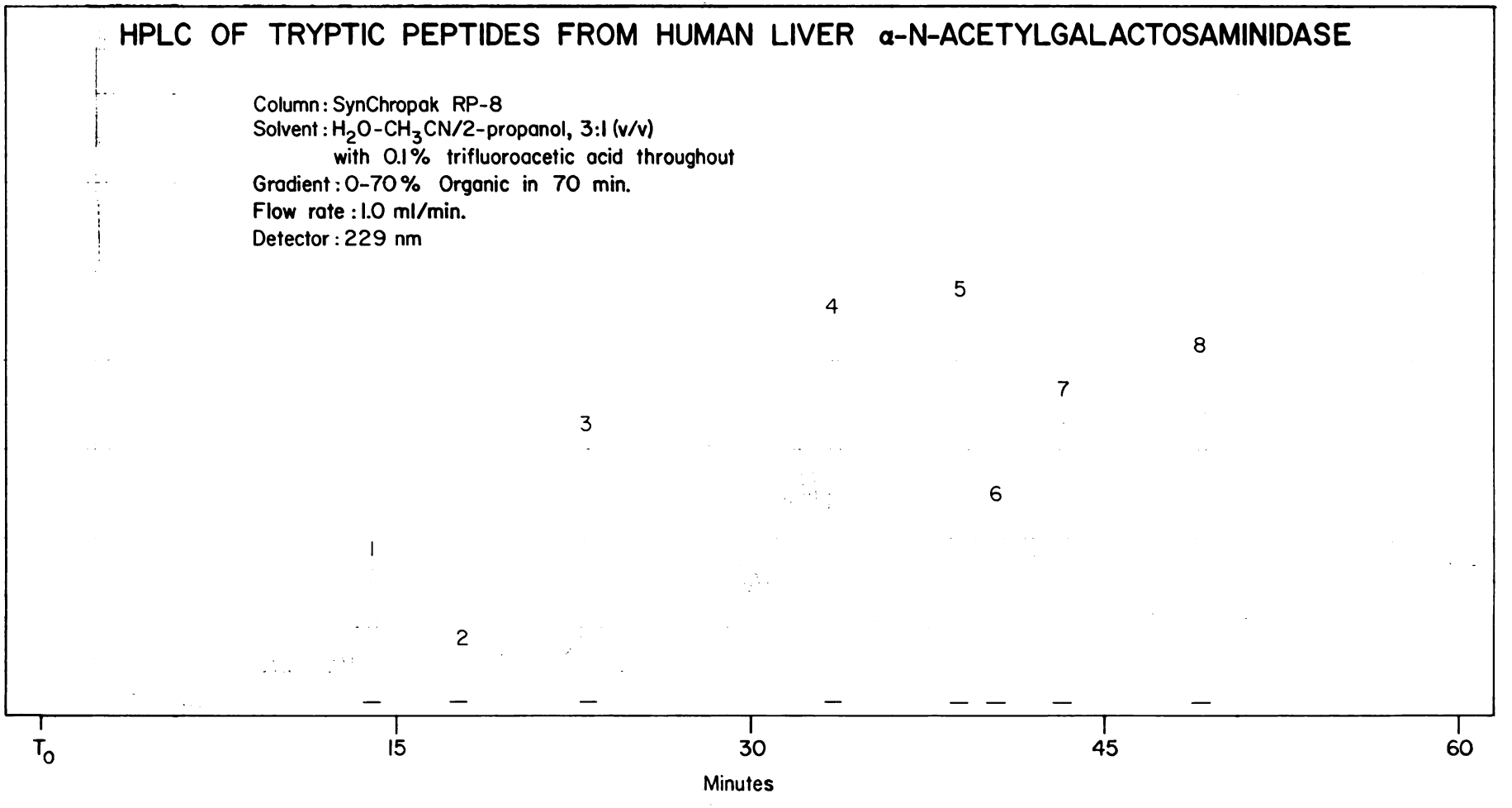
HPLC OF TRYPTIC PEPTIDES FROM HUMAN LIVER α-N-ACETYLGALACTOSAMINIDASE
Column: SynChropak RP-8
Solvent: H_2O-CH_3CN/2-propanol, 3:1 (v/v)
with 0.1% trifluoroacetic acid throughout
Gradient: 0-70% Organic in 70 min.
Flow rate: 1.0 ml/min.
Detector: 229 nm
1
2
3
4
5
6
7
8
T_0
15
30
45
60
Minutes

Figure 17. Repurification of an α-galactosidase A peptide

The material eluting at 31 minutes from Figure 15 was redissolved, injected, separated, and collected as described in the legend for Figure 19 for the repurification of α-galactosidase B peptides. Three peptides were collected as indicated. The major fraction has not yet been sequenced.

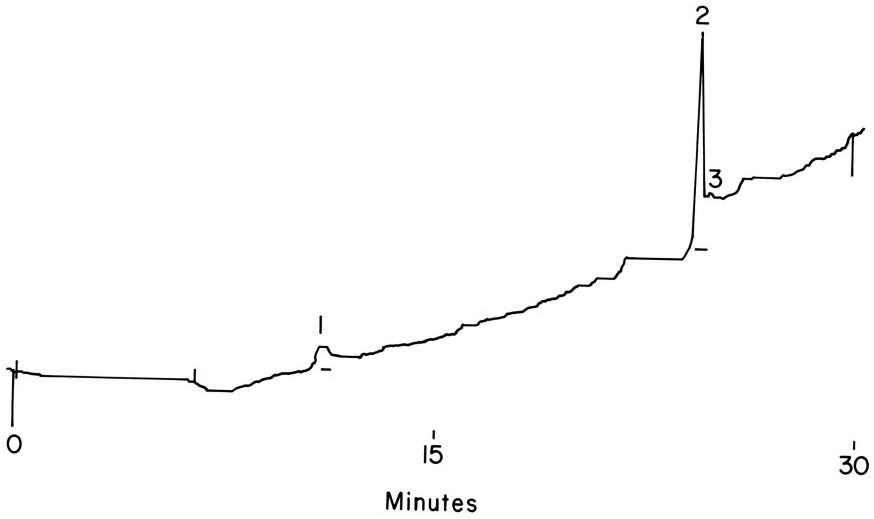
2
3
1
0
15
30
Minutes

Figure 18. Primary Separation of Tryptic Peptides of Human Liver α-Galactosidase B.

Approximately 500 μg of carboxymethylated α-galactosidase B were digested with 18 μg of TPCK-trypsin for ten hours at room temperature in one per cent NH_4HCO_3. TFA was added to the digest to 1.0% TFA, and the digest was applied to a Synchrom RP-8 HPLC column. The solvent system was H_2O-CH_3CN/2-propanol (3:1, v/v) with 0.1% TFA throughout. The flow rate was 1.0 ml per minute, and the absorbance detector was set at 229 nm. The effluent corresponding to the peaks on the chromatogram as shown by the bars were collected, and these peaks were further purified on a μBondapak Phenyl column. The difference between this figure and Figure 16. is that Figure 16 shows the entire chromatographic separation of all the tryptic peptides; this figure primarily shows the separation of smaller peptides. Additionally, peptides from this separation were successfully sequenced, while none were successfully sequenced from Figure 16.

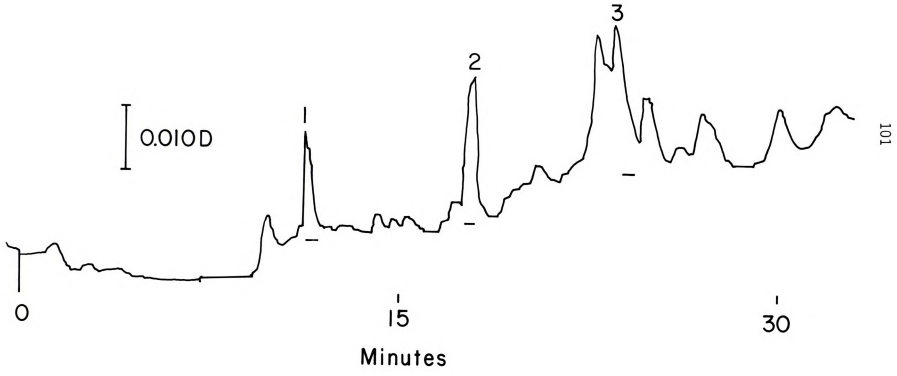
0.010D
1
2
3
0
15
30
Minutes

There was enough of several of these peptides for N-terminal sequencing in these two HPLC separations. Some of the peptides were repurified using the μBondapak Phenyl column before being submitted for sequencing (Figures 19, 20, and 21 demonstrate three successful peptide repurifications). Altogether, nine peptides of α-galactosidase B were sequenced at the University of Michigan Protein Sequencing Facility, and these sequences are given in Table 6, which also has the known sequences of CNBr and tryptic peptides of human placental α-galactosidase A.

Antibody Production

Polyclonal. Rabbit antibodies raised against human liver α-galactosidase A were successfully employed by others in this laboratory to determine the *in vivo* glycoprotein processing events of α-galactosidase A (31). The antibodies were found to be monospecific by immunoprecipitating single bands of precursor and mature forms of α-galactosidase A from Chang liver cells.

Monoclonal. Over 750 hybridomas derived from the fusion of mouse spleen cells and SP/2 cells were tested for the production of anti-α-galactosidase A antibodies. Two positive clones were found. Unfortunately, a collaborator left the cells on the bench overnight; the cells lived, but ceased production of the antibodies.

Figure 19. The separation of two α-galactosidase B peptides for amino acid sequencing.

The peak in a previous primary separation of tryptic peptides of α-galactosidase B corresponding to peak 1 in Figure 18 had a noticeable shoulder which indicated the presence of at least two peptides. The material from peak 1 as well as the corresponding material from the previous separation were separately dissolved in 6.0 M Guanidine-HCl, diluted with 0.1% TFA in water to less than 0.5 M Guanidine, and injected onto the Water's μ Bondapak Phenyl column. The solvent system was H_2O-CH_3CN/2-propanol (3:1, v/v) with 0.1% TFA throughout. There was an increase in organic phase of two per cent per minute, and the gradient was begun after the absorbance had returned to zero following sample injection (The peaks on the chromatogram to the left of the T_o mark result from the solvent from the multiple injections reaching the detector). The flow rate was 1.0 ml per minute, and the absorbance detector was set at 229 nm. Effluent corresponding to peptides 1 through 4 were collected, and the solvents removed under a water aspirator vacuum. Peptides 3 and 4 were sequenced by the University of Michigan Protein Sequencing Facility.

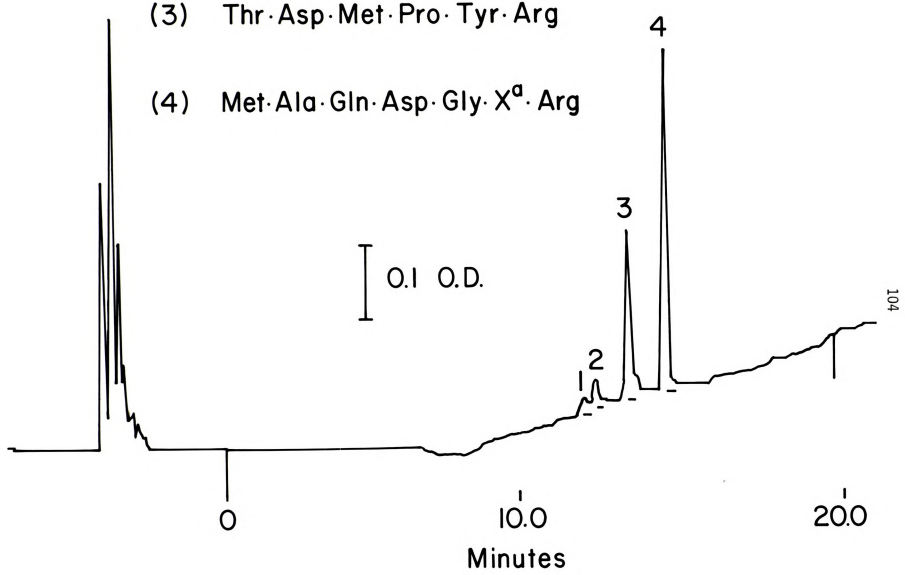
(3) Thr·Asp·Met·Pro·Tyr·Arg
(4) Met·Ala·Gln·Asp·Gly·X[a]·Arg
0.1 O.D.
1
2
3
4
0
10.0
20.0
Minutes
104

Figure 20. The purification of the major peptide from a mixture of three α-galactosidase B peptides for amino acid sequencing.

The amino acid sequence analysis of the material corresponding to peak 2 of Figure 18, but from another primary separation of α-galactosidase B tryptic peptides, indicated the presence of three peptides with one major component. The peptide was repurified in order to obtain more sequence information than the five amino acids in the first analysis. The material was dissolved, injected, separated, detected, and collected as described in the legend to Figure 19. Effluent corresponding to peaks 1 and 2 were collected, and the solvents were removed under a water aspirator vacuum. The sequence of peptide 2 was determined by the University of Michigan Protein Sequencing Facility.

(2) Val·Val·Gln·Asp·Ala·Glu·Thr·Phe·Ala·Glu·X^a·(Lys)

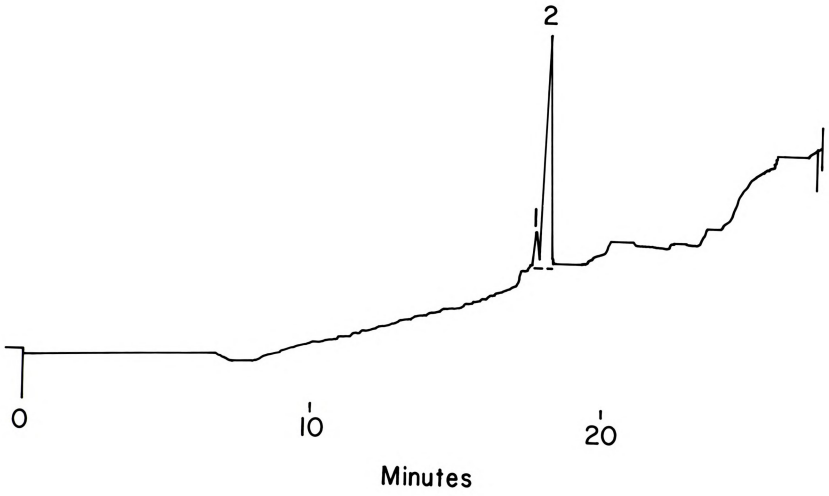

Figure 21. The purification of a peptide for amino acid sequencing from a complex mixture of α-galactosidase B peptides.

Panel A. Fraction 3 from Figure 18 was dissolved, injected, separated, detected, and collected as described in the legend to Figure 19. Effluent corresponding to nine peptides were collected as indicated.

Panel B. Peptide 7 from Panel A was re-injected neat onto the same Water's μBondapak Phenyl column after the column was re-equilibrated in 0.1% TFA in water. The elution and detection system was as described in the legend to Figure 19. The effluent corresponding to the peak was collected, and the solvent was removed under a water aspirator vacuum. The sequence of the peptide was determined by the University of Michigan Sequencing Facility.

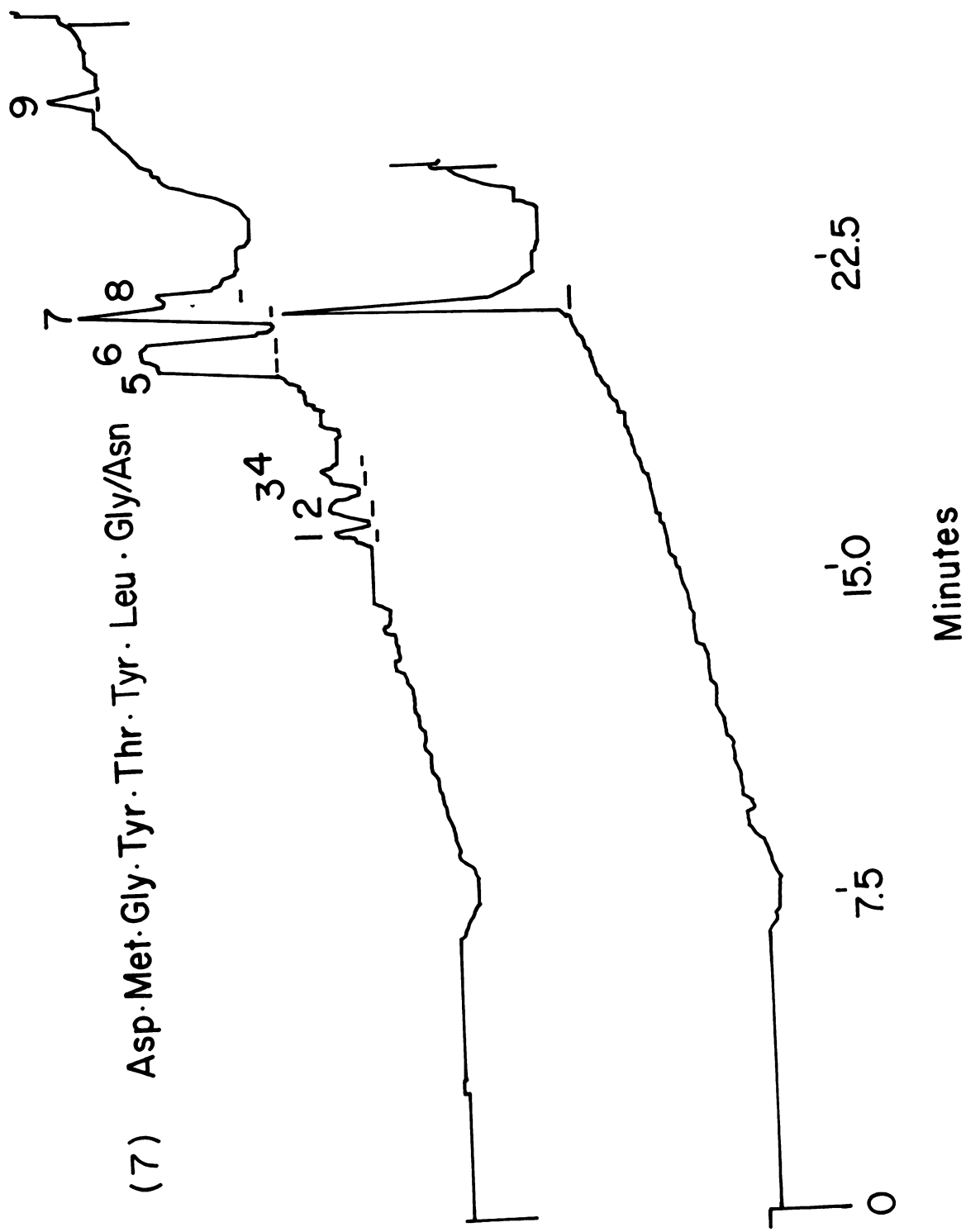
(7) Asp·Met·Gly·Tyr·Thr·Tyr·Leu·Gly/Asn
1
2
3
4
5
6
7
8
9
0
7.5
15.0
22.5
Minutes

Table 6. Peptide Sequences of Human α-Galactosidases A and B

Placental α-Galactosidase A (27)

Cleaved by CNBr

-(Met)-Ala-Leu-Leu-Lys-Arg-
-(Met)-Ile-Asn-Arg-Gln-Glu-
-(Met)-Leu-Val-Ile-Gly-Asn-

Digested with trypsin

-Ala-Leu-Gly-Phe-Tyr-
-Cys-Cys-Glu-Ser-Ala-
-Gln-Phe-Ala-Asp-Ile-
-Leu-Cys-Asp-Asn-Leu-
-Leu-Gln-Ala-Asp-Pro-
-Leu-Gln-Ala-Leu-Phe-
-Lys-Leu-Leu-Gln-Asp-
-Ser-Ile-Leu-Asp-Trp-
-Ser-Tyr-Gly-Ile-Ala-

Liver α-Galactosidase B (Present work)

Digested with Trypsin

-Ala-Gln-Met-Ala-
-Asp-Met-Gly-Tyr-Thr-Tyr-(Leu)-(Gly/Asn)-
-Leu-Asp-Asp-Leu-
-Leu-Leu-Ile-X^a-(Val)-
-Met-Ala-Gln-Asp-Gly-X^a-Arg
-Ser-Ala-Asp-(Gln)-(Val)-
-Thr-Asp-Met-Pro-Tyr-Arg
-Val-Glu-Tyr-
-Val-Val-Gln-Asp-Ala-(Glu)-Thr-Phe-Ala-(Glu)-X^a-(Lys)

The identity of the residues in parentheses are not known with certainty. The Glu's in the last peptide could be Gln's.

Synthesis of Conduritol C Epoxide

The principal intermediate in the synthesis of CCE was found to be the dibromotetraacetate (Figure 7, Compound V) by its melting point of 143° (Table 7) and by the appearance of two bromines in its mass spectrum (data not shown). The two bromines were removed by powdered zinc, and the product had a melting point of 89° which indicated it could be the tetraacetate of conduritol B, C, or F. An infrared spectrum of the presumed conduritol C tetraacetate was compared to the spectrum made by Stegelmeier (138) both of which are shown in Figure 22, and the two spectra are identical.

The acetyl groups were removed from (Figure 7, Compound VI) by triethylamine as described by Radin and Vunnam (139), but the melting point of the product did not match the literature value of 148-150° (140). A low resolution proton NMR spectrum indicated the presence of acetyl groups (data not shown). The partially de-acetylated material was treated with additional triethylamine until the melting point of the product matched the literature value for conduritol C which eliminated the possibility that the product could be any conduritol but C (Table 7). The infrared spectrum of the presumed conduritol C is similar, but not identical to the spectrum of conduritol B (Figure 23). The mass spectra of

Figure 22. Infrared spectra of conduritol C tetraacetate

Panel A An infrared spectrum of conduritol C tetraacetate from the PhD thesis of Stegelmeier (138).

Panel B An infrared spectrum of purported synthetic conduritol C tetraacetate. The spectrum was made on a Perkin-Elmer 167 Grating Spectrometer as were all other infrared spectra. The sample was a 1% KBr pellet.

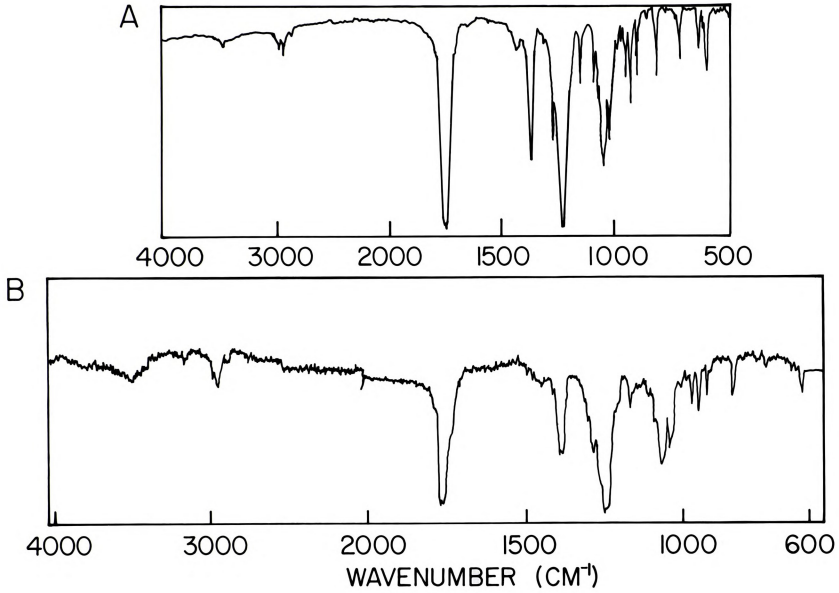
A
4000
3000
2000
1500
1000
500
B
4000
3000
2000
1500
1000
600
WAVENUMBER (CM-1)

Table 7. Melting points of intermediates and related compounds in the synthesis of conduritol C epoxide

Compound	Melting Point	
	Literature	Found
Dibromo tetraacetate (V)	144° (138)	143°
Conduritol A tetraacetate	Liquid (143)	
Conduritol B tetraacetate	91-92° (143)	
Conduritol C tetraacetate (VI)	91-92° (143)	89°
Conduritol D tetraacetate	102-104° (143)	
Conduritol F tetraacetate	92° (143)	
Conduritol A	141-142° (143)	
Conduritol B	205° (143)	
Conduritol C (VII)	148-150° (140)	149-150°
Conduritol E	179-180° (143)	
Conduritol F	103-104° (143)	
Conduritol B Epoxide	157-159° (140)	
Conduritol C Epoxide Trans (VIII)	135-137° (140) 145° (142)	139-141°
Conduritol C Epoxide Cis	126° (142)	

The Roman numerals in parentheses refer to the intermediates in Figure 7 where the reactions of the synthesis are illustrated.

Figure 23. Infrared spectra of conduritol B and conduritol C

Panel A An infrared spectrum of conduritol B. The sample was a 1% KBr pellet.

Panel B An infrared spectrum of purported synthetic conduritol C. The sample was a 3% KBr pellet.

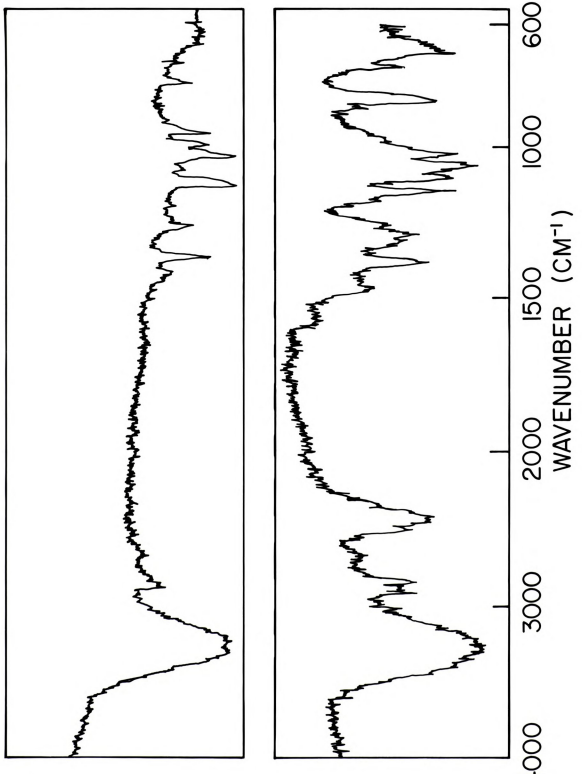
A
B
4000
3000
2000
1500
1000
600
WAVENUMBER (CM-1)

the TMS derivative of conduritol B and C were also similar, but not identical (Figure 24). The purity of the product as determined by GC was 97.8%.

Conduritol C was reacted with m-chloroperoxybenzoic acid to produce the trans epoxide. The product had a melting point of 139-141° compared to the two literature values of 135-137° (140) and 145° (142) and the 126° of the cis epoxide (142). The product gave a yellow color upon spraying with the methyl red reagent and had the same TLC mobility as authentic conduritol B epoxide. The infrared spectrum of the presumed conduritol C epoxide is shown in Figure 25 (there was not enough conduritol B epoxide available for a suitable infrared spectrum to be made). The mass spectrum of the TMS derivative of the product was compared to the spectrum of conduritol B epoxide; these spectra are similar but not identical (Figure 26). The molecular ion of CCE was found at m/z 450; it had an abundance of 0.06%. The purity of the product, as determined by GC of the TMS derivative, was 96.9%.

This conduritol C epoxide was used in inhibition studies of both α-galactosidases, but doubt was cast upon the identity of the product that had been synthesized because of the high Ki observed for the inhibition of α-galactosidase A towards 4-MU-α-Gal (145). Therefore high resolution ^{1}H-NMR spectra were made of the purported conduritol C and conduritol C epoxide to verify the

Figrure 24. Mass spectra of conduritol B and conduritol C.

The trimethylsilane derivatives of conduritol B and the purported conduritol C were formed by the method of Sweeley et al. (144). The samples were analyzed by GC-MS in the M.S.U. Mass Spectrometry Facility on a Hewlett-Packard 5985 GC/MS System. The column was a 6 foot long 4% SE-30, and there was a linear increase in temperature from 140 to 200^{o} at 4^{o} per minute.

Panel A. Conduritol B

Panel B. Conduritol C

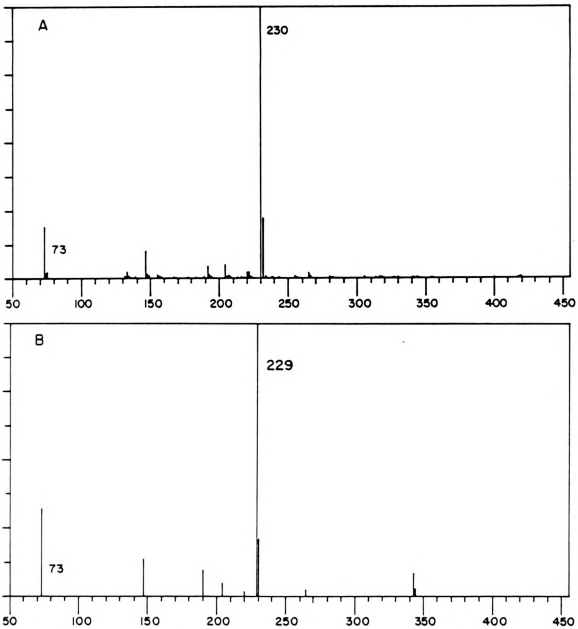
A
230
73
50
100
150
200
250
300
350
400
450
B
229
73
50
100
150
200
250
300
350
400
450

Figure 25. Infrared spectrum of conduritol C epoxide.

An infrared spectrum of purported synthetic conduritol C epoxide. The sample was a 3% KBr pellet.

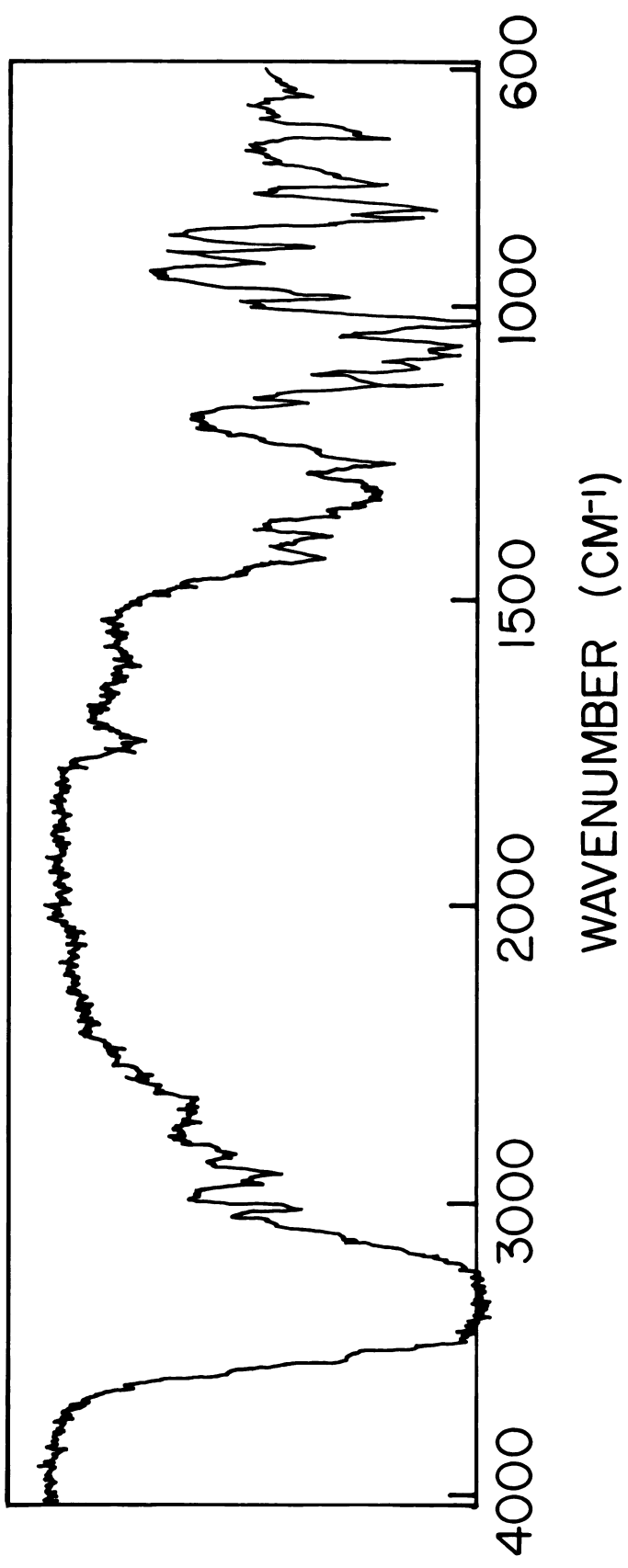
4000
3000
2000
1500
1000
600
WAVENUMBER (CM-1)

Figure 26. Mass spectra of conduritol B epoxide and conduritol C epoxide.

The TMS derivatives of conduritol B epoxide and the purported conduritol C epoxide were formed and analyzed by GC-MS as described in the legend to Figure 24.

Panel A. conduritol B epoxide

Panel B. conduritol C epoxide

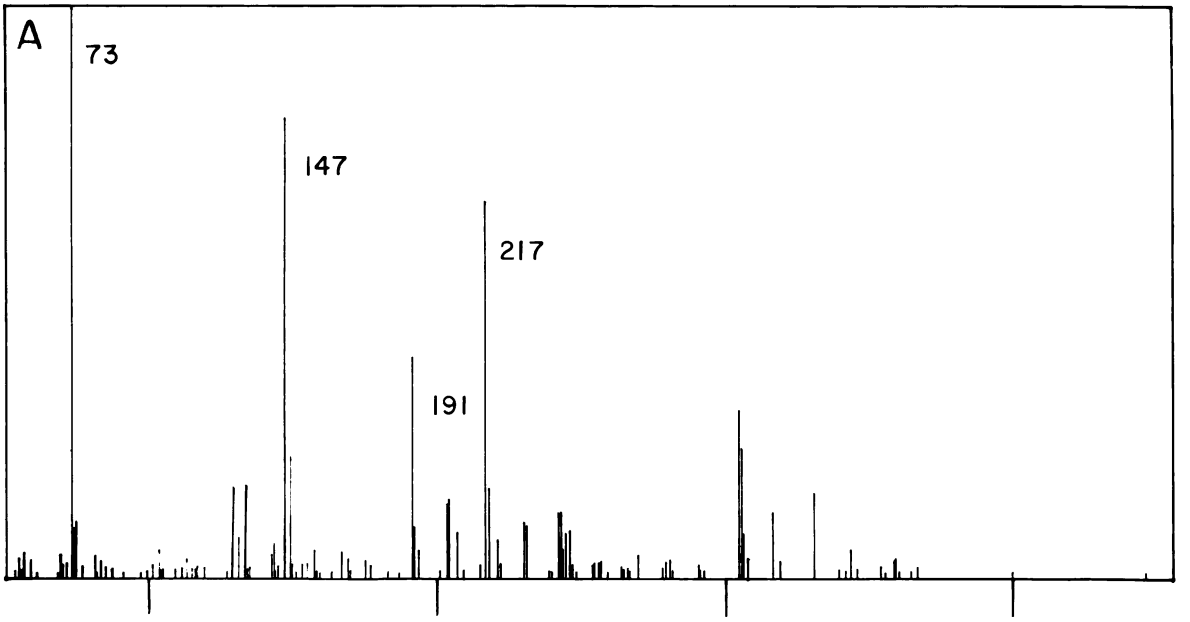
A
73
147
217
191

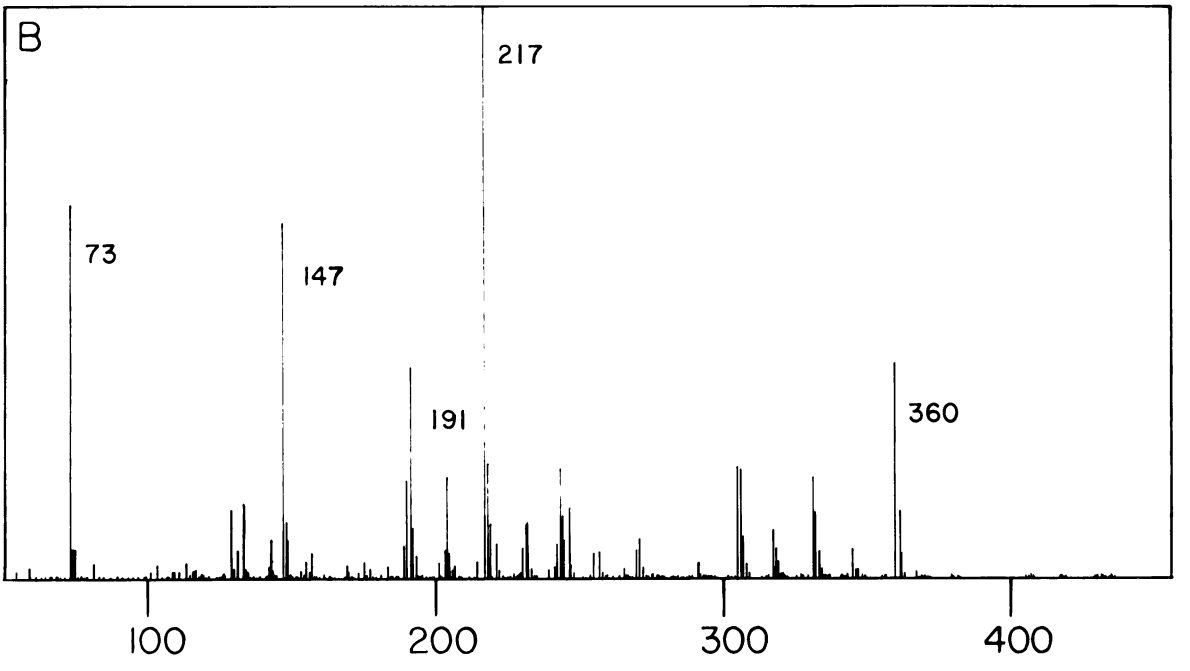
B
217
73
147
191
360
100
200
300
400

structures of these two compounds.

Peak Assignments in the ^{1}H-NMR Spectra of Conduritol C. In Figure 27, protons A and B are the olefinic protons, and the coupling constant of 10.6 Hz is characteristic of a cis double bond. Peaks C, D, E, and F are the other four ring protons. In the decoupled spectrum, Figure 28, Peak F is unaffected by the irradiation of either olefinic proton indicating that peak F is either proton 4 or 5 (Refer to Figure 31 for the numbering system as well as the structures of conduritol C and conduritol C epoxide). The coupling constant of 8.1 Hz appearing in peaks D and F indicates that proton D is coupled (or adjacent) to proton F in the molecule, and similarly, the coupling constant of 2.2 Hz appearing in peaks A and D indicates that these protons are adjacent. Panel F of Figure 28 shows that Peaks E and F are coupled. These data indicate that there are two possible circular permutations of the protons on the ring: -B-A-D-F-E-C- and -A-B-C-E-F-D-. The first was chosen because the coupling constant of 2.2 Hz between peaks A and D indicates a bond angle of 58^{o} between the two hydrogens, which is consistent with the structure of conduritol C, and because the protons at carbon four of simple sugars have the highest upfield chemical shift of the ring protons which would indicate Peak F would be proton four.

Peak Assignments in the ^{1}H-NMR Spectra of Conduritol C Epoxide. The interpretation of the high resolution

Figure 27. Proton NMR of conduritol C

Approximately 6 mg of presumed conduritol C were dissolved in D_2O, and the sample was scanned in a Bruker WM-250 Spectrometer under the direction of Dr. Klaas Hallenga of the M.S.U. Department of Chemistry. The spectrum was interpreted with the assistance of Dr. Kimihiro Kanemitsu of this laboratory as well as the staff of Dr. Hallenga. The chemical shifts in ppm and the coupling constants in Hz are as follows:

H #	Chem. Shift	J_{1-2}	J_{2-3}	J_{3-4}	J_{4-5}	J_{5-6}	J_{6-1}
1	5.60	10.63					ND
2	5.79	10.50	2.16				
3	4.27		2.20	8.15			
4	3.64			8.11	2.15		
5	4.09				ND	ND	
6	4.39					ND	ND

The peak at 4.75 ppm is due to H_2O.

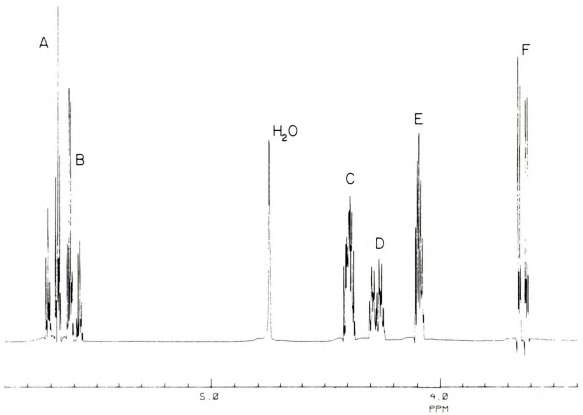
A
B
H_2O
C
D
E
F
5.0
4.0
PPM

Figure 28. Decoupled proton NMR spectrum of conduritol C

The sample of purported conduritol C used for Figure 27 was irradiated with an external source of radio-frequency radiation at each of the respective absorbances listed in Figure 27.

Panel A Irradiation of the proton at 5.79 ppm.

Panel B Irradiation of the proton at 5.60 ppm.

Panel C Irradiation of the proton at 4.39 ppm.

Panel D A normal coupled spectrum similar to Figure 27.

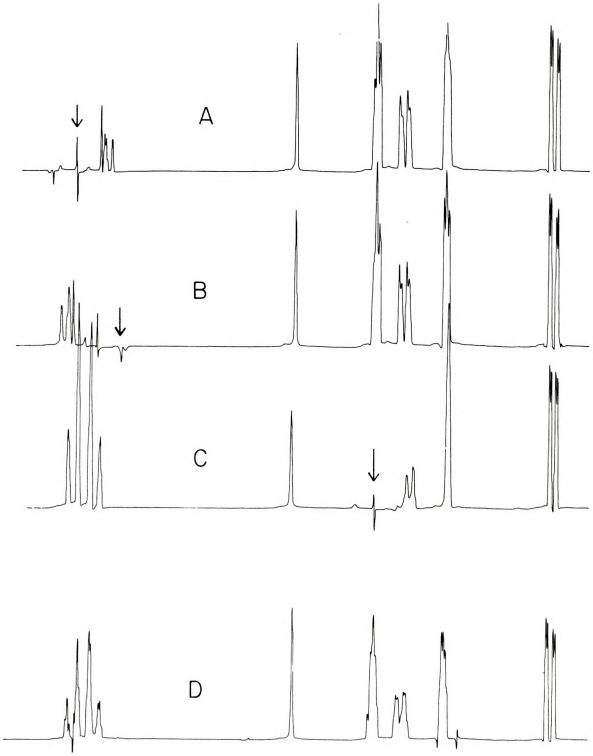
A
B
C
D

Figure 28. Continued.

Panel E Irradiation of the proton at 4.27 ppm.

Panel F Irradiation of the proton at 4.09 ppm.

Panel G Irradiation of the proton at 3.64 ppm.

Panel H A normal coupled spectrum similar to Figure 27.

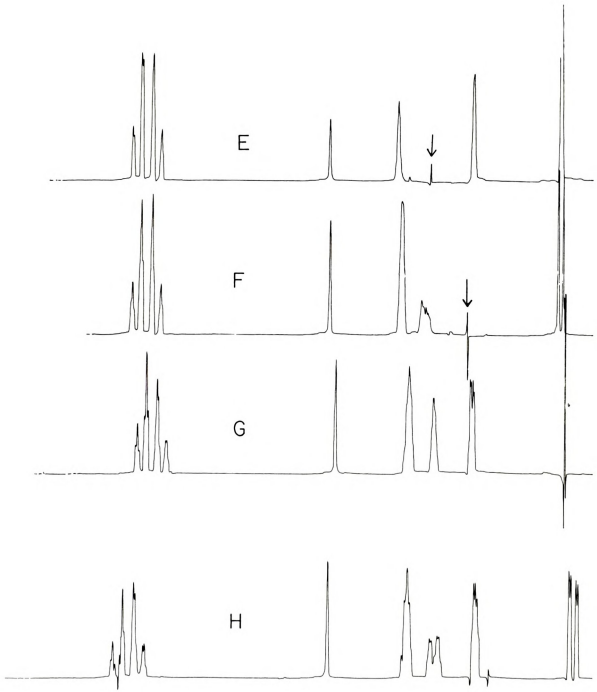
E
F
G
H

^{1}H-NMR spectrum of the purported conduritol C epoxide was facilitated by the assignment of the peaks in Figure 27 to specific protons in conduritol C, by a more distinctive decoupled spectrum than that of conduritol C, and by very well-defined peaks in Figure 29. From the decoupled spectra of CCE, Figure 30, it can be seen that peak A is coupled with both peaks D and E, that B is coupled with C and possibly F, that C is coupled with both B and E, D is coupled with A and F, E is coupled with A and C, and that F is coupled with D and possibly C. These data indicate a circular permutation of -A-D-F-B-C-E-. Peaks E and F of conduritol C were assigned positions 5 and 4, which should be changed little by the epoxidation, and these two resemble peaks C and E, respectively, in CCE so that peaks C and E were tentatively assigned to be protons 5 and 4, respectively. The distance in ppm between E and F in conduritol C and between C and E in CCE is 0.45 ppm which indicates that this assignment is correct. These data indicate that peaks A through F are protons 3-6-5-2-4-1, respectively. The coupling constants for peaks A, D, E, and F are very well-defined and can be used to determine bond angles between the protons by a plot of the Karplus equation. The coupling constants of peaks B and C are not as easily interpreted as the others, but since peak C in CCE is so similar to peak E in conduritol C, and the J_{3-4} and J_{4-5} are so similar in both molecules, the conformation of both molecules around carbons 3, 4, and 5

Figure 29. Proton NMR of conduritol C epoxide

Approximately 6 mg of purported conduritol C epoxide were dissolved in D_2O. The sample was scanned, and the spectrum was interpreted as described in the legend to Figure 27. The chemical shifts in ppm and the coupling constants in Hz are as follows:

H #	Chem. Shift	J_{1-2}	J_{2-3}	J_{3-4}	J_{4-5}	J_{5-6}	J_{6-1}
1	3.27	2.04					
2	3.51		2.29				
3	4.16		2.40	8.72			
4	3.47			8.72	1.61		
5	3.92				1.82	3.67	
6	3.96					3.90	

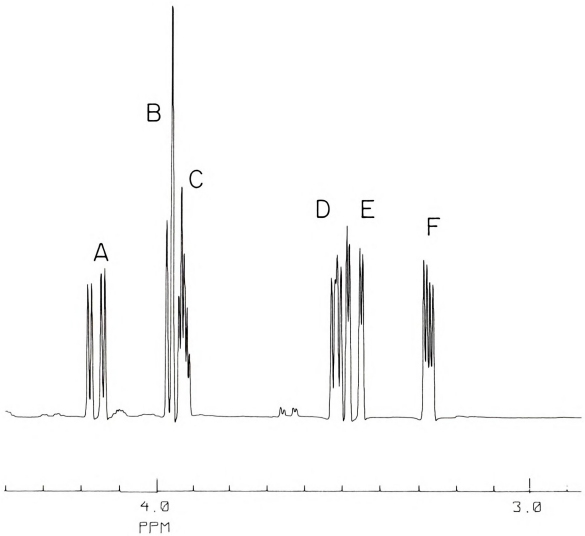
A
B
C
D
E
F
4.0
PPM
3.0

Figure 30. Decoupled Proton NMR spectra of conduritol C epoxide.

The sample of purported conduritol C epoxide used for Figure 29 was irradiated with an external source of radio-frequency radiation at each of the respective absorbances listed in the legend for Figure 29.

Panel A Irradiation of the proton at 4.16 ppm.

Panel B Irradiation of the proton at 3.96 ppm.

Panel C A normal coupled spectrum similar to Figure 29.

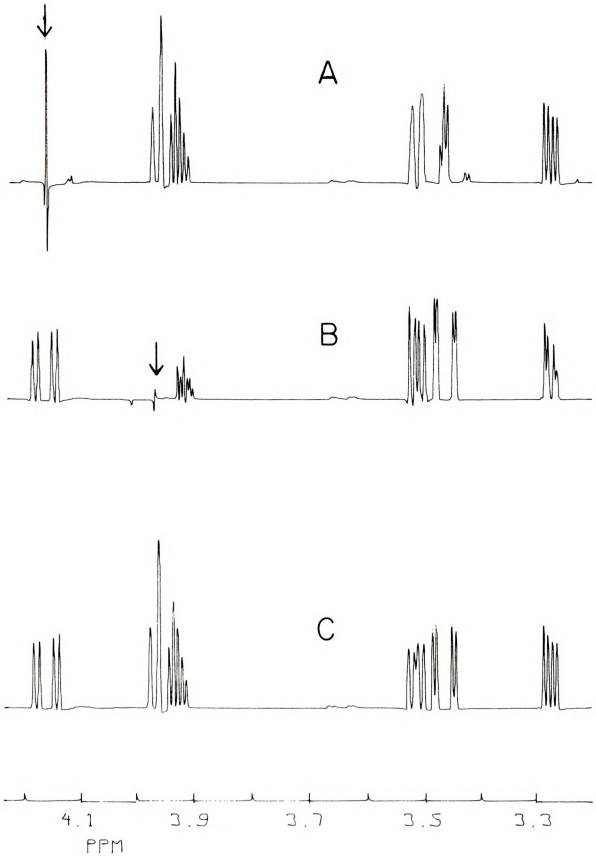
A
B
C
4.1
3.9
3.7
3.5
3.3
PPM

Figure 30 continued.

Panel D Irradiation of the proton at 3.92 ppm.

Panel E Irradiation of the proton at 3.51 ppm.

Panel F Irradiation of the proton at 3.47 ppm.

Panel G Irradiation of the proton at 3.27 ppm.

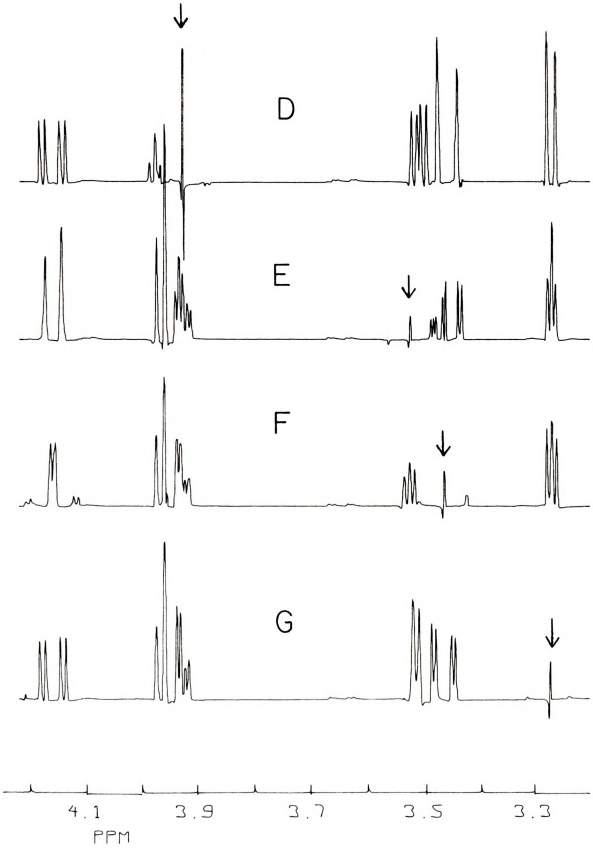
D
E
F
G
4.1
3.9
3.7
3.5
3.3
PPM

are almost identical.

Three-dimensional Structure of Conduritol C Epoxide.

The J_{1-2} of 2.04 for CCE is consistent with that for epoxides. The J_{2-3} of 2.34 Hz would indicate a bond angle of either 55 or 123° according to the Karplus plot. Since the epoxide is either cis (up) or trans relative to the plane of the molecule, and the expected bond angles would be either 0 or 150° for the cis and trans configuration, respectively, the epoxide is trans (down). The J_{3-4} of 8.72 Hz, the J_{4-5} of 1.72 Hz, the J_{5-6} of 1.7 Hz, and the J_{6-1} of 3.9 Hz indicate the respective angles between these pairs of hydrogens are 168, 58, 45, and 118°.

Substrate and Kinetic Studies of α-Galactosidases A and B.

Substrate Specificity. To show that the preparation of α-galactosidase B contained no α-galactosidase A, an assay was performed of both α-galactosidases using the natural substrate, $GbOse_3Cer$. The results of this study are shown in Figure 32, which shows that α-galactosidase A, but not B purified by the techniques as described here, hydrolyzes the natural substrate, $GbOse_3Cer$.

Kinetic Characterizations. Some of the kinetic parameters of the α-galactosidases were determined in order to compare these enzymes to those in the literature and to establish

Figure 31. Three-dimensional structures of conduritol C and conduritol C epoxide.

These structures were drawn like those made by Legler and Herrchen (142) and are consistent with the data of Figures 27, 28, 29, and 30.

A. Conduritol C

B. Conduritol C Epoxide

A.

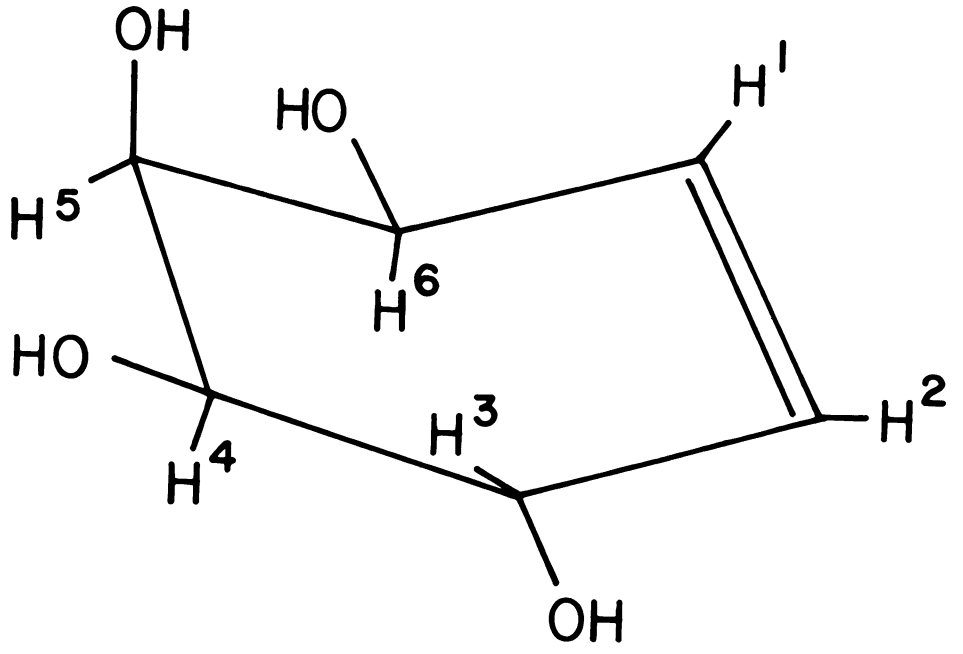

B.

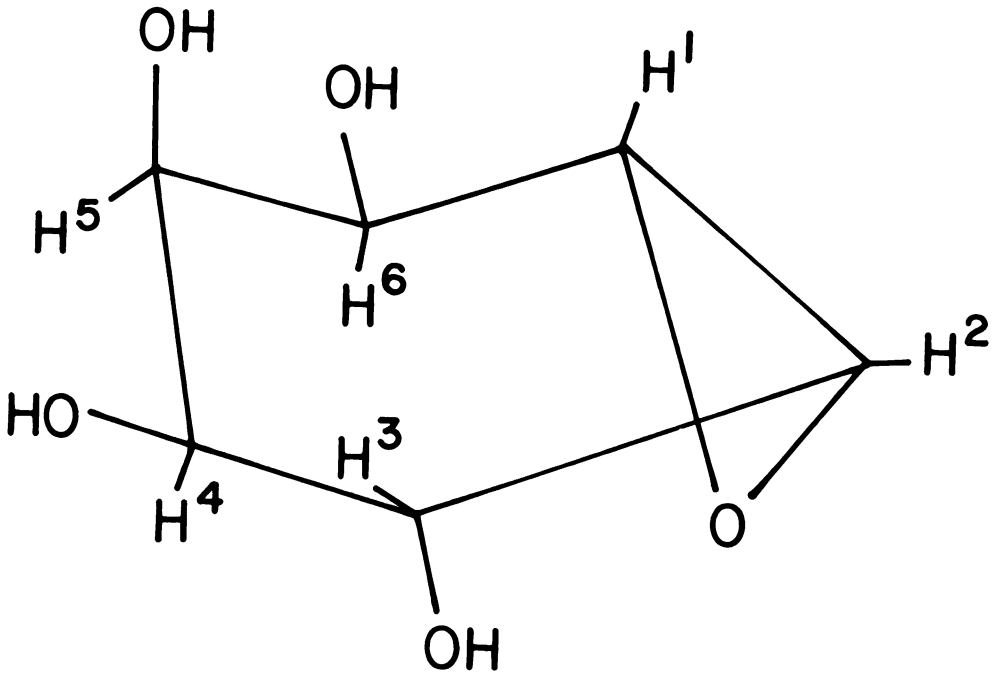

Figure 32. Hydrolysis of $GbOse_3Cer$ by α-galactosidases A and B.

Ten munits of each α-galactosidases were incubated at 37° with 100 nmoles of bovine $GbOse_3Cer$ in a reaction mixture also containing 50 μg of sodium taurocholate and 50 μl of Gomori Citrate-Phosphate pH 4.2. The reaction mixtures were incubated for one hour when an additional 10 munits of the respective enzyme were added. The reactions proceeded for an additional hour and were terminated by boiling. Comparable amounts of the respective reaction mixtures were spotted on a silica gel G plate which was developed in chloroform-methanol-water (65:25:4, v/v/v), and sprayed with the orcinol reagent to visualize the carbohydrates. Lane 1 contained standard LacCer. Lane 2 contained standard bovine $GbOse_3Cer$. Lane 3 contained the products from a reaction mixture that contained α-galactosidase A. Lane 4 contained the products from a reaction mixture that contained α-galactosidase B. Lane 5 contained the products from a reaction mixture that contained no enzyme. Lane 6 contained standard sodium taurocholate.

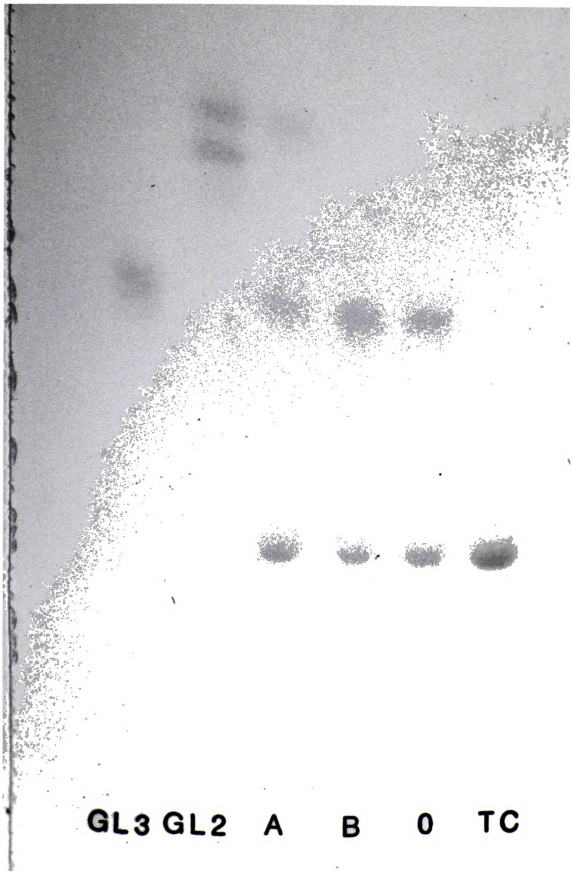
GL3 GL2 A B 0 TC

conditions for determining whether or not CCE is a suicide inhibitor of α-galactosidase A.

The initial velocities at each substrate concentration were determined using approximately one milliunit of enzyme and time points of less than ten minutes, and the initial velocities were calculated by linear regression of two or more non-zero time points. The kinetic constants were determined by a combination of the methods of Wilkinson (146) and Mannervik (147).

α-Galactosidase A. The Km of α-galactosidase A for the synthetic substrate 4-MU-α-Gal is 1.83 mM (Figure 33). Galactose was found to be a competitive inhibitor of α-galactosidase A with a Ki of 16.7 mM (Figure 34). N-Acetylgalactosamine is not an inhibitor of α-galactosidase A (Figure 35). Conduritol C epoxide appears to be a competitive inhibitor of α-galactosidase A with a Ki of 330 mM (Figure 36). This last value was based only upon one concentration of CCE due to a very limited amount of CCE. The Vmax of α-galactosidase A as determined in the presence or absence of the competitive inhibitors was 52.9 ±4.31 units/mg protein.

α-Galactosidase B. The Km of α-galactosidase B for the synthetic substrate 4-MU-α-Gal is 13.10 ± 2.45 mM (Figure 37). Galactose was found to be a competitive inhibitor of α-galactosidase B with a Ki of 27.9 mM (Figure 38).

Figure 33. Lineweaver-Burk plot of the hydrolysis of 4-MU-α-Gal by α-galactosidase A.

The Lineweaver-Burk plot of the hydrolysis of 4-MU-α-Gal by α-galactosidase A was linear with a Km of 1.83 mM and a Vmax of 63.9 ±2.62 μmoles/minute/mg of protein. The initial velocities at each substrate concentration were determined by linear regression analysis of two or more non-zero time points. The kinetic constants were determined by a combination of the methods of Wilkinson (147) and Mannervik (148). All subsequent kinetic data were analyzed in a similar fashion.

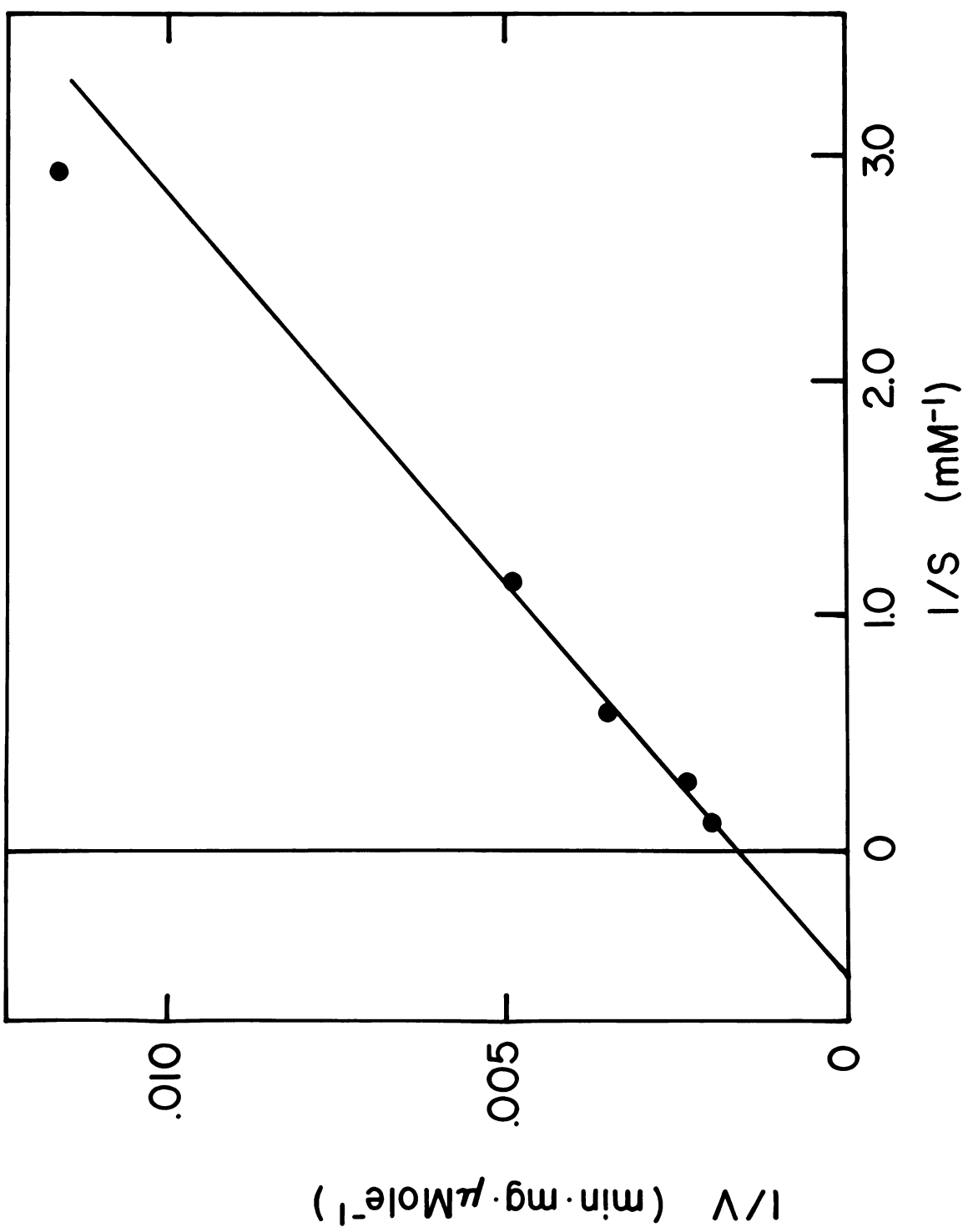
1/V (min·mg·μMole⁻¹)
.010
.005
0
0
1.0
2.0
3.0
1/S (mM⁻¹)

Figure 34. The competitive inhibition by galactose of 4-MU-α-Gal hydrolysis by α-galactosidase A.

The hydrolysis of 4-MU-α-Gal by α-galactosidase A was examined in the presence of galactose at 37° and pH 4.6. Galactose was found to be a competitive inhibitor of α-galactosidase A with a Ki of 16.7 mM.

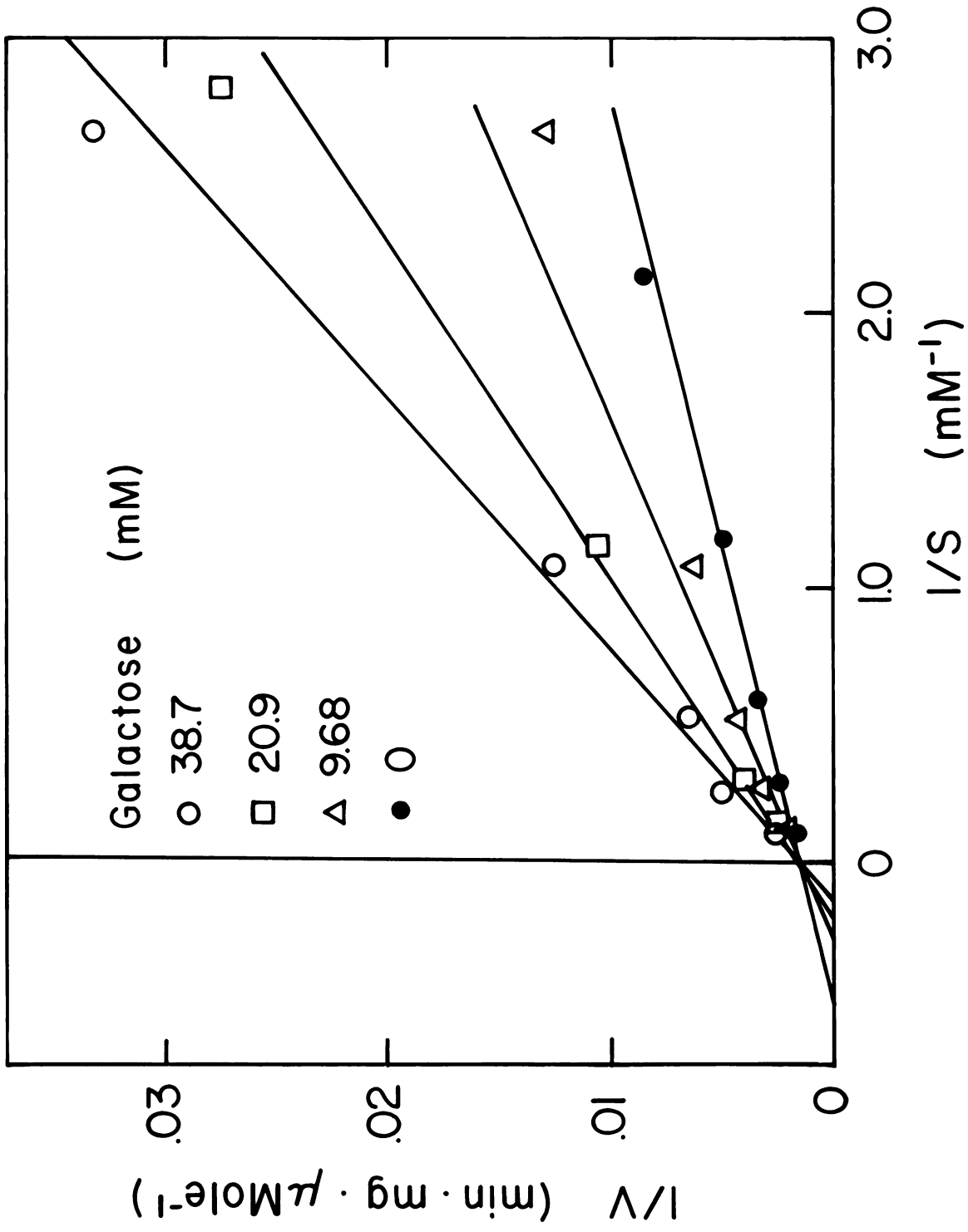
Galactose (mM)
38.7
20.9
9.68
0
1/V (min · mg · μMole⁻¹)
1/S (mM⁻¹)
0
.01
.02
.03
1.0
2.0
3.0

Figure 35. The effect of GalNAc on the hydrolysis of 4-MU-α-Gal by α-galactosidase A.

The hydrolysis of 4-MU-α-Gal by α-galactosidase A was examined in the presence of GalNAc at 37° and pH 4.6. GalNAc was found not to be an inhibitor of α-galactosidase A.

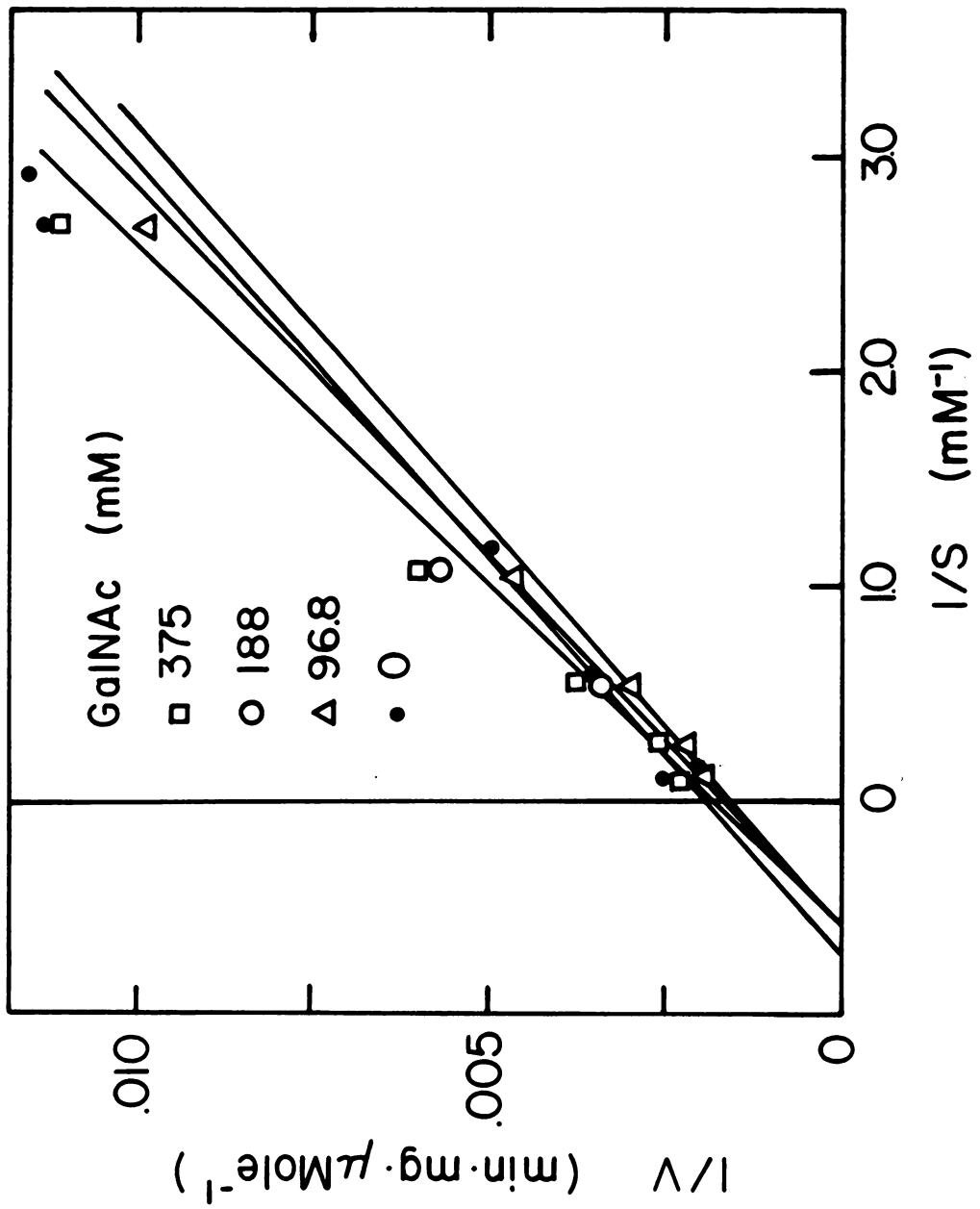
GalNAc (mM)
□ 375
○ 188
△ 96.8
● 0
0
.005
.010
1/V (min·mg·μMole⁻¹)
0
1.0
2.0
3.0
1/S (mM⁻¹)

Figure 36. The inhibition by conduritol C epoxide of 4-MU-α-Gal hydrolysis by α-galactosidase A.

The hydrolysis of 4-MU-α-Gal by α-galactosidase A was examined in the presence of conduritol C epoxide at 37° and pH 4.6. Conduritol C epoxide appeared to be a competitive inhibitor with a Ki of 330 mM.

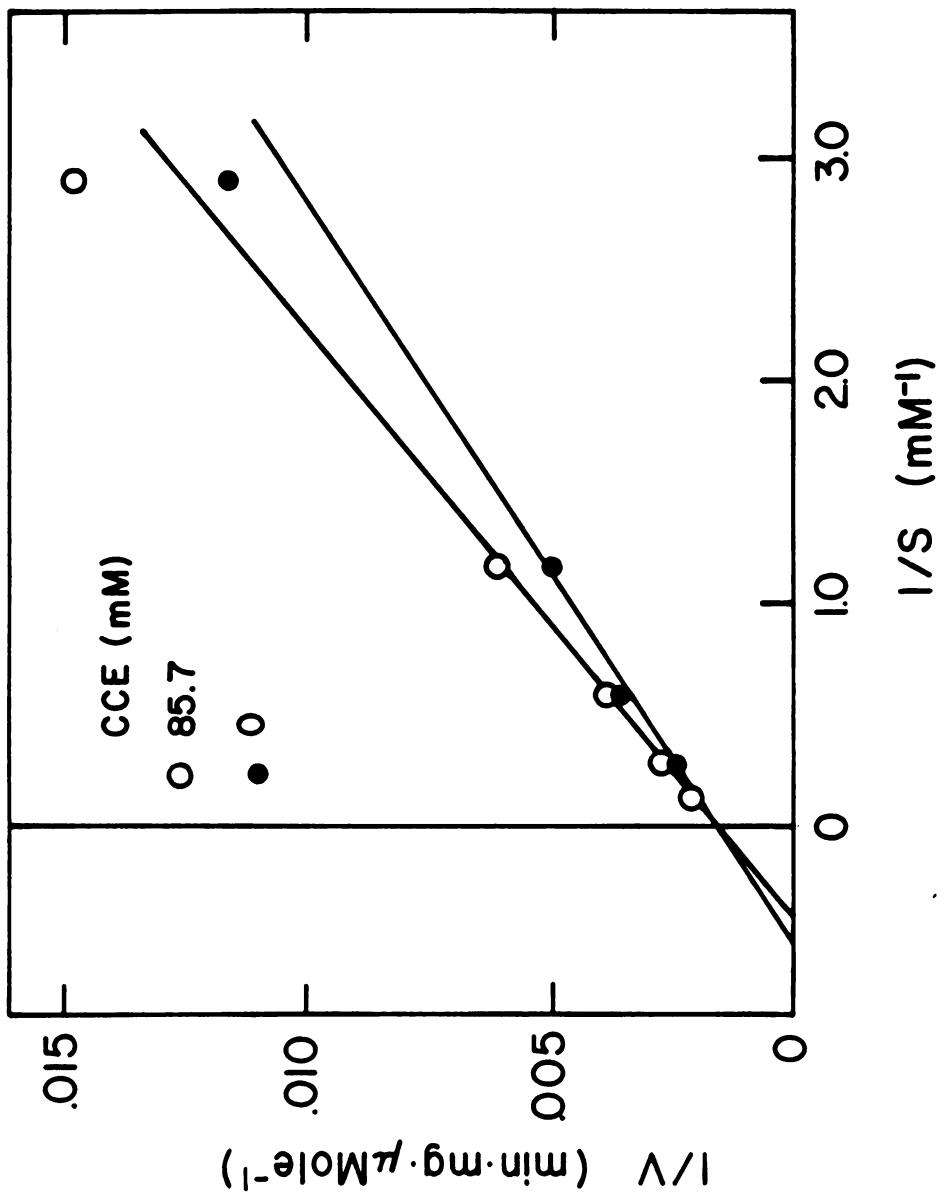
1/V (min·mg·μMole⁻¹)
.015
.010
.005
0
0
1.0
2.0
3.0
1/S (mM⁻¹)
CCE (mM)
85.7
0
0

Figure 37. Lineweaver-Burk plot of the hydrolysis of 4-MU-α-Gal by α-galactosidase B.

The Lineweaver-Burk plot of the hydrolysis of 4-MU-α-Gal by α-galactosidase B was linear with a Km of 13.10 ±2.45 mM and a Vmax of 13.9 ±1.68 moles/minute/mg of protein.

1/V (min·mg·μMole-1)
0.1
0.05
0
0
0.5
1.0
1/S (mM-1)

Figure 38. The competitive inhibition by galactose of 4-MU-α-Gal by α-galactosidase B.

The hydrolysis of 4-MU-α-Gal was examined in the presence of galactose at 37° and pH 4.6. Galactose was found to be a competitive inhibitor of α-galactosidase B with a Ki of 27.9 mM.

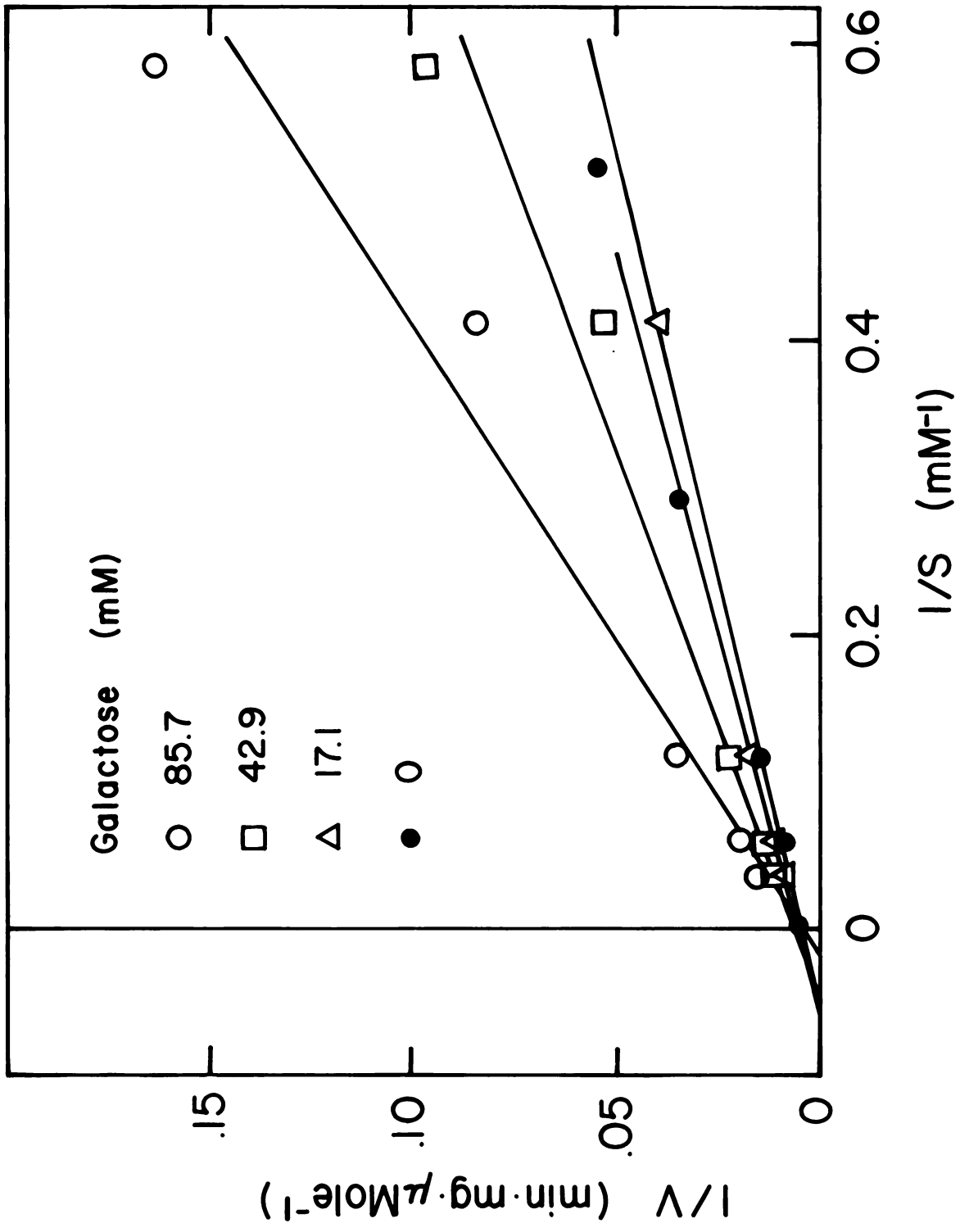
1/V (min·mg·μMole⁻¹)
.15
.10
.05
0
0
0.2
0.4
0.6
1/S (mM⁻¹)
Galactose (mM)
85.7
42.9
17.1
0

N-Acetyl-D-galactosamine was found to be a competitive inhibitor of α-galactosidase B with a Ki of 1.65 mM (Figure 39). The Vmax of α-galactosidase B in the presence or absence of the competitive inhibitors was 13.9 ± 1.68.

Conduritol C Epoxide Inhibition of α-Galactosidase A

It was reported to us (148) that conduritol C epoxide inhibits α-galactosidase A at 37° with a T 1/2 of 210 minutes at a concentration of 10 mM CCE. Later, we were told that a concentration of at least 100 mM CCE was required for inactivating splenic α-galactosidase A (149). Because of the thermal and pH instability of α-galactosidase A, reaction conditions were determined that would allow reaction between CCE and the enzyme and yet maintain enzyme activity in the absence of CCE. A pH of 6.5 and a temperature of 4° were found to be satisfactory.

Pure α-galactosidase B and partially purified α-galactosidase A were incubated at 4° at pH 6.5 for several days in 100 mM CCE, and samples were assayed at various times for enzyme activity. The results of this study are shown in Figure 40, and the data are expressed as 100 times the ratio of the amount of product formed in the presence of CCE (E_I) relative to the amount of product formed in the absence of CCE (E_o) and plotted on a natural log scale. Conduritol C epoxide inhibited both enzymes in a time-dependent fashion, but the rate of

Figure 39. The competitive inhibition by GalNAc of 4-MU-α-Gal hydrolysis by α-galactosidase B.

The hydrolysis of 4-MU-α-Gal by α-galactosidase B was examined in the presence of GalNAc at 37^{o} and pH 4.6. GalNAc was found to be a competitive inhibitor of α-galactosidase B with a Ki of 1.65 mM.

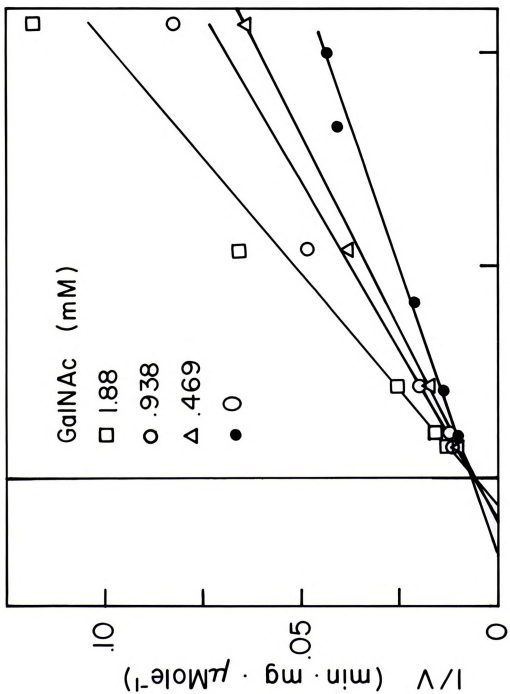
GalNAc (mM)
□ 1.88
○ .938
△ .469
● 0
1/V (min · mg · μMole⁻¹)
0
.05
.01
0
.25
.5
1/S (mM⁻¹)

Figure 40. Time-dependent inactivation of α-galactosidases A and B by conduritol C epoxide.

Human liver α-galactosidases A (closed circles) and B (open circles) were incubated at 4^{o} in 10 mM sodium phosphate pH 6.5 containing 100 mM Conduritol C Epoxide for various times up to 168 hours. α-Galactosidases A and B were assayed for two minutes with 4-MU-α-Gal and p-NP-α-GalNAc respectively. The data are expressed as 100 times the ratio of the amount of product formed in the presence of CCE (E_I) relative to the amount of product formed in the absence of CCE (E_0) and plotted on a natural log scale. The rates of inactivation were determined by regression analysis and found to be 5.40×10^{-2} and 1.10×10^{-2} $hr^{-1} \cdot mole^{-1} \cdot l$ for α-galactosidase A and B, respectively. The correlation coefficients for the rates are .9889 and .6625 for α-galactosidase A and B, respectively.

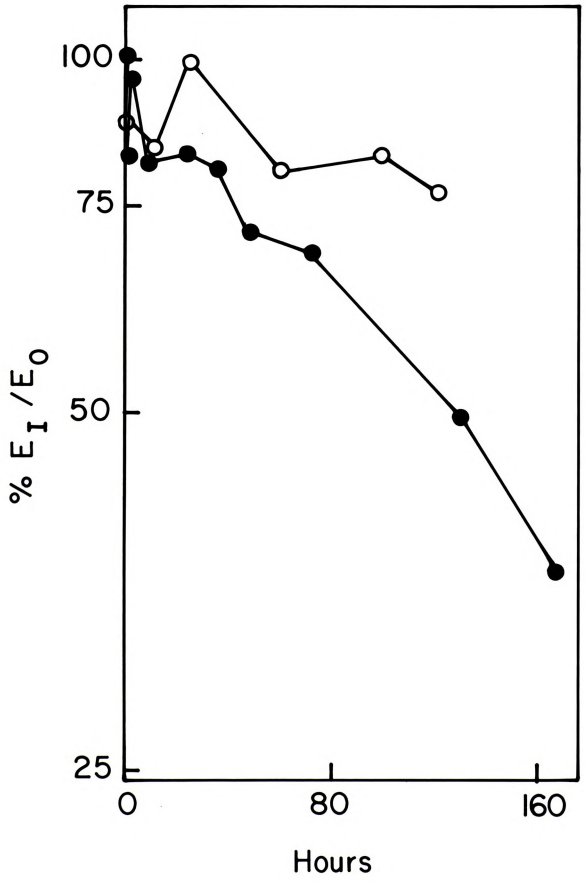
100
75
50
25
% E_I / E_0
0
80
160
Hours

inactivation of α-galactosidase B, as determined by regression analysis, was 20.5% that of α-galactosidase A. This inactivation is characteristic of suicide inhibitors. The regression line for α-galactosidase A included all time points, except for the time points from one through six hours when the data points were quite variable. Since the inactivation of α-galactosidase B was so slow (The T 1/2 for inactivation would be 26 days), subsequent experiments with conduritol C epoxide were performed only with α-galactosidase A.

After galactose was found to be a competitive inhibitor of α-galactosidase A with a Ki of 16.7 mM, a series of experiments were performed to determine if CCE is a suicide inhibitor of α-galactosidase A. Pure α-galactosidase A was incubated at 4^{o} in 10 mM sodium phosphate, pH 6.5, containing 1.0 mg/ml BSA to stabilize the enzyme. Four series of tubes were used in the experiment: the first had no inhibitor and these were used as controls, the second contained galactose, the third contained CCE, and the fourth contained both galactose and CCE. The concentration of inhibitor was 100 mM in all cases. Two or more samples were assayed with 4-MU-α-Gal at each time point for times up to 128 hours (It is important to note that the concentration of inhibitor was about 15 mM in the assay mixture). The data are expressed as 100 times the ratio of the amount of product formed in the presence of inhibitor (E_I) relative to the amount of product

formed in the absence of inhibitor (E_o) and plotted on a natural log scale as shown in Figure 41. These data show that the enzyme is inhibited by CCE alone to a similar extent (T 1/2 of inhibition was 75 hours) as seen in Figure 40, and that the enzyme is inhibited to a similar extent by galactose and by galactose in combination with CCE. These data show that the time-dependent inactivation of α-galactosidase A by conduritol C epoxide is substantially reduced (90.7%) by galactose, a competitive inhibitor of α-galactosidase A. The protection experiment demonstrated that CCE is a suicide inhibitor of α-galactosidase A.

Purification of Commercially Tritiated Conduritol C Epoxide. As can be seen in Figure 42, very little of the radioactivity, 100 mCi, co-migrated with authentic CCE. The material was purified by column chromatography on Iatrobeads and gel filtration on G-25. Those fractions having the same TLC mobility as CCE were pooled, and the yield was approximately 27% or 30 mg of CCE. The specific activity of the material was 2.5×10^9 cpm per mmole or 2.5×10^3 cpm per nmole.

Inactivation of α-Galactosidase A with Tritiated Conduritol C Epoxide. Fifteen milliunits of purified α-galactosidase A (330 μg) were incubated at 4^o in 2 ml of 10 mM sodium phosphate buffer (pH 6.5) containing the 30 mg of tritiated conduritol C epoxide. Aliquots were removed from the reaction mixture and assayed with 4-MU-α-Gal to assess the

Figure 41. Protection of α-galactosidase A by galactose from inactivation by conduritol C epoxide.

Human liver α-galactosidase A was incubated at 4^{o} in 10 mM sodium phosphate, pH 6.5, containing 0.5% BSA in the presence or absence of inhibitors for various times up to 128 hours. The samples were assayed with 4-MU-α-Gal for two minutes. Results are expressed as 100 times the ratio of the amount of product formed in the presence of inhibitor (E_I) relative to the amount of product formed in the absence of inhibitor (E_0) and plotted on a natural log scale. One series of tubes contained 100mM galactose (closed circles), another 100mM of both galactose and CCE (open circles), and the other had 100mM CCE (open squares). The rates for inactivation were analyzed by regression analysis, and the rates for inactivation in the presence of galactose, galactose plus CCE, and CCE alone were found to be 6.07×10^{-5}, 9.03×10^{-3}, and 9.64×10^{-2} hr^{-1}. $mole^{-1} \cdot l$, respectively. The correlation coefficients for the rates of inhibition are .1099, .6370, and .9689 for gal, gal plus CCE, and CCE, respectively.

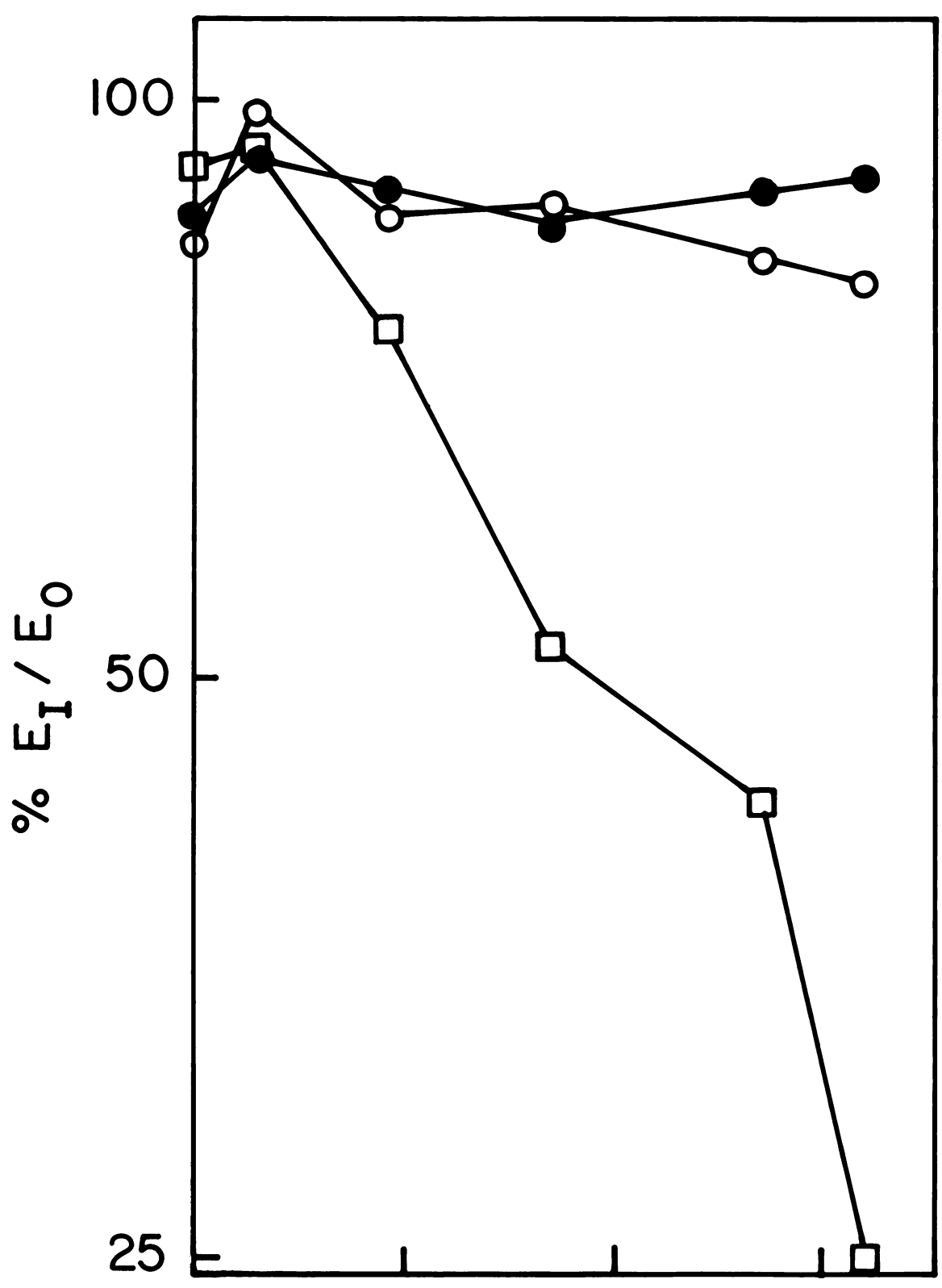
100
50
25
% E_I / E_O
0
40
80
120
Hours

Figure 42. Purity determination of tritiated conduritol C epoxide.

An aliquot of the commercially tritiated conduritol C epoxide was spotted on a silica gel TLC plate which was developed in EtOH, EtOAc, water (2:8:1, v/v/v). The plate was sprayed with methyl red reagent (131) to visualize the CCE. A scan of the plate with a Berthold LB 2760 TLC scanner indicated that less than 1% of the radioactivity migrated with authentic conduritol C epoxide which indicated the material needed to be further purified.

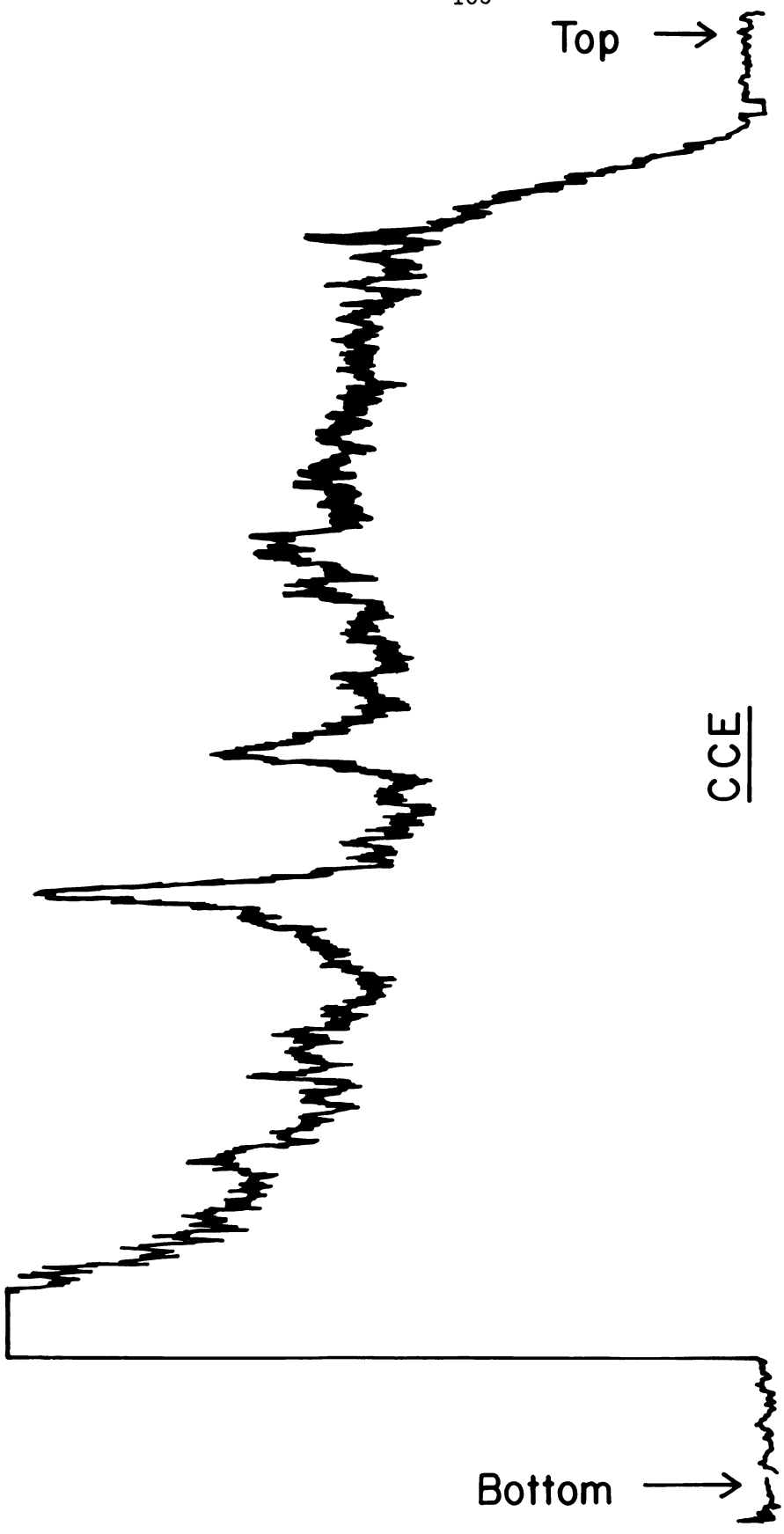
Top
CCE
Bottom

extent of inactivation over 300 hours. Data are expressed as 100 times the ratio of the amount of product in the presence of CCE (E_I) relative to the original amount of enzyme activity (E_o) and plotted on a natural log scale (Figure 43). The data through 180 hours were analyzed by least squares, and the T 1/2 for the inactivation of α-galactosidase A was 75 hours. The specific activity of the radiolabeled enzyme was 15,700 cpm/nmole of monomer, which indicates that six molecules of CCE reacted per monomer of α-galactosidase A.

Figure 43. Inhibition of α-galactosidase A by tritiated conduritol C epoxide.

Fifteen units of α-galactosidase A were incubated with 30 mg of tritiated CCE in 2ml of 10 mM sodium phosphate, pH 6.5, buffer at 4^{o} for thirteen days. Aliquots were removed at various times and assayed with 4-MU-α-Gal. The data are expressed as 100 times the amount of activity in the presence of inhibitor (E_I) relative to the initial activity (E_0) and are plotted on a natural log scale. The data through 180 hours were analyzed by regression analysis, and the regression line is shown. The T 1/2 for the inactivation of α-galactosidase was 75 hours.

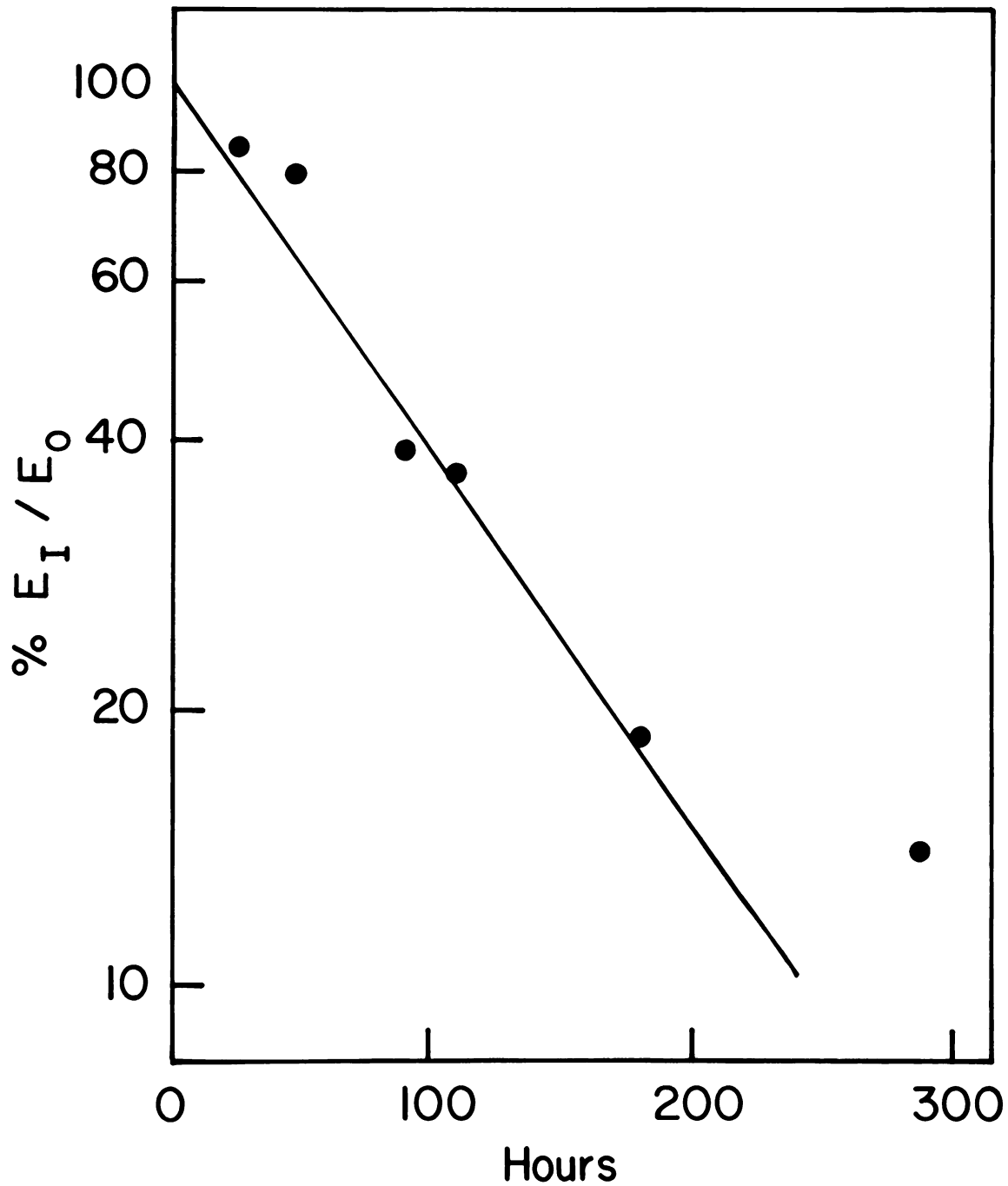
100
80
60
40
20
10
% E_I / E_0
0
100
200
300
Hours

DISCUSSION

The Purification Procedure. The first few steps of the enzyme purification were straight-forward, and the yields were good primarily because very little enzyme was discarded in order to maximize the yield. These extra steps included the re-extraction of the pellets from the first homogenization, extracting with Con-A Sepharose of some rather gooey material that contained several units of enzyme, the elution of the DE-52 column with 1.0 M NaCl to save a few more units of enzyme, and saving the side fractions from the DE-52 and G-150 columns.

Two procedures that were previously used in the purification of human liver α-galactosidases (104,105), hydroxyapatite and ampholyte displacement chromatography, were eliminated from the purification scheme. In this study, the yield at the hydroxyapatite chromatography step was 70 to 80%, but the hydroxyapatite did not remove any contaminant that could not be removed by affinity chromatography. Ampholyte displacement was removed from the purification scheme because the yield at that step was 36%, and the enzyme was about 40% pure (it is my opinion that the two major impurities could have been removed by gel filtration on G-150, but the overall yield would have been 24%).

In one purification, the Con-A Sepharose extract was

concentrated and applied to the G-150 column with the intention of by-passing the DEAE column. Something in the enzyme preparation bound to the Sephadex causing the beads to shrink and the column to stop. Apparently the DE-52 removes this component from the enzyme preparation.

The Affinity Resin. The affinity resin first used was identical to that of Bishop and Desnick (16) which involved the coupling of the affinity ligand N-6-aminohexanoyl-α-D-galactopyranosylamine to carboxyhexyl-Sepharose with a carbodiimide. Initial attempts to purify either α-galactosidase gave yields of from five to fifty per cent, but generally less than twenty-five per cent. In addition the bulk of unwanted proteins bound to the affinity resin which indicated that there were numerous free carboxyl groups remaining from the carboxyhexyl-Sepharose. It was decided to reduce the non-specific interaction of the affinity resin by attaching the affinity ligand directly to Sepharose 4B with cyanogen bromide. In the first use of such an affinity resin, Harpaz and Flowers (109) used a spacer arm synthesized from two molecules of 6-aminohexanoic acid. It was decided to attach the affinity ligand with a spacer arm of only one molecule of 6-aminohexanoic acid because Lowe et al. (150) showed that affinity resins having a spacer arm of from six to eight methylene groups are much more effective that those with ten or more methylenes.

The unwanted proteins were eluted from the affinity

resin with Gomori citrate-phosphate buffer (pH 4.6) containing 0.15 M NaCl until the A_{280} of the effluent was zero before beginning the pH-salt gradient. In one purification the affinity resin was washed with the pH 4.6 buffer as usual, the pH-salt gradient was run, then the resin was washed with Gomori citrate-phosphate, pH 6.0, containing 0.5 M NaCl until the A_{280} of the effluent was zero before the enzyme was eluted with galactose. The yield of enzyme in the galactose eluate was three per cent. The lost enzyme was found in the fractions from the pH 6.0 wash; it was found that a pH above 5.5 elutes α-galactosidase A from the affinity resin.

The yield of α-galactosidase A at the affinity chromatography step with the new spacer arm was consistently between twenty-five and fifty per cent. Since the pI of the liver enzyme is 4.6 (105), it was decided to acidify the enzyme only to pH 5.0 prior to applying the enzyme to the affinity resin. In both a trial and a large purification of α-galactosidase A, the yield was 70%. Acidification to a slightly higher pH, but below the 5.5 at which the enzyme non-specifically elutes from the resin, may improve the yield even more. The acidification of α-galactosidase B to pH 4.7 does not lead to poor yields of the enzyme even though its pI is 4.5 (104). The main precaution about the affinity purification of α-galactosidase B is that the enzyme activity in addition to the A_{280} of the pH 4.7 eluted fractions should be

monitored as the enzyme can non-specifically bleed off. The α-galactosidase B should be eluted with Gomori citrate-phosphate, pH 4.6, containing 0.15 M NaCl and 0.4 M galactose after the bulk of the unwanted proteins have eluted but before much of the enzyme has bled off. The yield of α-galactosidase B at the affinity chromatography step was generally about 80%.

In another experiment, the Con-A extract was acidified to pH 4.7 and mixed with the affinity resin. The enzyme was eluted from the affinity resin, but the yield was only 25%, and the enzyme was very impure. It would be reasonable for future investigators to apply enzyme acidified to pH 5.0 or 5.2 from an earlier step in the purification procedure to the affinity resin. If the yield is over 70% at that step, the overall yield would be greatly improved. Such a procedure has been developed for the purification of human liver α-L-fucosidase by Alhadeff et al. (15). These investigators purified α-L-fucosidase from a 100,000 X g supernatant of the total homogenate with two passes over a comparable fucosylamine affinity resin as was used in this study.

Dual Affinity Chromatography. The separation of the mixture of α-galactosidases A and B from the DEAE step presented a challenge as both enzymes have similar molecular weights (104 and 90 Kd, respectively) and nearly identical isoelectric points (4.6 and 4.5, respectively). A variety of unsuccessful attempts were made to completely

resolve them including differential elution from Con A-Sepharose, re-chromatography on DEAE, chromatography on hydroxylapatite, and heat inactivation of α-galactosidase A. It was then thought that since both α-galactosidases bind to the affinity resin and GalNAc inhibits α-galactosidase B, but not A, that GalNAc would selectively elute -galactosidase B from the affinity resin. A concentration of 50 mM GalNAc was chosen to elute the α-galactosidase B because 50 mM GalNAc preferentially inactivates the α-galactosidase B in the assay for α-galactosidase A. This idea proved to be correct, and this separation has proven very useful in improving the yield of both enzymes. The importance of this procedure was proven in that 79% of the α-galactosidase A that was sequenced was originally in the A plus B fraction that eluted from the DEAE column.

Yields of Enzymes. The overall yield of α-galactosidase A of 58% in the procedure developed here compares favorably to the 5.6% yield from placenta (17), the 27% yield from liver (105), and the 31% yield from spleen (16), especially since the placental and liver enzymes were not pure. The overall yield of α-galactosidase B of 37% in this procedure is comparable to the 35% from placenta (17) and the 21% yield from liver (104), both of which appeared to be pure by gel electrophoresis.

Physical Characterizations of the Purified α-Galactosidases

The purified α-galactosidase A has a subunit molecular weight of 47,800 daltons, as determined by SDS-gel electrophoresis, and this value is similar to the 49,800 daltons reported for the splenic enzyme. Since the native molecular weight is 104,000 (105), and N-terminal sequencing yielded a unique sequence, α-galactosidase A must be a homodimer, which had heretofore only been postulated.

The subunit molecular weight of α-galactosidase B is 46,800 compared to the 47,700 reported for the placental enzyme (17). Since the native molecular weight of the liver enzyme has been reported to be 90,000 (105), and the N-terminal sequencing gave a single sequence, α-galactosidase B is composed of homodimers as is the A enzyme.

The specific activity of α-galactosidase A of 45.2 units/mg of protein, compares favorably with the 31.3 reported for the splenic enzyme (16). The specific activity of 4.18 units/mg of α-galactosidase B purified here is comparable to the 4.52 reported for the placental (17) and somewhat lower than the 6.56 previously reported for the liver enzyme (104).

The two α-galactosidases had very similar amino acid compositions (Table 4), but this similarity did not extend to other human lysosomal enzymes.

The results of N-terminal sequencing were gratifying

because 1) some other human lysosomal glycosidases have been found to have a blocked N-terminus (15,19); 2) the sequencing gave single sequences for both proteins, indicating that both proteins were pure and that the proteins were homodimers so that it would not be necessary to separate the subunits if they had been heterodimers; and 3) we postulated that the homologous N-terminal region of the α-galactosidases was either a general marker for all lysosomal hydrolases or just a region of homology between two enzymes that have similar functions.

The possibility that the N-terminal sequence found in the two α-galactosidases exists in other glycosidases and serves as a signal for glycosylation, peptide cleavage, or delivering the enzymes to the lysosome was discounted by the absence of a similar N-terminal sequence in either placental α-L-fucosidase (25) or β-glucocerebrosidase (26). To determine if both α-galactosidases have homology throughout, tryptic peptides of both α-galactosidases were generated. We were successful at purifying peptides of α-galactosidase B for N-terminal sequencing, while other workers obtained those from α-galactosidase A (27). It can be seen in Table 6 that none of the tryptic peptides of α-galactosidase A are identical to those of α-galactosidase B, which indicates that the region of homology between these two enzymes is restricted to the N-terminal region.

Kinetic Characterizations. The Km of 1.83 mM for the hydrolysis of the artificial substrate 4-MU-α-Gal by

α-galactosidase A is quite similar to the 3.4 mM (103) and 1.55 mM (17) for the placental enzymes, 2.9 mM previously reported for the liver enzyme (105) and 2.03 mM for the splenic enzyme (16); of these other determinations only the splenic enzyme was pure. The Vmax of 63.9 units/mg of protein is greater than the 46.7 units/mg for the splenic enzyme (16). The Km of 13.1 mM of α-galactosidase B towards the artificial substrate 4-MU-α-Gal is identical to the 13.1 reported for the placental enzyme and higher than the 6.7 mM previously reported for the liver enzyme (104). The Vmax of 13.9 for the α-galactosidase B purified here is less than the 18.9 reported previously for the liver enzyme (104) which is the only other report of a Vmax for this enzyme.

Galactose was found, as expected, to be a competitive inhibitor of both α-galactosidases with a Ki of 16.7 and 27.9 mM for A and B, respectively. Galactose was previously reported to be a competitive inhibior of splenic α-galactosidase A with a Ki of 21 mM (16). GalNAc was found to be a competitive inhibitor of α-galactosidase B with a Ki of 1.65 mM; o-NP-α-GalNAc, another artificial substrate for α-galactosidase B, was previously reported to be a competitive inhibitor of α-galactosidase B with a Ki of 2.7 mM (112).

In a non-quantitative hydrolysis of $GbOse_3Cer$ α-galactosidase A, but not α-galactosidase B, hydrolyzed the lipid to lactosyl ceramide. This is consistent with

the findings of Kusiak et al. (17) who found that α-galactosidase A is 300 times more effective than α-galactosidase B in hydrolyzing this lipid. It was previously reported (104,105) that α-galactosidase B is 38% as effective as α-galactosidase A in hydrolyzing $GbOse_3Cer$. It is possible that the previous purification of α-galactosidase B from liver (104) contained some α-galactosidase A, which would account for the significant differences in Km, Vmax and specific activity that were noted above.

Inactivation of α-Galactosidases A and B by Conduritol C Epoxide. Conduritol B cis epoxide is a structural analogue of ß-D-glucose. CBE has previously been shown to be a competitive inhibitor of the lysosomal enzyme ß-glucocerebrosidase (48). CBE (40,42) and a related compound (43) were shown to be active site directed reagents and useful in determining the active site sequences of three non-lysosomal glycosidases. We decided that if any conduritol epoxide were an inhibitor of either α-galactosidase, that it would be conduritol C trans epoxide, and in searching the literature, we found that coffee bean α-galactosidase was inhibited by CCE (142).

CCE was synthesized and was found to inhibit both α-galactosidases in a time-dependent fashion at 4^{o} and pH 6.5, which is fully two pH units above the pH optimum of both enzymes (104,105). These data suggested that conduritol C epoxide is a suicide inhibitor of both

enzymes. Since the rate of inactivation of α-galactosidase B was so slow, further inhibition studies were performed only on α-galactosidase A.

To verify that conduritol C epoxide is a suicide inhibitor of α-galactosidase A, an experiment was performed that showed that galactose, a competitive inhibitor of α-galactosidase A, blocked the time-dependent inactivation of α-galactosidase A. Although conduritol B epoxide can be inferred to be a suicide inhibitor of ß-glucocerebrosidase because CBE has been shown to reduce the in vivo level of ß-galactocerebrosidase in mice (47), this is the first demonstration of a suicide inhibitor of any lysosomal glycosidase.

In addition, CCE appeared to be a competitive inhibitor of α-galactosidase A with a Ki of 330 mM which is also characteristic of a suicide inhibitor. This Ki is much higher than the 1.2 μ M of CBE for ß-glucocerebrosidase (48). This may be due to CCE having a more rigid conformation than CBE (The proton NMR spectra of conduritol C and CCE indicate they have very similar structures, while the spectrum of conduritol B, data not shown, indicates conduritol B is a less rigid molecule). Conduritol B epoxide may rapidly change conformations, one of which may be similar to the ß-glucosyl moiety hydrolyzed by ß-glucocerebrosidase. Additionally, it has been shown the ß-glycosidases are inhibited 50 to 200 times more rapidly with the corresponding conduritol epoxide than are

the respective α-glycosidases with their conduritol epoxide (Reviewed reference 151).

The suicide inhibitor-enzyme mixture is generally diluted prior to assaying the enzyme, which was done here. Since the concentration of CCE in the assay mixture was about 15 mM and the Ki of CCE towards α-galactosidase A was found to be 330 mM, the CCE should inhibit the α-galactosidase A about 1.3% in the assay mixture.

There are three lines of evidence that conduritol C epoxide is a suicide inactivator rather than only inhibiting enzyme activity: 1) CCE very poorly inactivated α-galactosidase B, which efficiently hydrolyzes many of the same water-soluble oligosaccharides as α-galactosidase A (108), 2) Galactose, a competitive inhibitor of α-galactosidase A, blocked the time-dependent inactivation of α-galactosidase A, which indicates the inactivation occurs at the active site, and 3) α-Galactosidase A was inactivated by as much as 75% in these studies, and this would have required 3.3 M CCE in the assay mixture as calculated from the Ki of 330 mM.

CCE was commercially tritiated, purified, and used to label 15 milliunits of pure α-galactosidase A. This was performed in order that a radioactive peptide could be purified by HPLC, and the peptide sequenced. The protein was not digested to peptides because of the difficulties previously mentioned in separating α-galactosidase A peptides. Another difficulty was that the enzyme appeared

to be labelled by six molecules of tritiated CCE per monomer. This may have been due to incomplete dialysis of the CCE from the protein, the formation of a reactive compound during tritiation of the CCE, or the formation of a reactive compound during catalysis that moved from the active site of the enzyme then reacted with the enzyme.

BIBLIOGRAPHY

BIBLIOGRAPHY

1. deDuve, C., Pressman, B. C., Gianetto, R., Wattiaux, R., and Appelmans, F. (1955) Biochem. J. 60, 604-617

2. deDuve, C. (1969) in Lysosomes in Biology and Pathology (Dingle, J. T., and Fell, H. B. eds.) North-Holland Publishing Co. Amsterdan pp. 3-40

3. deDuve, C. (1963) Harvey Lect. 59, 49-87

4. Stanbury, J. B., Wyngaarden, J. B., Fredrickson, D. S., Goldstein, J. L., and Brown, M. S., Editors (1983) Metabolic Basis of Inherited Disease 751-969 McGraw Hill

5. Jones, M. Z., and Laine, R. A. (1981) J. Biol. Chem. 256, 5181-5184

6. Jones, M. Z., and Dawson, G. L. (1981) J. Biol. Chem. 256, 5185-5188

7. Galjaard, H., and Reuser, A. J. J. (1984) In Lysosomes in Biology and Pathology (Dingle, J. T., Dean, R. T., and Sly, W. S., eds.) Elsevier Amsterdam pp. 315-345

8. Glossl, J. Truppe, W., and Kresse, J. (1979) Biochem. J. 181, 37-46

9. von Figura, K. (1977) Eur. J. Biochem. 80, 525-533

10. Warner, T. G., Dambach, L. M., Shin, J. H., and O'Brien, J. S. (1980) Am. J. Human Genet. 32, 869-879

11. Draper, R. K., Fiskum, G. M., and Edmond, J. (1976) Arch. Biochem. Biophys. 177, 525-538

12. McGovern, M. M., Vine, D. T., Haskins, M. E., Desnick, R. J. (1982) J. Biol. Chem. 257, 12605-12610

13. McGovern, M. M., Aula, P., and Desnick, R. J., (1983) J. Biol. Chem. 258, 10743-10747

14. Contractor, S. F., Mason, R. M., and Oakey, M. (1982) Placenta 3, 45-56

15. Alhadeff, J. A., Miller, A. L., Wenass, H., Vedick, T., and O'Brien, J. S. (1975) J. Biol.Chem. 250, 7106-7113

16. Bishop, D. F., and Desnick, R. J. (1981) J. Biol. Chem. 256, 1307-1316

17. Kusiak, J. W., Quirk, J. M., Brady, R. O., and Mook, G. E. (1978) J. Biol. Chem. 253, 184-190

18. Lo, J-t., Mukerji, K., Awasthi, Y. C., Hanada, E., Suzuki, K., and Srivastava, S. K. (1979) J. Biol. Chem. 254, 6710-6715

19. Frost, R. G., Holmes, E. W., Norden, A. G. W., and O'Brien, J. S. (1978) Biochem. J. 175, 181-188

20. Strasberg, P. M., Lowden, J. A., and Mahuran, D. (1982) Can. J. Biochem. 60, 1025-1031

21. Brot, F. E., Bell, Jr., C. E., and Sly, W. S., (1978) Biochem. 17, 385-391

22. deBarsy, T., Jacquemin, P., Devos, P., and Hers, H-G. (1972) Eur. J. Biochem. 31, 156-165

23. Geiger, B., and Arnon, R. (1976) Biochem. 15, 3484-3493

24. Jones, C. S., Shankaran, P., Davidson, D. J., Poulos, A., and Callahan, J. W. (1983) Biochem. J. 209, 291-297

25. Fukushima, H., de Wet, J. R., and O'Brien, J. S. (1985) Proc. Nat. Acad. Sci. U. S. A. 82, 1262-1265

26. Martin, B. M., Murray, G. J.Coligan, J. E., Raum, M., Brady, R. O., and Barranger, J. A. (1984) Amer. Soc. Biol. Chem. Abstr. #2640

27. Martin, B. M., Murray, G. J., Merkle-Lehman, D., Ginns, E. I., Zirzow, G. C., and Barranger, J. A. (1985) Fed. Proc. Abstr. #3801

28. Rohrborn, W., and von Figura, K. (1978) J. Physiol. Chem. 359, 1353-1362

29. Alhadeff, J. A., and Freeze, H. (1977) Mol. Cell. Biochem. 18, 33-37

30. Sweeley, C. C., LeDonne, N. C., Jr., and Robbins, P. W. (1983) Arch. Biochem. Biophys. 223, 158-165

31. LeDonne, N. C., Jr., Fairley, J. L., and Sweeley, C. C. (1983) Arch. Biochem. Biophys. 224, 186-195

32. Takahashi, T., Schmidt, P. G., and Tang, J. (1983) J. Biol. Chem. 258, 2819-2830

33. Takasaki, S., Murray, G. S., Furbish, F. S., Brady, R. O., Barranger, J. A., and Kobata, A. (1984) J. Biol. Chem. 259, 10112-10117

34. Cuatrecasas, P., and Roth, T. (1983) Receptor-Mediated Endocytosis Chapman and Hall London and New York 304pp.

35. Ohkuma, S., and Poole, B. (1978) Proc. Nat. Acad. Sci. U. S. A. 75, 3327-3331

36. Gartner, S., Conzelman, E., and Sandhoff, K. (1983) J. Biol. Chem. 258, 12378-12385

37. Conzelmann, E., and Sandhoff, K. (1978) Proc. Nat. Acad. Sci. U. S. A. 75, 3979-3983

38. Shapiro, L. J., Aleck, K. A., Kaback, M. M., Itabashi, H., Desnick, R. J., Brand, N., Stevens, R. L., Fluharty, A. L., and Kihara, H. (1979) Pediatr. Res. 13, 1179-1181

39. Stevens, R. L., Fluharty, A. L., Kihara, H., Kaback, M. M., Shapiro, L. J., Marsh, B., Sandhoff, K., and Fischer, G. (1981) Am. J. Hum. Genet. 33, 900-906

40. Bause, E., and Legler, G. (1974) Z. Physiol. Chem. 355, 438-442

41. Legler, G., and Harder, A. (1978) Biochem. Biophys. Acta 524, 102-108

42. Quaroni, A., and Semenza, G. (1976) J. Biol. Chem. 251, 3250-3253

43. McKelvy, J. F., Eshdat, Y., and Sharon, N. (1970) Israel J. Chem. 8, 170

44. Fowler, A. V., Zabin, I., Sinnott, M. L., and Smith, P. J. (1978) J. Biol. Chem. 253, 5283-5285

45. Lalegerie, P., Legler, G., and Yon, J. M. (1982) Biochimie 64, 977-1000

46. van Diggelen, O. P., Galjaard, H., Sinnott, M. L., and Smith, P. J. (1980) Biochem. J. 188, 337-343

47. Kanfer, J. N., Legler, G., Sullivan, J., Raghavan, S. S., and Mumford, R. A. (1975) Biochem. Biophys. Res. Commun. 67, 85-91

48. Mumford, R. A., Raghavan, S. S., and Kanfer, J. N. (1976) J. Neurochem. 27, 493-498

49. Hasilik, A., Waheed, A., and von Figura, K. (1981) Biochem. Biophys. Res. Commun. 98, 761-767

50. Reitman, M. L., Varki, A., and Kornfeld, S., (1981) J. Clin. Invest. 67, 1574-1579

51. Proia, R. L., d'Azzo, A., and Neufeld, E. F. (1984) J. Biol. Chem. 259, 3350-3354

52. d'Azzo, A., Proia, R. L., Kolodny, E. H., Kaback, M. M., and Neufeld, E. F. (1984) J. Biol. Chem. 259, 11070-11074

53. Frisch, A., Baran, D., and Navon, R. (1984) Biochem. Biophys. Res. Commun. 119, 101-107

54. Silhavy, T. J., Benson, S. A., and Emr, S. D. (1983) Microbiol. Rev. 47, 313-344

55. Erickson, A. H., Conner, G. E., and Blobel, G. (1981) J. Biol. Chem. 256, 11224-11231

56. Gilmore, R., and Blobel, G. (1983) Cell 35, 677-685

57. Meyer, D. I., Krause, E., and Dobberstein, B. (1982) Nature 297, 503-508

58. Struck, D. K., Lennarz, W. J., and Brew, K. (1978) J. Biol. Chem. 253, 5786-5794

59. Struck, D. K., and Lennarz, W. J. (1980) In The Biochemistry of Glycoproteins and Proteoglycans (Lennarz, W. J., ed.) Plenum Press New York and London pp. 35-83

60. Li, E., Tabas, I., and Kornfeld, S. (1978) J. Biol. Chem. 253, 7762-7770

61. Hubbard, S. C., and Robbins, P. W. (1979) J. Biol. Chem. 254, 4568-4576

62. Green, M. (1982) J. Biol. Chem. 257, 9039-9042

63. Hsieh, P., Rosner, M. R., and Robbins, P. W. (1983) J. Biol. Chem. 258, 2555-2561

64. Nakamura, K., and Compans, R. W. (1979) Virology 95, 8-23

65. Grinna, L. S., and Robbins, P. W. (1979) J. Biol. Chem. 254, 8814-8818

66. Mellis, S. J., and Bainziger, J. U. (1983) J. Biol. Chem. 258, 11546-11556

67. Tabas, I., and Kornfeld, S. (1979) J. Biol. Chem. 254, 11655-11663

68. Waheed, A., Pohlmann, R., Hasilik, A., and von Figura, K. (1981) J. Biol. Chem. 256, 4150-4152

69. Varki, A., and Kornfeld, S. (1980) J. Biol. Chem. 255, 10847-10858

70. Reitman, M. L., and Kornfeld, S. (1981) J. Biol. Chem. 256, 11977-11980

71. Weisman, U. N., Lightbody, J., Vassela, F., and Herschkowitz, N. N. (1971) N. Eng. J. Med. 284, 109-110

72. Brown, W. J., and Farquhar, M. G. (1983) Cell 36, 296-307

73. Sahagian, G. G., Distler, J., and Jourdian, G. W. (1981) Proc. Nat. Acad. Sci. U. S. A. 78, 4289-4293

74. Kornfeld, S., Reitman, M. L., Varki, A., Goldberg, D., and Gabel, C. A. (1982) in Membrane Recycling (Evered, D., and Collins, G. M. eds.) Pitman Press Bath, Great Britain pp. 138-156

75. Owada, M., and Neufeld, E. F. (1982) Biochem. Biophys. Res. Commun. 105, 814-820

76. Waheed, A., Pohlmann, R., Hasilik, A., von Figura, K., van Elsen, A., and Leroy, J. G. (1982) Biochem. Biophys. Res. Commun. 105, 1052-1058

77. Kornfeld, S. (1985) Lecture at the Gordon Conference on Complex Carbohydrates

78. Tabas, I., and Kornfeld, S. (1978) J. Biol. Chem. 253, 7779-7786

79. Tulsiani, D. R. P., Hubbard, S. C., Robbins, P. W., and Touster, O. (1982) J. Biol. Chem. 257, 3660-3667

80. Schachter, H. (1984) Clin. Biochem. 17, 3-14

81. Yamashita, K., Tachibana, Y., and Kobata, A. (1978) J. Biol. Chem. 253, 3862-3869

82. Erickson, A. H., and Blobel, G. (1983) Biochem. 22, 5201-5205

83. Van den Bergh, F. A. J. T. M., Rietra, P. J. G. M., Kolk-Vegter, A. J., Bosch, E., and Tager, J. M. (1976) Acta Med. Scand. 200, 249-256

84. Hobbs, J. R., Hugh-Jones, K., Barrett, A. J., Byrom, N., Chambers, D., Henry, K., James, D. C. O., Lucas, C. F., Rogers, T. R., Benson, P. F., Tansley, L. R., Patrick, A. D., Mossman, J., and Young, E. P. (1981) Lancet ii, 735-739

85. Bayever, E., Feig, S. A., Philippart, M., and Brill, N. (1983) Clin. Res. 31, 107A

86. Gaspar, P. W., Thrall, M. A., Wenger, D. A., Macy, D. W., Ham, L., Dornsife, R. E., McBiles, K., Quackenbush, S. L., Kesel, M. L., Gillette, E. L., and Hoover, E. A. (1984) Nature 312, 467-469

87. Desnick, R. J., Dean, J. J., Grabowski, G., Bishop, D. F., and Sweeley, C. C. (1979) Proc. Nat. Acad. Sci. U. S. A. 76, 5326-5330

88. Ashwell, G., and Harford, J. (1982) Ann. Rev. Biochem. 51, 531-554

89. Desnick, R. J., and Sweeley, C. C. (1983) in Metabolic basis of Inherited Diseases (eds. Stanbury, J. B., Wyngaarden, J. B., Fredrickson, D. S., Goldstein, J. L., and Brown, M. S.) 906-944 McGraw Hill

90. Sweeley, C. C., and Klionsky, B. (1963) J. Biol. Chem. 238, PC 3148-3150

91. Siddiqui, B., Kawanami, J., Li, Y-T., and Hakomori, S-I. (1972) J. Lipid Res. 13, 657-667

92. Hanada, E., Konno, K., Handa, S., and Yamakawa, T. (1977) J. Biochem. 81, 1079-1083

93. Eto, T., Ichikawa, Y., Nishimura, K., Ando, S., and Yamakawa, T. (1968) J. Biochem. 64, 205-213

94. Hanada, E., Handa, S., Konno, K., and Yamakawa, T. (1978) J. Biochem. 83, 85-90

95. Wherrett, J. R., and Hakomori, S-I., (1973) J. Biol. Chem. 248, 3046-3051

96. Hanfland, P. Assman, G., and Egge, H. (1978) Z. Naturforsch. 33c, 73-78

97. Watanabe, K., Hakomori, S-I., Childs, R. A., and Feizi, T. (1979) J. Biol. Chem. 254, 3221-3228

98. Brady, R. O., Gal, A. E., Bradley, R. M., Martensson, A. L., Warshaw, and Laster, L. (1967) N. Eng. J. Med. 276, 1163-1167

99. Kint, J. 1970 Science 167, 1268-1269

100. Beutler, E., and Kuhl, W. (1972) Nature New Biol. 239, 207-208

101. Kint, J. A., Huys, A., and Hooft, C. (1971) Arch. Int. Biochem. 79, 633-634

102. Schram, A. W., Hamers, M. N., Brouwer-Kelder, B., Konker-Koopman, W. E., and Tager, J. M. (1977) Biochem. Biophys. Acta 482, 125-137

103. Beutler, E., and Kuhl, W. (1972) J. Biol. Chem. 247, 7195-7200

104. Dean, K. J., and Sweeley, C. C. (1979) J. Biol. Chem. 254, 10001-10005

105. Dean, K. J., and Sweeley, C. C. (1979) J. Biol. Chem. 254, 9994-10000

106. Mayes, J. S., Cray, E. L., Dell, V. A., Scheer, J. B., and Sifers, R. N. (1982) Am. J. Hum. Genet. 34, 602-610

107. Mayes, J. S., and Beutler, E. (1977) Biochim. Biophys. Acta 484, 408-416

108. Dean, K. J., and Sweeley, C. C. (1979) J. Biol. Chem. 254, 10006-10010

109. Harpaz, N., and Flowers, H. M. (1974) Methods Enzymol. 34B, 347-350

110. Romeo, G., DiMatteo, G., D'Urso, M., Li, S-C., Li, Y-T. (1975) Biochim. Biophys. Acta 391, 349-360

111. Beutler, E., Guinto, E., and Kuhl, W. (1973) Am. J. Human Genet. 25, 42-46

112. Dean, K. J., Sung, S-S. J., and Sweeley, C. C. (1977) Biochem. Biophys. Res. Commun. 77, 1411-1417

113. Schram, A. W., Hamers, M. N., and Tager, J. M. (1977) Biochim. Biophys. Acta 482, 138-144

114. Sung, S-S. J., and Sweeley, C. C. (1980) J. Biol. Chem. 255, 6589-6594

115. Thomas, D. B., and Winzler, R. J. (1969) J. Biol. Chem. 244, 5943-5946

116. Gahmberg, C. G., and Hakomori, S-I. (1975) J. Biol. Chem. 250, 2438-2446

117. Siddiqui, B., and Hakomori, S-I. (1971) J. Biol. Chem. 246, 5766-5769

118. Hakomori, S-I., Stellner, K., and Watanabe, K., (1972) Biochem. Biophys. Res. Commun. 49, 1061-1068

119. Frei, J. (1984) Personal Communication

120. Schwyzer, R., Iselin, B. M., and Feurer, M. (1962) Chem. Abstr. 56, 4864

121. Frusch, H. L., and Isbell, H. S. (1951) J. Res. Natl. Bur. Stds. 47, 239-247

122. Gordon, J. A., Blumberg, S., Lis, H., and Sharon N. (1972) Methods Enzymol. XXVIII, 365-368

123. Pierce, J. W., Jr. (1980) Personal Communication

124. March, S. C., Parikh, I., and Cuatrecasas, P. (1974) Anal. Biochem. 60, 149-152

125. Desnick, R. J., Allen, K. Y., Desnick, S. J., Raman, M. K., Bernlohr, R. W., and Krivit, W. (1973) J. Lab. Clin. Med. 81, 157-171

126. Gomori, G. (1955) Methods Enzymol. 1, 138-146

127. Sung, S-S. J., and Sweeley, C. C. (1976) In Current Trends in Sphingolipidoses and Allied Disorders (Volk, B. W., and Schneck, L., eds.) Plenum Press-New York and London pp.323-337

128. Dean, K. J. (1978) PhD Thesis, Department of Biochemistry, Michigan State University East Lansing, Michigan

129. Laemmli, U. K. (1970) Nature 227, 680-685

130. Wray, W., Boulikas, T., Wray, V. P., and Hancock R. (1981) Anal. Biochem. 118, 197-203

131. Lowry, O. H., Rosebrough, N. J., Farr, A. L., and Randall, R. J. (1951) J. Biol. Chem. 193, 265-275

132. Rutter, W. J. (1967) In Methods in Developmental Biology (Wilt, F. H., and Wessels, N. K. eds.) Thomas Y. Crowell Co. New York 671-683

133. Bohlen, P., Stein, S., Dairman, W., and Udenfried, S. (1973) Arch. Biochem. Biophys. 155, 213-220

134. Gracy., W. C. (1977) Methods Enzymol. XLVII, 195-204

135. Hermodson, M. A., Ericcson, L. H., Neurath, H., and Walsh, K. A. (1972) Biochem. 12, 3146-3152

136. Tarr, G. E., Black, S. D., Fujita, V. S., and Coon, M. J. (1983) Proc. Nat. Acad. Sci. U. S. A. 80, 6552-6556

137. Galfre, G., Howe, S. C., Milstein, C., Butcher, G. W., and Howard, J. C. (1977) Nature 266, 550-552

138. Stegelmeier, H. (1979) Thesis, Faculty of Mathematics and Natural Sciences, University of Cologne

139. Radin, N. S., and Vunnum, R. R. (1981) Methods Enzymol. 72, 673-684

140. Legler, G. (1966) Z. Physiol. Chem. 345, 197-214

141. Oesch, F., Jerina, D. M., and Daly, J. (1971) Biochim. Biophys. Acta 227, 685-691

142. Legler, G., and Herrchen, M. (1981) FEBS Lett. 135, 139-144

143. Posternak, T. (1965) The Cyclitols Holden-Day, Inc. San Francisco

144. Sweeley, C. C., Bentley, R., Makita, M., and Wells, W. W. (1963) J. Amer. Chem. Soc. 85, 2497-2505

145. Ghatt, S. (1985) Personal Communication

146. Wilkinson, G. N. (1961) Biochem. J. 80, 324-332

147. Mannervik, B. (1984) Methods Enzymol. 87, 370-390

148. Legler, G. (1982) Letter dated October 27

149. Legler, G. (1983) Personal Communication

150. Lowe, C. R., Harvey, M. J., Craven, D. B., and Dean, P. D. G. (1973) Biochem. J. 133, 499-506

151. Lalegerie, P., Legler, G., and Yon, J. M., (1982) Biochimie 64, 977-1000